NUTRIENTS, SALINITY AND SHADING IN AN ALGAE GROWTH MODEL

by

Song Gao

A Dissertation Submitted to the Faculty of the

DEPARTMENT OF AGRICULURAL AND BIOSYSTEMS ENGINEERING

In Partial Fulfillment of the Requirements

For the Degree of

DOCTOR OF PHILOSOPHY

In the Graduate College

THE UNIVERSITY OF ARIZONA

2017

THE UNIVERSITY OF ARIZONA
GRADUATE COLLEGE

As members of the Dissertation Committee, we certify that we have read the dissertation prepared by Song Gao, titled Nutrient, salinity and shading in an algae growth model and recommend that it be accepted as fulfilling the dissertation requirement for the Degree of Doctor of Philosophy.

_____ Date: 11/22/2017
Peter Waller

_____ Date: 11/22/2017
Kimberly Ogden

_____ Date: 11/22/2017
Stephen Poe

_____ Date: 11/22/2017
Kevin Fitzsimmons

Final approval and acceptance of this dissertation is contingent upon the candidate's submission of the final copies of the dissertation to the Graduate College.

I hereby certify that I have read this dissertation prepared under my direction and recommend that it be accepted as fulfilling the dissertation requirement.

_____ Date: 11/22/2017
Dissertation Director: Peter Waller

STATEMENT BY AUTHOR

This dissertation has been submitted in partial fulfillment of the requirements for an advanced degree at the University of Arizona and is deposited in the University Library to be made available to borrowers under rules of the Library.

Brief quotations from this dissertation are allowable without special permission, provided that an accurate acknowledgement of the source is made. Requests for permission for extended quotation from or reproduction of this manuscript in whole or in part may be granted by the head of the major department or the Dean of the Graduate College when in his or her judgment the proposed use of the material is in the interests of scholarship. In all other instances, however, permission must be obtained from the author.

SIGNED: Song Gao

ACKNOWLEDGEMENTS

First and foremost, I would like to express my sincere gratitude to my advisor Dr. Peter Waller for the continuous support of my Ph.D study. I started my research without much knowledge on programing and modeling. It was his patience, encouragement and explanation that helped me to overcome all the difficulties. Without his guidance, this thesis would never be completed.

My sincere gratitude is also reserved for the rest of my dissertation committee. A large portion of my research was completed with Dr. Kimberly Ogden's laboratory and facility. Her support was critical for the completion of this thesis. I consider myself very fortunate to have Dr. Kevin Fitzsimmons in my committee for his immense knowledge of algae and insightful comments. I'm also grateful to Dr. Steve Poe for helping me keep my study and research on the right track.

My acknowledgements are extended to Dr. Michael Huesemann, who developed the original model and provided important experimental data, Dr. Murat Kacira from whom I learned sensor applications, and Dr. Judith Brown whose laboratory provided most of the stock culture and inoculum used in the project.

Dozens of people have helped me during my research. I would like to thank: George Khawam for his help on model modification; Said Attalah, Owen Bertelsen, Eleanore Leichtenberg, Kai Lepley and Irene Liang for their work on carrying out raceway

experiments; Yaser Mehdipour for his effort on constructing bioreactors; Margarita Acedo, Renhe Qiu and Lydia Toscano-Palamar for their help on biomass biochemical analysis.

Very special thanks to the ABE department. I came to the U.S. alone, and the department was always by my side. Without the support from the department, it would have been impossible for me to complete this dissertation.

Lastly, I would like to thank my family for their love and support that sustained me in my pursuits. My gratitude to them is beyond words. I would also like to thank Min Ju, for her love and encouragement during this journey. I will forever remember all of my friends who has been good companions to me during these years in Tucson. Thank you, and love you!

TABLE OF CONTENTS

LIST OF FIGURES

LIST OF TABLES

NOMENCLATURE

A	Azimuth angle (from North, clockwise)
AFDW	Ash free dry weight concentration, g L^{-1}
B	Biomass concentration, g L^{-1}
BF	Bias factor
C_n	*AFDW* on day *n*
D	Culture depth, m
DW	Dry weight biomass concentration, g L^{-1}
H	Board height, m
HABG model	Huesemann Algae Biomass Growth model
L	Channel width in Algae Raceway Integrated Design, m
I	Light intensity received by cell
I_0	Incident light intensity at the surface, μmol m^{-1} s^{-1}
I_k	Half saturation constant in photosynthesis-irradiance response
I_z	Light intensity at depth z, μmol m^{-1} s^{-1}
I_{z0}	Light intensity in unshaded area at depth z, μmol m^{-2} s^{-1}
I_{zx}	Light intensity at point at distance x and depth z, μmol m^{-2} s^{-1}
k_a	Particle light absorption coefficient, m g L^{-1}
k_{sca}	Corrected particle light absorption coefficient in HABG model, m g L^{-1}

K_B	Light scattering coefficient related to biomass concentration
K_S	Monod half-saturation constant, mg L^{-1}
$K_{S,N}$	Monod half-saturation constant of nitrogen, mg L^{-1}
$K_{S,P}$	Monod half-saturation constant of phosphorus, mg L^{-1}
K_Z	Light scattering coefficient related to depth
n_a	Refractive index of air
n_w	Refractive index of water
N_0	Initial media nutrient concentration
N_A	Nitrogen availability
N_n	Media nutrient concentration on day n
P	Specific rate of photosynthesis
P_m	Maximum specific rate of photosynthesis
Q	Nutrient quota, g/g-biomass
Q_0	Subsistence quota, g/g-biomass
Q_N	Nitrogen cell quota, g-N/g-biomass
Q_P	Phosphorus cell quota, g-P/g-biomass
RAFT	Regional Algal Feedstock Testbed
R_{Iz}	Shading factor at depth z
R_N	Nitrogen stress factor

R_S	Salinity factor
r_{zx}	Light ratio at depth z and distance x from the board
S	Substrate concentration, mg L^{-1}
w_z	Shade width at depth z, m
Y	Substrate yield, g g^{-1} or g mg^{-1}
z	Depth of a specific layer, m
θ_1	Zenith angle
θ_2	Refractive angle
μ	Specific growth rate, day^{-1} or h^{-1}
μ_m	Maximum specific growth rate, day^{-1} or h^{-1}
μ_m'	Hypothetic maximum growth rate at infinite Q, day^{-1}
μ_n	Specific growth rate on day n, day^{-1}

ABSTRACT

Microalgae have been recognized as one of the most promising feedstocks for biofuel production. In the Regional Algal Feedstock Testbed (RAFT) project, scientists and engineers have been working on various topics including improving cultivation strategy, optimizing culture system, developing production models, controlling contamination, and so on. One of the objectives in this project is to improve an algae cultivation model for productivity prediction and techno-economic assessment. The model adopted in this project is the Huesemann Algae Biomass Growth (HABG) model which is based upon strain characteristics obtained from laboratory experiments. However, because the model assumed optimal growth conditions for microalgae, it over-predicted biomass growth significantly when its results were compared to outdoor raceway experimental data. For example, in an attempt to control contamination, culture salinity was raised to a high level. The high salinity may limit growth of contaminants, but it also causes stress on salinity sensitive strains of microalgae. Researchers also lowered nutrient fertilization rates in order to minimize fertilizer input and cost of production. However, this introduced nutrient stress and lowered the growth rate of microalgae. In the raceways used in the RAFT project, shade covered a large fraction of the culture surface when solar angle was low. All of these growth limiting factors were not included in the original model. In this study, salinity stress, nitrogen limitation and shading effect were incorporated into the model. Growth rate reduction due to salinity stress and nitrogen limitation were quantified through laboratory experiments. An innovative concept of nitrogen availability was introduced, which estimates the nitrogen stress factor without measuring intracellular nitrogen. The shading factor was calculated based on solar position during the day and raceway geometry. The modification greatly improved the model accuracy. In addition to HABG model improvements, this study also

focused on nutrient application. Several experiments were performed in both indoor and outdoor systems to improve field cultivation practices. The nitrogen experiments provided not only the growth kinetics that improved the growth model, but also demonstrated that high lipid accumulation rate was triggered at different nitrogen stress intensities for different strains. Stress should be applied depending the saturation demand of the final lipid product. In order to quickly evaluate the nitrogen status in the culture, a nitrogen stress index using optical density was proposed. Experiments in RAFT experiments supported the feasibility of applying the method in outdoor cultivation. This study also investigated maximum biomass yields of nitrogen and phosphorus for producing *S. obliquus* biomass with indoor bench scale experiments. The results were tested in the outdoor raceways and demonstrated the potential of using fertilizer more efficiently in microalgae cultivation.

Keywords: microalgae, growth model, salinity, shading, nutrient, yield

Chapter 1 Introduction

1. Literature review

1.1 The basic of biofuels research

Climate change is one of the primary concerns for humanity in the 21st century (Tingem and Rivington, 2009). In the last century, the global mean surface temperature has increased by 0.4 to 0.8 ℃ (Panwar et al., 2011). The rise in temperature is mainly caused by greenhouse gas emissions. In the last 200 years, atmospheric CO_2 levels have increased 31% (Panwar et al., 2011). A large portion of greenhouse gas emission is related to transportation and electricity generation through burning of fossil fuels (Mata et al., 2010). With the growing population, global energy demand is continuously increasing. In 2008, the annual world primary energy consumption was estimated at 11,295 million tons of oil equivalent, of which fossil fuels accounts for 88% (BP Global, 2009). In 2015, fossil fuels remained the dominant source of energy powering the world economy, accounting for 85% of 13,147 million tons of oil equivalent energy supplies (BP Global, 2017). The burning of fossil fuels is the major contributor to the 2.1% annual growth of net CO_2 emissions (BP Global, 2017). The intensifying greenhouse effect and the problems associated with it requires governments to control greenhouse gas emissions. In response, agreements, such as Kyoto Protocol (United Nations, 1998) and Climate Change Act (Great Britain, 2008), were made to set limits and goals for CO_2 emission control. Biofuel was proposed as one possible solution to the problem. Unlike fossil fuels, biofuels originate from photosynthetic organisms. Atmospheric carbon is fixed into biomass through photosynthesis. Ideally, the net carbon release from burning biofuels to the atmosphere is zero, but there might be consumption of external energy at different points of the

production process. Nevertheless, biofuel production is one of the most strategically important technologies for energy sustainably (Nigam and Singh, 2011).

Biofuels produced from sugars, grains or seeds are identified as first-generation biofuels (Naik et al., 2010). Ethanol from sugar fermentation of crop plants and oily seeds is a widely-used biofuel currently on the market (United Nations, 2008); however, these feedstocks are also important food sources, which encouraged the search for non-edible biomass feedstock (Patil et al., 2008). Second-generation biofuels use non-edible residues of food crop production such as stems, leaves and husks (Inderwildi and King, 2009) which is more appropriate for a world with increasing food demand. However, conversion technologies for second-generation biofuels remain challenging, which highly limit their commercial production (Brennan and Owende, 2010). Third-generation biofuels, using microbes, lack these two major drawbacks to the first and second generation biofuels. Among various possible feedstocks, microalgae have been recognized as one of the most promising organisms because of their high lipid content, rapid growth and diverse cultivation patterns (Chisti, 2007).

1.2 Alternative uses of algae

Prior to biofuels, microalgae have been cultured for many purposes. Human consumption of microalgae dates back to 2000 years ago (Spolaore et al., 2006). Nowadays, various algal products can be found on the market in tablets, capsules and many other forms (Yamaguchi, 1997).

Many algae, such as *Scenedemus*, *Chlorella*, and *Spirulina*, have protein contents that are more than half of the dry mass (Becker, 2007). In addition, the amino acid (AA) composition of algal protein is favorable to humans and animals. The essential AAs provides great health value, and enables algae to be a high quality food source. Long-chain polyunsaturated fatty acids (PUFAs)

from microalgae also provide nutritional benefits to human health. Omega-3 and omega-6 series such as eicosapentaenoic (EPA), docosahexaenoic (DHA), and arachidonic acid are pharmacologically important to dietetics and therapeutics (Pulz and Gross, 2004). Pigments from microalgae also have a wide range of applications. For instance, the carotenoid pigment astaxanthin is an important antioxidant (Koller et al., 2014; Naguib, 2000). Its price reached $2500-7000/kg, and its market potential was estimated at $447 million in 2014 (Borowitzka, 2013; Koller et al., 2014; Milledge, 2010; Pérez-López et al., 2014). Table 1.1 shows market value and demand of some algal products within fields other than biofuels.

Table 1.1 Global market of selected microalgal high-value compounds (Markou and Nerantzis, 2013)

Added-value compound	Global Market (million US$/annum)	Production kt/annum	Price $/kg
Carotenoids	1200	-	-
β-Carotene	261	-	300-700
Lutein	233	-	-
Astaxanthin	240	-	2000-7000
Bioplasticss	-	64	-
Fatty acids (omega-3)	>700	85	0.88-3.8
Vitamins and supplement	68	-	-
Glycerol	-	1995.5	0.3-1
Phycobilins	>60	-	-
C-phycocyanin	-	5	-
B-phycoerythrin	-	-	50000

Microalgae is an important animal feed source, especially for aquatic animals. Many fish, mollusks and shrimps require microalgae as the major food source in early life stages (Spolaore

et al., 2006). Algal pigments are also important in providing nature color in seafood products such as salmon flesh and oysters (Baker, 2001; Martínez-Fernández and Southgate, 2007).

1.3 Characterization of the algal growth cycle

In general, batch microalgae culture shares the same typical growth phases as other microorganisms. The growth curve, generally, consists of six phases, namely, lag phase, exponential phase, linear phase, stationary phase, and death phase (Figure 1.1). Lag phase is usually caused by physiological adjustment, genetic regulation and/or low inoculum size. Under autotrophic growth condition, the exponential phase of microalgae is relatively short because self-shading effect increases rapidly with growing cell density and limits the growth (Grima et al., 1999). Declining growth phase starts when nutrient or light is close to its carrying capacity. Accumulation of secondary byproducts and/or other stresses can also lower the growth rate. When there is no growth, the stationary phase starts. Storage molecules such as lipid and starch are accumulated during this phase.

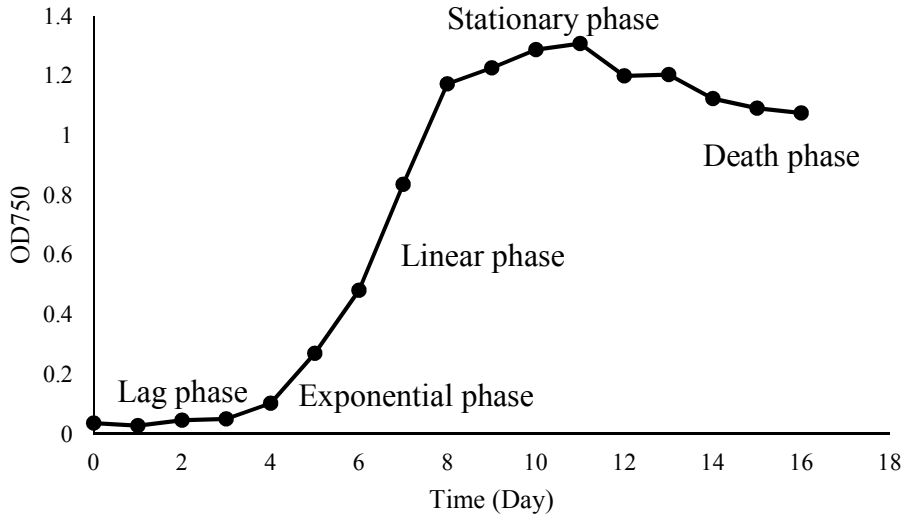

Figure 1.1 Growth curve of *Chlorella sorokiniana* in a batch culture. Nitrogen was provided only once at the beginning and was gradually depleted during the experiment

Various environmental conditions can determine the shape of the growth curve. In order to model the growth of microalgae, a number of models have been developed by scientists and engineers. In these models, light intensity, temperature and nutrients are as the most common input variables.

1.3.1 Light

In autotrophic microalgae culture, light is one of the most critical environmental factors. Modeling algae growth using light intensity as the independent variable was among the earliest kinetic studies. Many light kinetic models adopted Monod-like equation to quantify photosynthetic response to light intensity via the following formula:

$$P = \frac{P_m \cdot I}{I_k + I}$$

The model generates a hyperbolic curve of specific photosynthesis rate to light intensity. In the dark, there is no photosynthesis. As light intensity increases to I_k, photosynthesis rate increases to half of maximum photosynthesis rate. As light intensity is strong enough, photosynthesis rate reaches the saturation value and no longer increases with more light (Jeon et al., 2005). Photoinhibition is commonly observed in photosynthesis studies (Harris and Lott, 1973; Marra, 1978). The Monod-like model cannot model the inhibition effect of intense light; thus, other models were developed. Lee et al. (1987) observed best model performance by implementing an inhibition model in a model of bioenergetic yield and growth rate of *Spirulina platensis.*

Determination of a biological kinetic model is only part of growth modeling in a dense microalgae culture. Due to self-shading, light distribution beneath the water surface needs to be calculated and incorporated with the biological model. The Beer-Lambert law has been the most widely used models for estimation of light intensity within the culture (Bosma et al., 2008;

Evers, 1990; Guterman et al., 1990). However, the accuracy of Beer-Lambert law was determined to be inaccurate in a dense culture due to scattering effect (Quinn et al., 2011). Therefore, Suh and Lee (2003) introduced light scattering coefficients and achieved better prediction of light intensity distribution with depth in the culture. This approach is species-specific, and has been successfully integrated into recent algae growth models (Huesemann et al., 2016). Another alternative for accounting for light scattering was developed by Cornet (1992): the two-flux model. Regardless of the modeling approach and the complexity of estimating light intensity in a dense algae culture, determination of light distribution is critical to model accuracy. The coefficients should be calibrated for each species by experimental measurements.

1.3.2 Temperature

Temperature is also an important environmental factor for algal growth. Within a certain range, increasing temperature usually accelerates photosynthesis and growth. When temperature exceeds this range, overheating causes decreased growth rate or even kills the algae (Butterwick et al., 2005; Carvalho and Malcata, 2003).

Several models have been developed for quantifying the response of algae to temperature. For instance, Duarte (1995) introduced the Arrhenius function into an algal growth model and combined it with a mechanistic light function to predict algal productivity. However, the reduction effect of high temperature cannot be captured well by this approach (Ahlgren, 1987). Bernard and Rémond (2012) borrowed the concept of the cardinal temperature model with inflexion from a bacterial modeling study, and they proposed a model consisting of minimum, maximum and optimum temperatures. Respiration is also sensitive to temperature. Night time biomass loss of *Spirulina platensis* ranged from 3.6% to 31.5% dry weight, depending on temperature and other growth conditions (Torzillo et al., 1991). Collins and Boylen (1982)

modeled the specific respiration rate of *A. variabilis*. As temperature in outdoor culture systems may change significantly on a seasonal and even daily basis, the impact of temperature on respiration must be considered. Edmundson and Huesemann (2015) showed that respiration is not solely dependent on temperature, but also light status during the previous day, which was quantified in laboratory experiments and implemented in algae growth modeling.

1.3.3 Nutrients

As the building blocks for algal growth, nutrients are of great importance in algal cultivation. To better estimate biomass production, especially in attempts to minimize fertilizer cost, nutrient kinetic models should be integrated into algal growth models.

One of the most widely used models that describes the relationship of microbial growth rate and nutrient concentration is the Monod model (Monod, 1949):

$$\mu = \mu_{max}\frac{S}{K_S+S}$$

The Monod model has been tested against experimental data on several nutrients, including carbon, nitrogen, and phosphorus, and was proven to quantify the effect of nutrient concentration on algal growth (Aslan and Kapdan, 2006; Goldman et al., 1974; King and Novak, 1974; Li et al., 2010; Novak and Brune, 1985). For instance, Goldman et al. (1974) reported that, in a CFSTR (continuous flow stirred tank reactor) culture, the growth rates of two microalgae, *Scenedesmus quadricauda* and *Selenastrum capricornulum*, were determined by total dissolved inorganic carbon (TIC) following the Monod model. Novak and Brune (1985) have observed a similar pattern in carbon limited *Chlorella*, *Oscillatoria* and *Microcoleus* cultures. Aslan and Kapdan (2006) applied the Monod model to nitrogen and phosphorus removal in a batch reactor

using *Chlorella vulgaris*. Good fit of the data was achieved by using saturation constants for nitrogen and phosphorus ($K_{S\text{-}N}$ = 31.5 mg L^{-1} and $K_{S\text{-}P}$ = 10.5 mg L^{-1}).

The Monod model assumption is that the growth rate is controlled by external nutrient concentration. However, this assumption does not hold in many cases in which the model is not applicable. According to the Monod model, there should be no growth if external nutrients are unavailable. In reality, many studies have reported sustained growth of microalgae in the absence of external nutrients (Eixler et al., 2006; Li et al., 2008; Rhee, 1972; Tantanasarit et al., 2013; Tischner and Lorenzen, 1979). Growth kinetics in these cases cannot be explained by the Monod model.

An alternative nutrient kinetic model considering intracellular nutrient storage was first proposed by Droop (1968), and is known as the Droop model or the cell quota model:

$$\mu = \mu'_m(1 - \frac{Q_0}{Q})$$

The assumption for this model is that the growth rate is related to the intracellular nutrient concentration, defined as the cell quota (Q). With this model, continuous growth after depletion of external nutrients is reasonable. It has been successfully applied in many phytoplanktonic studies in nitrogen and phosphorus limited water (Grover, 1991a, 1991b; Lemesle and Mailleret, 2008; Sommer, 1991). By studying continuous cultures with different phosphorus supply patterns, Grover (1991b) demonstrated that, for *Chlorella* sp. and *Scenedesmus* sp., the phosphorus cell quota more accurately determined growth rate than the Monod model. Sommer (1991) also concluded that the cell quota model provides accurate prediction of microalgal growth in eutrophic water where nitrogen was limited.

The cell quota model also has its weaknesses. Compared to measuring external nutrient concentration, measuring intracellular nutrient quota is more difficult. This technical difficulty largely limits the applicability of this model. Also, cell quota was expressed in different ways such as cellular quota, biomass quota and carbon-based quota. Interpretation of the cell quota may vary from case to case (Flynn, 2002; Sommer, 1991).

Independently studying light, temperature and nutrient kinetic models provides the fundamental basis for constructing a more comprehensive model that can be applied to complicated real-world culture conditions. Grobbelaar et al. (1990) combined light and temperature models to predict growth of microalgae in large outdoor cultures. Light, temperature and carbon kinetics were considered by James and Boriah (2010) in modeling algae growth in an open-channel raceway. Quinn et al. (2011) developed a bulk growth model for industrial scale systems with sub models for light distribution, photosynthetic rate, temperature and nitrogen kinetics. In general, these models are case-specific or too complicated to parameterize, calibrate or apply. At this point, the Huesemann Algae Biomass Growth (HABG) model with incorporation of several submodels for calculating growth limiting factors appears to be the most promising approach.

1.4 Nutrients application in microalgae cultivation

Nitrogen and phosphorus are the major nutrients essential to algal growth. They provide the basic building blocks for cells, such as amino acids, nucleotides and chlorophyll, genetic materials, such as DNA and RNA, and other important functional molecules, such as ATP and enzymes (Cai et al., 2013). In the natural environment, nitrogen and phosphorus are usually the growth limiting factors. To achieve high biomass productivity, fertilization is required in most algal cultivation systems.

Life cycle assessments have evaluated the economic and environmental impact of fertilizer application in algal biomass production. Within a paddlewheel driven raceway system, urea usage is one of the major costs, accounting for more than 18% of the total operating cost (Rogers et al., 2014). In production of algal biomass for biofuel, energy investment on nitrogen fertilizer production also limits the value of the products. Currently, nitrogen fertilizer production relies on the Haber-Bosch process, an energy intensive process (Galloway et al., 2008). Energy consumption embedded in nitrogen fertilizer application contributes 6% - 40% of the total energy demand during the cultivation phase (Slade and Bauen, 2013). Sensitivity analysis showed that 10% increase in urea usage increases energy consumption by 4% (Clarens et al., 2010). Moreover, greenhouse gas emissions are also associated with nitrogen fertilizer production (Clarens et al., 2010). Nitrogen fertilizer application limits the carbon neutrality of microalgal biofuel. Controlling nitrogen fertilizer usage is important to lower production cost, lower energy consumption, and maintain carbon neutrality.

The other major nutrient input in algae cultivation is phosphorus. Currently, the major source of phosphorus fertilizers is phosphate rock, a non-renewable resource which may be depleted in 50-100 years (Cordell et al., 2009). Fertilizer application rates in the US. for agriculture are far less than the rates recommended for algae culture systems. An additional 53 million tons of phosphorus fertilizers per year would be required if complete replacement of petroleum biofuels occurred in the US (Hannon et al., 2010). Due to supply and demand, the price of phosphorus fertilizer increased drastically in the past, spiking by 700% in 2007 and 2008 (Elser and Bennett, 2011). For these and other reasons (Clarens et al., 2010; Lardon et al., 2009), reduction of nitrogen and phosphorous usage is necessary.

Coupling wastewater treatment with algal cultivation is a promising solution to lower the cost and nutrient requirements of growing biomass. Excessive nitrogen and phosphorus in wastewater support the growth of microalgae, while microalgae remove large amounts of nutrients from wastewater and prevent eutrophication problem after treated water is discharged to the environment (Tam and Wong, 1989). The method can be adapted to different wastewaters at different stages of treatment process (Teles et al., 2013). Additionally, compared to conventional energy intensive nutrient removal technology, integrating microalgae into the treatment process improves the energy balance considerably (Menger-Krug et al., 2012). Lastly, removing phosphorous and nitrogen from biomass after fuel production and recycling can limit the requirement for nitrogen and phosphorous production (Ayala-Parra et al., 2017).

1.5 Lipid content

Apart from affecting biomass production, nutrients and temperature also have a strong impact on microalgal biomass lipid content. Several environmental factors influence lipid accumulation. For instance, *C. vulgaris* accumulated 47% (of DW) more lipid when iron was supplemented (Liu et al., 2008). Increased lipid content was observed when *S. dmorphus* was cultured under high salinity. By raising growth temperature from 20℃ to 25℃, researchers increased the lipid content of *Nannochloropsis oculata* from 8 % to 15% (Converti et al., 2009).

Nutrient starvation is recognized as the most successful and most widely used strategy to increase lipid content (Hu et al., 2008). Under nitrogen limited condition, excess carbon is diverted to storage compounds such as lipids and starch when carbon fixation rate exceeds carbon demand for nitrogen assimilation (Turpin, 1991). Since photosynthesis cannot be shut down completely, lipid synthesis also works as a protective mechanism for siphoning off ATP and NAD(P)H, and preventing photodamage (Roessler, 1990). Restricting nitrogen can double

lipid content in some green algae (Thompson, 1996). Converti et al. (2009) decreased nitrogen concentration by 75% in the culture medium and lipid content of both *N. oculata* and *C. vulgaris* increased from 7.9% to 15.3, and from 5.9 to 16.4%, respectively. In a photobioreactor culture, lipid accumulation rate increased by more than 6 times after the depletion of nitrogen (Unkefer et al., 2017). Phosphorus stress can stimulate triacylglycerol (TAG) production and increase lipid content (Kamalanathan et al., 2015; Khozin-Goldberg et al., 2002). *C. protothecoides* accumulated 33% lipid content under phosphorus limited conditions, but the highest lipid content (55.8%) was observed within a culture under co-limitation of nitrogen and phosphorus (Li et al., 2014). *Scenedesmus* sp. also increased lipid content from 30% to 53% under co-deficiency of nitrogen and phosphorus (Li et al., 2010). However, Li et al. (2010) also pointed out that lipid productivity was not enhanced by increasing lipid content because of lowered biomass productivity. Therefore, a two-stage cultivation process was suggested: Culture is provided with nutrient rich media until reaching the desired density or stationary phase to obtain high biomass productivity, and then nitrogen and/or phosphorus are reduced to create a nutrient limited condition and higher lipid content.

2. Problem statement

Most of the work presented in this dissertation was conducted with the support of the RAFT (Regional Algal Feedstock Testbed) project, a Department of Energy funded microalgae biofuel research project. Developing cultivation models and improving resource usage were two of the major objectives of this project. Problems related to these two objectives occurred during the project. Research performed in this dissertation was mainly designed to solve the problems that arose during the project.

2.1 Over-prediction in microalgae growth model

In the RAFT project, the HABG model was used as a tool for biomass productivity prediction, cultivation strategy evaluation, and techno-economic assessment. Compared to other existed microalgae growth models, the HABG model is a relatively simple growth model that is easy to apply in commercial scale outdoor cultivation system. The model requires two easy-to-measure variables, culture temperature and incident light intensity. The combination of these two inputs was used in an interpolation scheme to find growth rate / respiration rate coefficients from laboratory measured growth rate matrices. The model was designed to be simple in order to increase the accuracy of the temperature and light coefficients, but important factors in real-world practice are ignored by doing so; thus, the model may provide inaccurate predictions if other factors are not optimal. In this research, growth limiting factors such as contamination, salinity, nutrient limitation and water/nutrient replenishment may post stress the culture. These growth reduction factors were introduced to our outdoor experiments through raceway operation, system geometry and contamination control. In fact, they commonly exist in microalgal cultivation, particularly in research. The original model didn't include any these impacts, and thus over-predicted the growth. Figure 1.2 shows the difference between predicted biomass concentration with the HABG model and observed biomass concentration in the RAFT experiment in the ARID raceway. Based on only measured water temperature and incident light intensity data, the model significantly over-predicted the growth.

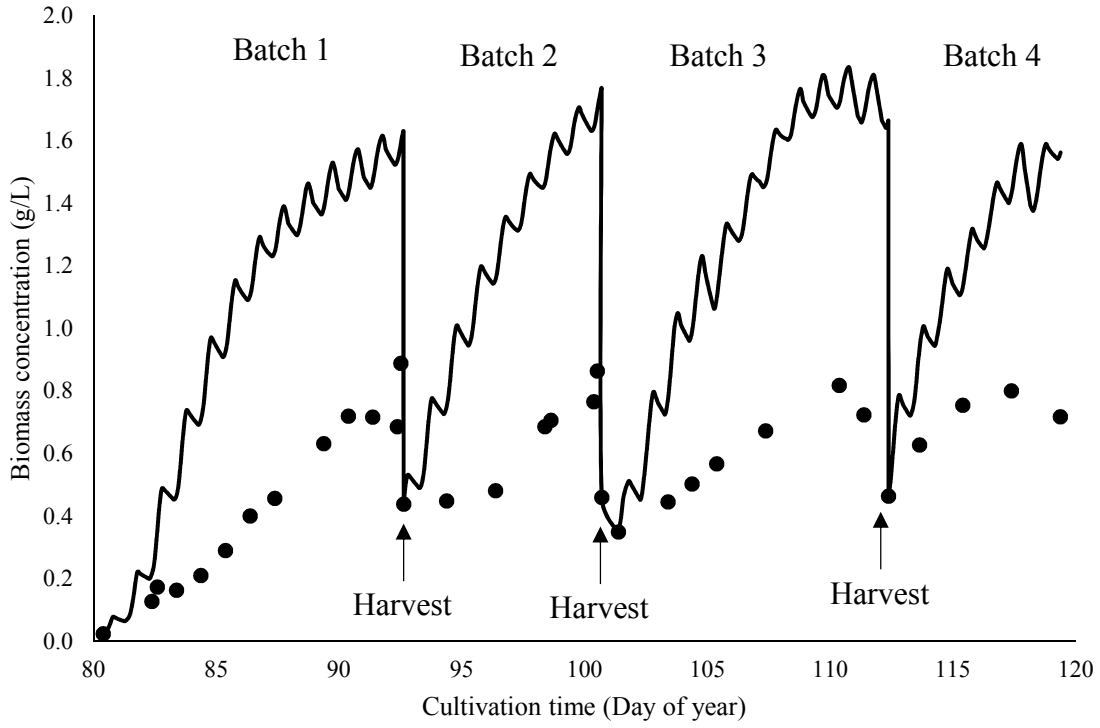

Figure 1.2 Comparison of simulated growth of original HABG model (-) and observed data (●) in RAFT 07, March 2015, in the ARID raceway (baffle version)

2.2 Large variation in nutrient efficiency

Although there are many studies on nutrient effects on algal growth, there are few studies on how to manage nutrients in biomass production systems. In RAFT raceway experiments, fertilization decisions were made empirically. Up to the time of writing this dissertation, the RAFT research group has conducted 90 outdoor experiments, with both ARID (Algae Raceway Integrated Design) raceways and conventional paddlewheel reactors. The ratio of added nutrient / produced biomass was defined as nutrient yield, and Figure 1.3 summarizes nutrient yields from majority of the *S. obliquus* experiments conducted in RAFT experiments. Although nutrients were added following similar procedures in most of experiments, nutrient yields varied by as much as 27 times. The large variation of nutrient yields through these experiments

indicated nutrients were utilized efficiently in some of the experiments, but were wasted in others. The results suggested a large opportunity for nutrient performance improvement and the necessity of better nutrient management strategy.

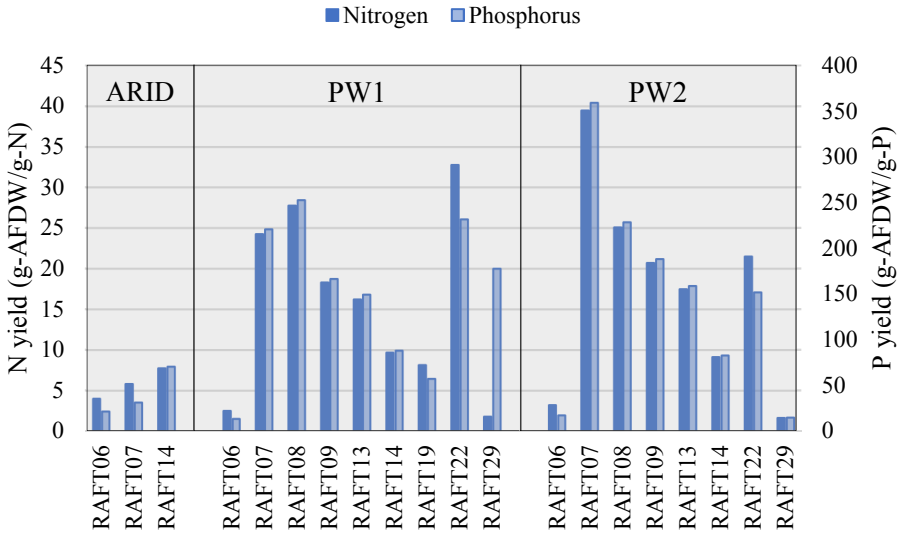

Figure 1.3 Nitrogen (N) yield and phosphorus (P) yield of *Scenedesmus obliquus* experiments in RAFT project: ARID raceway (ARID), Paddlewheel reactor 1 (PW1) and Paddlewheel reactor 2 (PW2).

3. Dissertation structure

Solutions adopted to solve the two above-mentioned problems are explained in chapters 2 and 3. Chapter 2 begins with a brief introduction of the HABG model. The model was constructed based on strain growth characteristics in response to light intensity and water temperature under indoor laboratory conditions. However, the model over-predicted microalgae growth when its results were compared to the outdoor raceway experimental data. By examining the growth conditions and cultivation system geometry, several possible growth limiting factors were identified, which were not included in the original model. Appendix A is associated with this chapter.

Chapter 3 focuses on better management of nutrient application through detection of nitrogen stress, measuring maximum biomass yields for nitrogen and phosphorous, and decision-making based on product lipid composition requirement. The results enable balancing high biomass productivity, controlling fertilizer usage and managing biomass biochemical composition. Appendices B, C, D are associated with this chapter.

Appendix A incorporates salinity effect, nitrogen stress and shading effect into the HABG algae growth model. Results are compared with experimental data from the ARID raceway. Laboratory experiments measured microalgae growth response to salinity stress and nitrogen stress. In the simulations, the measured salinity and nitrogen fertilizer usage were used to calculate the reduction in growth due to the salinity and nitrogen concentrations. In addition, a solar path model was added into the model which calculates solar angles during the day. Combined with raceway geometry, as well as measured light distribution in shaded area, a shading factor was calculated. The model simulations that incorporated the three factors were compared with observed raceway growth data. To measure the prediction accuracy, two statistics were applied, RMSE (Root Mean Square Error) and BF (Bias Factor). The hypothesis is that quantifying the effects of salinity, nitrogen stress and shading in the algae culture will improve the agreement between observed culture data and model, which means lowered RMSE and BF.

Appendix B is a summary of the chemical compositions in each culture media recipe used in the RAFT project. In general, most of the chemicals were applied in a much lower concentration than the standard algae culture media, BG-11.

Appendix C describes a two by two factorial experiment with nitrogen and phosphorus fertilization rates for *Scenedesmus obliquus* cultivation. The goal was to find the maximum biomass yields of nitrogen and phosphorus. Flat-panel photobioreactor (PBR) and outdoor

raceway experiments were used to evaluate the bench-scale experiment results. MANOVA (multivariate analysis of variance) was used to evaluate the growth effect of nutrients on algae growth and lipid content from triplicate samples. The hypothesis of this study is that by supplying the culture with two different levels of nitrogen and phosphorus, biomass yield of the limited one is maximized. If this is true, then the PBR and raceway experiment results should agree with the result from indoor bench-scale experiment results.

Appendix D describes the relationships between algae growth rate and cellular nitrogen, and an optical health indicator in microalgae cultures. The experiments determined nitrogen kinetics for the three microalgae species cultured in RAFT project, as well as nitrogen stress index based on chlorophyll content. The kinetic model parameters were determined by fitting experimental data (growth rates and cellular nitrogen) to the Droop model. Goodness of fit is represented by R^2. The R^2 statistics was also used to measure the linearity between the stress index and cellular nitrogen. There were two hypotheses in this study. One is that algae growth rate is dependent on internal nitrogen and can be described by the Droop model. The other is that the stress index based on chlorophyll content, which is strongly affected by cellular nitrogen, is tightly correlated with cellular nitrogen and can be used to measure culture nitrogen status.

Chapter 2 HABG model and addition of growth limiting factors

The microalgae growth model applied in this work is the Huesemann Algae Biomass Growth (HABG) model (Huesemann et al., 2016). The model is briefly introduced in the introduction section including the modified Beer-Lambert's Law for light intensity calculation, growth rate / dark respiration rate as a function of light status and water temperature, over-prediction in the model and growth limiting factors that needs to be considered. Adjustment of the model for these growth limiting factors was summarized in a manuscript and was presented in Appendix A: Incorporation of the effects of salinity, nitrogen stress, and shading into an algae growth model and evaluation in the ARID raceway.

1. Introduction

1.1 Light intensity as a function of depth

Light is one of the most important environmental factors because it drives photosynthesis; hence, microalgal growth rate is highly dependent on light intensity. Beer-Lambert's Law is widely used to calculate light intensity as a function of depth (Goldman and Hole, 1979; Packer et al., 2011) in many microalgal growth models.

$$I_z = I_0 \times e^{-k_a \cdot B \cdot z}$$

where, I_0 is the incident light intensity at the surface, I_z is the light intensity at depth z, k_a is the particle light absorption coefficient.

The linear relationship between $\log_{10}(I_z/I_0)$ in Beer-Lambert's Law is valid only for monochromatic radiation and negligible scattering in the medium. However, in dense microalgal culture, scattering effect cannot be neglected (Quinn et al., 2011). Directly applying this equation

causes error in light intensity estimation. In the HABG model, a scatter-corrected biomass light attenuation coefficient was quantified at Pacific Northwest National Laboratory (PNNL) and was incorporated into the model (Huesemann et al., 2016). The new coefficient for calculating light intensity at depth z, $k_{sca,}$ is calculated via

$$k_{sca} = k_a \times \frac{K_B}{K_B + B} \times \frac{K_Z}{K_Z + Z}$$

where K_B and K_Z are the light scattering coefficients related to biomass concentration (B) and depth (z), respectively.

The scattering and light absorption coefficients vary significantly between different microalgal strains. For instance, with the same biomass concentration, light penetration is shorter in *Chlorella sorokiniana* culture than in *Scenedesmus obliquus* culture (Figure 2.1).

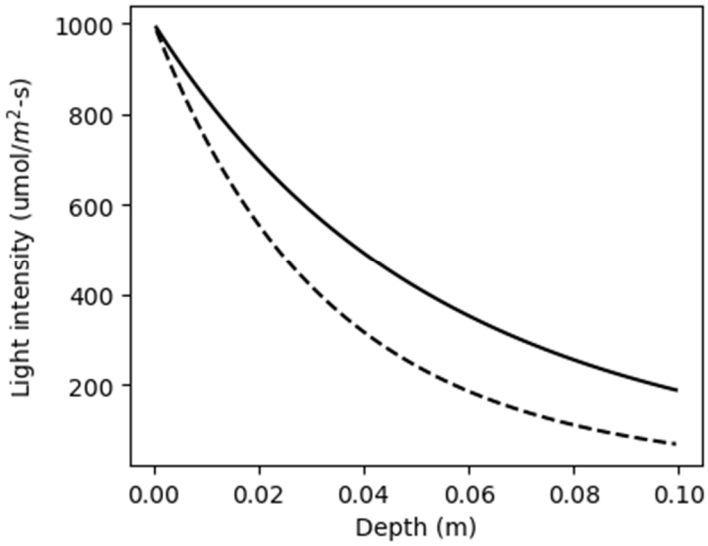

Figure 2.1 Light intensity as a function depth for *Chlorella sorokinina* (dashed line) and *Scenedesmus obliquus* (solid line) at same biomass concentration (0.1 g-AFDW/L) with photosynthetic photon flux of 1000 umol/m^2-s perpendicular to water surface

1.2 Growth rate as function of light intensity and water temperature

The growth rate coefficients used in this model were determined individually for each microalgal strain in laboratory experiments at PNNL marine laboratory. Figure 2.2 is a surface plot of the specific growth rate of *Scenedesmus obliquus* in response to temperature and light intensity. Within 0 to 2000 μmol/m^2-s photon flux range, the optimal temperature for *S. obliquus* is approximately 30 ℃. *C. sorokiniana* has higher heat tolerance, and it has higher growth rate at 36℃ than at 31 ℃. In comparison, *Monoraphidium minutum* is more competitive at lower temperature. Its highest growth rate was observed within the range of 22 to 27 ℃. For achieving high annual biomass productivity, different strains should be selected for different seasons and different locations. In most of the RAFT experiments, *C. sorokiniana* was cultured in summer, and *S. obliquus* and *M. minutum* were cultured in winter.

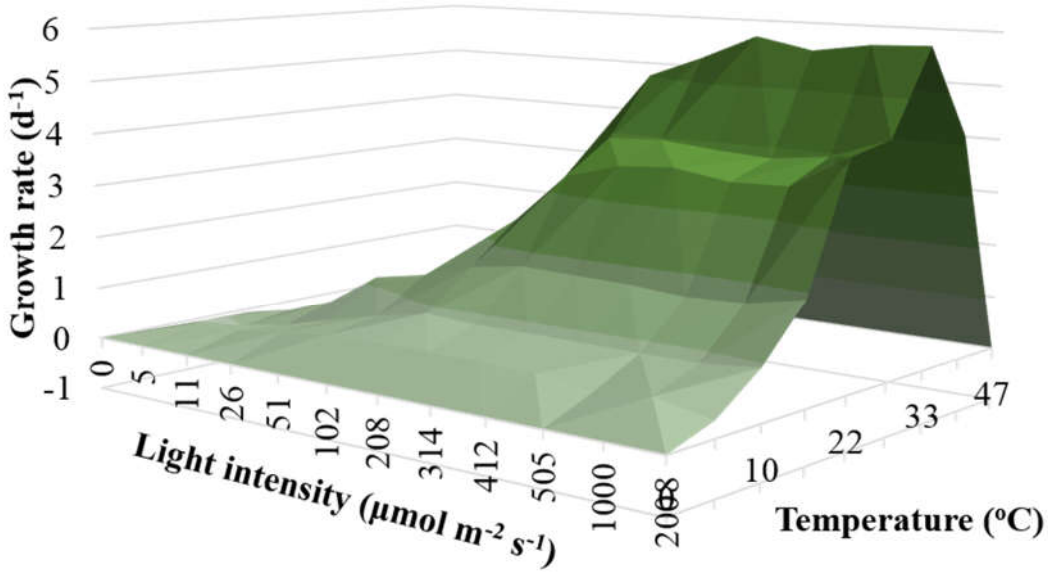

Figure 2.2 Surface plot of growth rate of *Scenedesmus obliquus* as a function of temperature and light intensity

Respiration plays an important role in algae growth as cell maintenance is performed in parallel with photosynthesis (De Vries et al., 1974). Energetics of endogenous respiration of microalgae are often much smaller than the light photosynthetic rate; The consumption of biomass was not considered important in the energy budget of vascular plants (Geider and Osborne, 1989). However, experimental data showed that this may not be the case in mass algae culture. Depending on culture condition (light intensity and temperature), night time biomass loss could reach 31.5% of the dry biomass (Torzillo et al., 1991). To accurately predict continuous microalgal growth, respiration needs to be quantified. Researchers have applied different methods to model dark respiration in microalgae culture. For instance, Goldman and Hole (1979) introduced one parameter, k_d, to summarize respiration rate, which includes photorespiration and cell death. Quinn et al. (2011) assumed constant respiration rate in a bulk growth model. In reality, estimation of dark respiration rate is difficult because cellular respiration is subject to temperature and light intensity (Béchet et al., 2013; Collins and Boylen, 1982). Compare to assuming constant value, or using theoretical equations in other models, the HABG model estimates dark respiration rate based on experimental data, and can be applied in more complicated situations. Similar to the daytime growth rate coefficients, dark respiration rate is a function of temperature and light status (Edmundson et al., n.d.; Edmundson and Huesemann, 2015). Figure 2.3 shows dark respiration response surface to the two factors of *S. obliquus*.

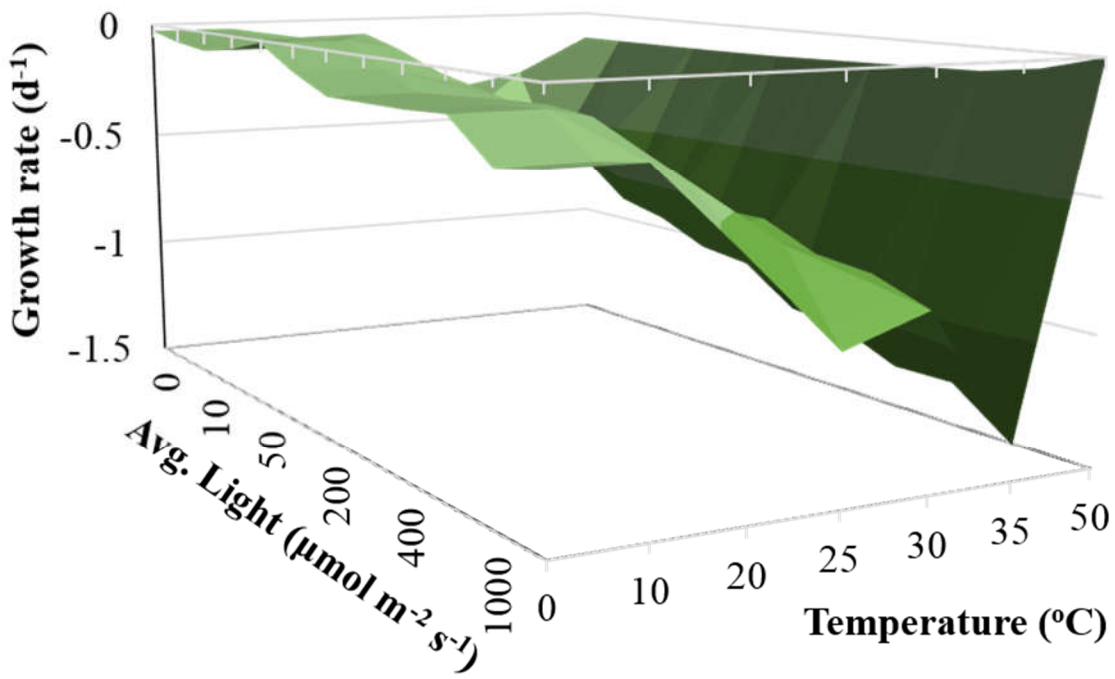

Figure 2.3 Dark respiration rate of Scenedesmus obliquus as a function of average daily light intensity and temperature

Figure 2.4 is an example of a typical sawtooth shape growth curve produced by the HABG model. The diurnal biomass concentration fluctuation is caused by photosynthesis and dark respiration. Biomass accumulates during the day, and is consumed by dark respiration during the night.

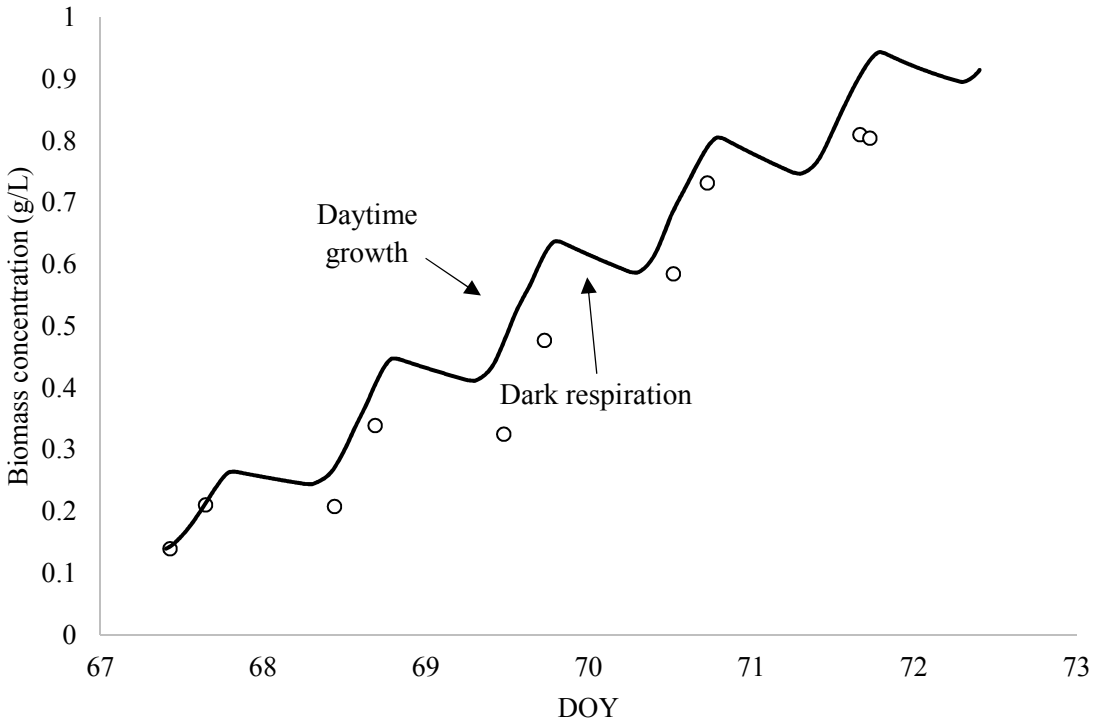

Figure 2.4 Typical growth curve produced by HABG model (PWARID, 2017). The solid line represents simulated growth and black circles represent observed biomass concentration

1.3 Over-prediction

In some cases, the HABG model has accurate growth prediction, however, over-prediction appeared many times when modeled growth was compared to outdoor experimental data. For instance, simulation of outdoor experiment RAFT07 had an overall 90% over-prediction when compared to experimental data (Figure 2.5). Similar results were observed in many other growth simulations.

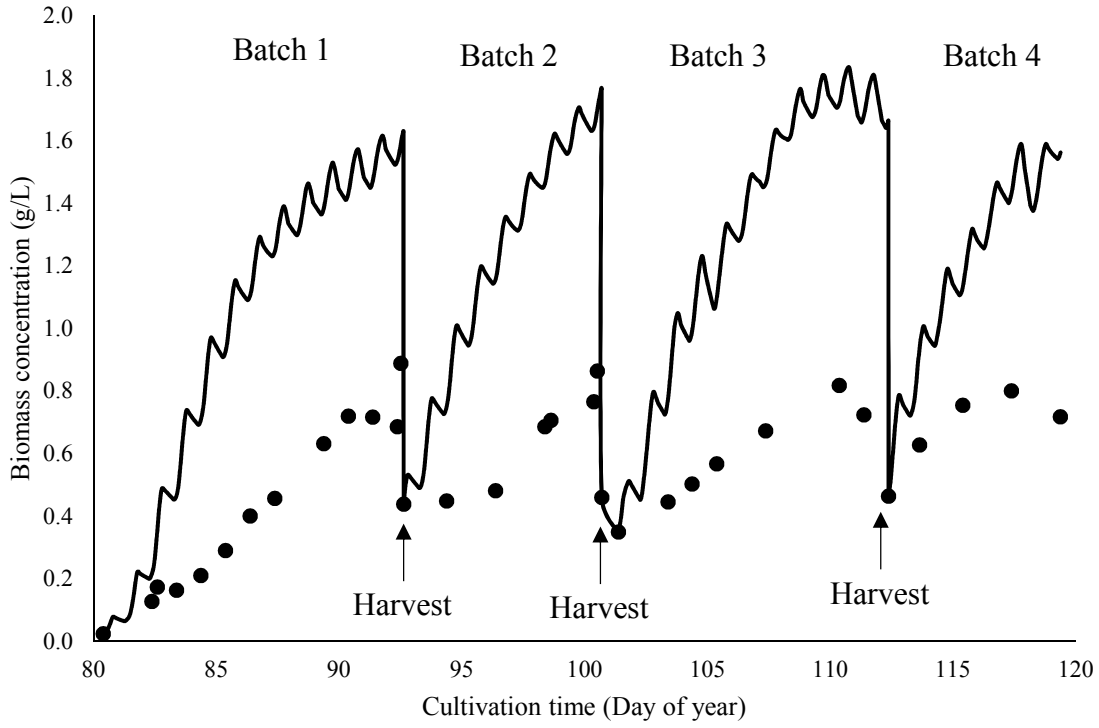

Figure 2.5 Observed (●) and predicted (—) biomass concentration over time. Three harvests divided the experiment into 4 successive batch culture runs (RAFT07 ARID raceway)

1.4 Causes of over-prediction

In the original HABG model, the light and temperature coefficients obtained in laboratory experiments were evaluated in indoor experimental raceways with an overhead LED light array, which provided perpendicular light to the culture surface, and BG-11 culture medium, which provided sufficient nutrients. Other conditions are also well controlled and assumed to be optimal. However, outdoor cultivation conditions are much more complicated, and some of the assumptions may not be satisfied.

Contamination is one of the major challenges in growing microalgae in outdoor open cultivation systems (Forehead and O'Kelly, 2013; Lincoln et al., 1983; Moreno-Garrido and Cañavate, 2000). One possible solution is using high salinity culture media. Rao et al. (2012) showed that

raising culture salinity could keep the culture monospecies in an open raceway pond for high salinity adapted algal strains such *Dunaliella*. In some of our raceway experiments, we implemented this idea by adding NaCl into the culture in an attempt to control contamination. In these experiments, salinity was raised to approximately 5 g/L. However, a freshwater algal strain such as *S. obliquus* is sensitive to high salinity. Evidence has shown that 0.05 M (1.42 g/L) sodium chloride can cause significant decrease in growth rate (Kaewkannetra et al., 2012). Under our salinity conditions, the original HABG model over-predicts growth.

Because nutrients are one of the major costs in microalgal biomass production (Rogers et al., 2014), the RAFT project researchers reduced the nutrient inputs in an attempt to reduce cost and environmental impact. For instance, total nitrogen concentration in BG-11 medium is approximately 250 mg/L, whereas in RAFT experimental media (Pecos 07 and Pecos 09), nitrogen concentration was reduced to 25-50 mg/L. Although lowering nutrient concentration helps to avoid unnecessary fertilizer application, it also leads to possible nutrient stress. Moreover, the application of fertilizer was not consistent throughout the research. For example, there were four culture batch runs in experiment RAFT07, and a different amount of fertilizer was added to each run (Figure 2.6). Nutrient status varied from one run to another. These many runs with reduced nutrients provided an opportunity to model the effect of nutrient stress on algal growth. In this study, more attention was paid to nitrogen stress because experiments have shown that nitrogen is one of the major nutrient requirements for algal growth and has a strong impact on biomass productivity (Converti et al., 2009; Hsieh and Wu, 2009; Wijffels and Barbosa, 2010).

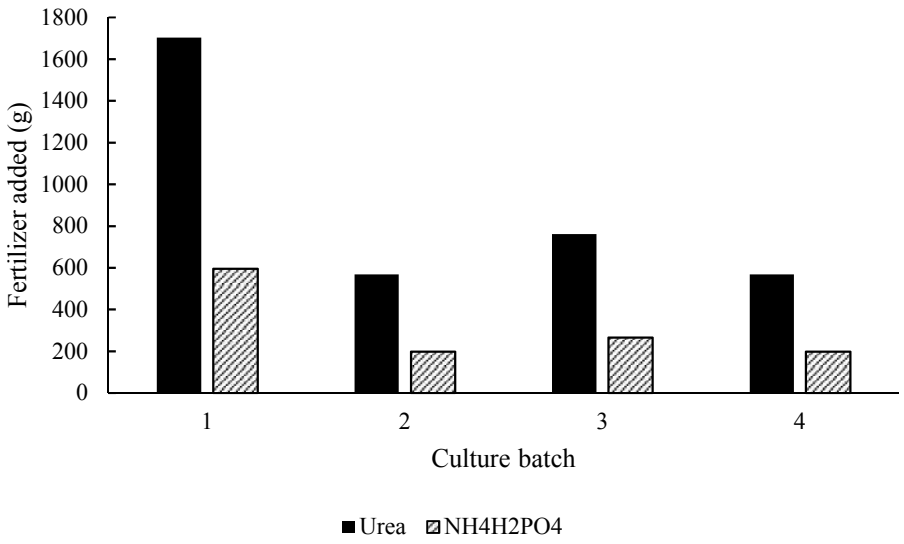

Figure 2.6 Fertilizer added in each culture phase (RAFT07, ARID raceway)

In outdoor cultivation activities, light received by algal cells is usually less than sensor-detected light intensity. Depending on solar angle and raceway geometry, part of solar radiation is reflected at the water surface, and part of solar radiation is blocked by shade generated by reactors walls or channel dividers (Figure 2.7). Since light is one of the most influential inputs of this model, and algal growth is sensitive to light intensity (Difusa et al., 2015; Sorokin and Krauss, 1958; Yoshimura et al., 2013), a small amount of light reduction may have a strong impact on growth rate. The incident light intensity must be adjusted for reflectance and shading effect in order to develop an accurate simulation of algae growth.

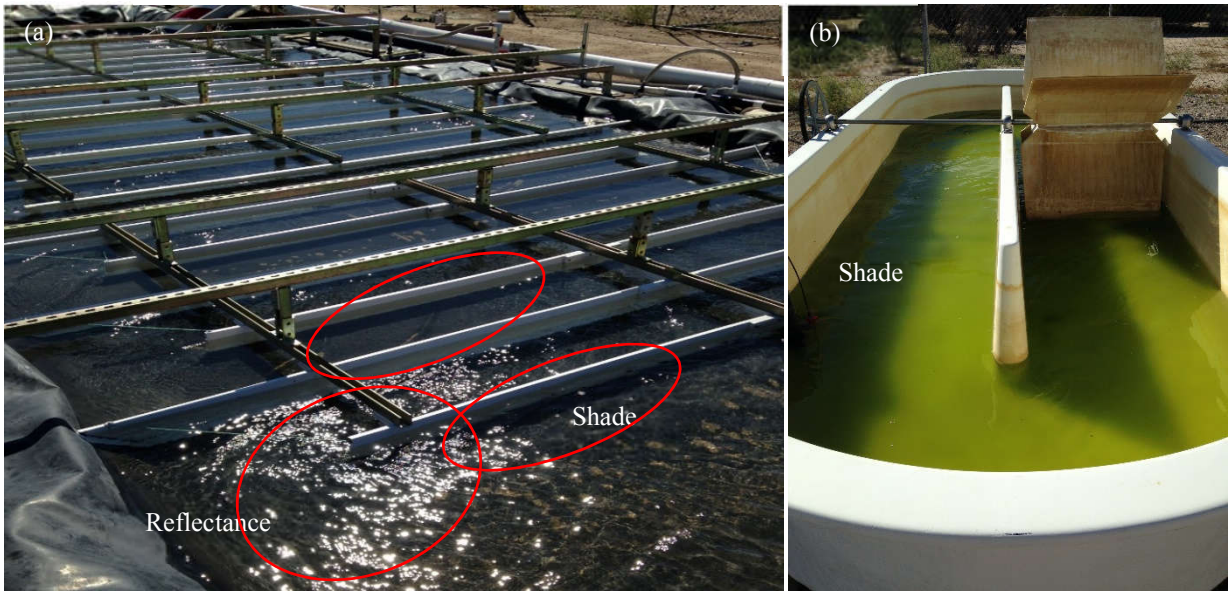

Figure 2.7 Reflectance and shade in ARID raceway (a) and paddlewheel raceway (b)

The work on incorporation of the effects of salinity stress, nitrogen stress and shading into the HABG model is described in Appendix A. The work on estimating shading effect in paddlewheel reactor cultures is under corporation with George Khawam, and is not presented in this dissertation.

Chapter 3 Nutrients and microalgae growth

1. Introduction

This chapter includes two nutrient studies, nutrient biomass yields and nitrogen kinetics and detection. Background information for these two studies were provided in this section.

1.1 Nitrogen and phosphorus biomass yields

One of RAFT research objectives is to control cost of microalgal biomass production, including fertilizer usage. For this purpose, nutrient recipes used in the RAFT project were modified and consisted of less nitrogen and phosphorus than BG-11 (Rippka et al., 1979), a widely used culture medium in microalgae cultivation. Table 3.1 shows the composition of PECOS07 and PECOS09, which were used in most of the outdoor raceway experiments at the University of Arizona Campus Agriculture Center. Other nutrient recipes used can be found in Appendix B.

Table 3.1 PECOS07 and PECOS09 culture media composition*

Chemicals	PECOS07	PECOS09
Urea	0.1	0.05
NaNO3		
NH4H2PO4	0.035	0.01
KH2PO4		
Potash K2O + SO4	0.175	0.175
Potash KCl		
MgSO4*7H2O	0.012	0.012

NaCl	0	0
Citraplex 20% Iron	0.005423	0.005423
H_3BO_3	0.00286	0.00286
$MnCl_2•4H_2O$	0.00181	0.00181
$ZnSO_4•7H_2O$	0.000137	0.000137
$Na_2MoO_4•2H_2O$	0.00039	0.00039
$CuSO_4•5H_2O$	0.000079	0.000079
$Co(NO_3)_2•6H_2O$	0.000055	0.000055
$NiCl_2•6H_2O$	0.0001	0.0001

*Unit in g L^{-1}

The Stumm empirical formula for microalgae cells is $C_{103}H_{263}O_{110}N_{16}P$ (Cai et al., 2013). Biomass yields of nitrogen and phosphorus are approximately 10 g/g-N and 78 g/g-P, respectively. However, as shown in Figure 1.3, the nitrogen and phosphorus yields of *S. obliquus* can vary greatly. In the RAFT project, producing 1g biomass of *S. obliquus* required 1.65 – 39.5 g-N and 13.5 – 359 g-P. Similarly, nitrogen and phosphorus yields of *C. sorokiniana*, another microalgal strain used in the RAFT project, also had large variation (Figure 3.1). Many life cycle assessment analyses estimate fertilizer usage based on empirical formulas, which may introduce inaccurate results (Collet et al., 2011; Lardon et al., 2009). Modification of the nutrient recipe improved nutrient yields in some of the RAFT experiments. The large variation and inconsistency in nutrient yields indicated that there is a large space for improving fertilizer application in microalgae cultivation.

In order to gain a better understanding of fertilizer application in microalgal cultivation, a nutrient yield study was carried out in bench scale flasks. The yield results were then tested in a photobioreactor experiment under laboratory conditions and two outdoor paddlewheel reactors experiments using *S. obliquus*. The work is summarized in a manuscript and is shown in *Appendix C: Nitrogen and phosphorus yields in Scenedesmus obliquus cultivation.*

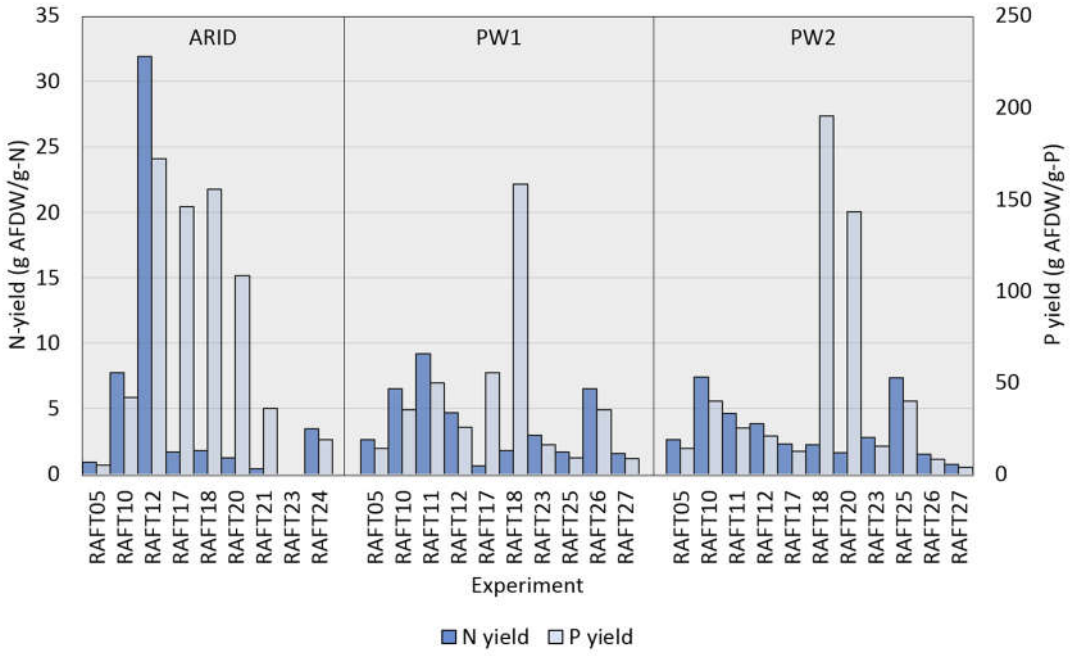

Figure 3.1 Nitrogen (N) yield and phosphorus (P) yield of *Chlorella sorokiniana* experiments in RAFT testbed projects: ARID raceway (ARID), Paddlewheel reactor 1 (PW1) and Paddlewheel reactor 2 (PW2)

1.2 Nitrogen kinetics and nitrogen stress detection

This work has two major contributions to this research, it provided growth kinetics which was incorporated into the growth model and improved the model accuracy, and nitrogen stress detection method which is easy to perform in algae cultivation.

1.2.1 Nitrogen kinetics

In the initial nutrient yield experiments, as nitrogen was depleted from the culture medium, microalgal growth rate decreased. The relationship between growth rate and culture nitrogen status tended to follow the cell quota model, but because of light attenuation in the culture, the correlation was skewed. For better quantification of the nitrogen stress effect on growth rate, another experiment was conducted within a flat panel photobioreactor by comparing cellular nitrogen and growth rate during the light period. Growth rates at different nitrogen stress levels were measured from batches with same starting biomass concentration so that the light attenuation difference between batches was eliminated. The nitrogen kinetic model was transformed by introducing the concept of nitrogen availability, which is the total nitrogen added to the culture divided by the algal biomass in the culture. This part of the work was incorporated into the growth model presented in Chapter 2.

1.2.2 Nitrogen stress detection

In addition to determining microalgae nitrogen growth kinetics, a quick method of using optical density to measure culture nitrogen status was proposed. The method takes advantage of the high sensitivity of chlorophyll content to nitrogen stress and the light absorption characteristics of chlorophyll, and is easy to apply either with external sensors or automatically with in-line sensors.

This work is summarized a manuscript and is presented in Appendix D: *Nitrogen stress and health indicator in microalgae cultures*.

Chapter 4 Conclusions and Future Work

1. Conclusions

In this dissertation, two problems were addressed, over-prediction in growth prediction with the HABG model and optimization of nutrient application in algae cultivation. Solutions to both problems were determined based on laboratory experiments and verified with outdoor large-scale raceway experiments.

Several growth limiting factors in outdoor raceway experiments were identified, and their effects on algae growth rate were quantified in this dissertation. Results showed that incorporation of these factors into the model improved model accuracy significantly. Evaluation of the model needs to be done with inclusion of these and other factors. Otherwise, the simulation is not realistic and large error will occur.

The two major nutrients inputs, nitrogen and phosphorus, in microalgae cultivation were studied in this dissertation. The yield experiments provide the minimum nutrient demand for culturing algae. An optimal ratio was obtained maximize both nitrogen and phosphorus yields. Furthermore, an optical based nitrogen stress index can be used for quick detection of the culture nitrogen status. By knowing the demand of nutrient, and the timing of adding nutrients, excessive fertilizer application can be avoided.

2. Future work

Although incorporation of salinity stress, nitrogen limitation and shading effect into the model improved model accuracy significantly, it did not fully solve the over-prediction problem. There are a few stress factors that may limit microalgae growth but not included in the model yet. For instance, one of the major challenges of growing algae in an open system is contamination which

also existed in the RAFT project. Sudden environmental condition change such as inoculation, harvest and water replenishment often result in lagged growth. Future work on model assumption verification, contamination stress identification and lag phase estimation will further improve the prediction power of the HABG model.

The difficulty in optimizing nutrient application in algae cultivation is caused by the complex relationship among growth rate, production cost and biomass composition such as lipid content and fatty acid composition. Although this dissertation has presented how they respond to nitrogen status, to better apply the knowledge in practice requires further quantitative studies. In fact, modeling the biomass composition can be part of the growth model, which will be able to predict not only the biomass productivity, but also the lipid productivity, as well as making decision on nutrient addition for production cost control.

Complete Dissertation References

Ahlgren, G., 1987. Temperature functions in biology and their application to algal growth constants. Oikos1 49, 177–190.

Aslan, S., Kapdan, I.K., 2006. Batch kinetics of nitrogen and phosphorus removal from synthetic wastewater by algae. Ecol. Eng. 28, 64–70. doi:10.1016/j.ecoleng.2006.04.003

Ayala-Parra, P., Liu, Y., Field, J.A., Sierra-Alvarez, R., 2017. Nutrient recovery and biogas generation from the anaerobic digestion of waste biomass from algal biofuel production. Renew. Energy 108, 410–416. doi:10.1016/j.renene.2017.02.085

Baker, R.T.M., 2001. Canthaxanthin in aquafeed applications: Is there any risk? Trends Food Sci. Technol. 12, 240–243. doi:10.1016/S0924-2244(01)00091-7

Béchet, Q., Muñoz, R., Shilton, A., Guieysse, B., 2013. Outdoor cultivation of temperature-tolerant *Chlorella sorokiniana* in a column photobioreactor under low power-input. Biotechnol. Bioeng. 110, 118–126. doi:10.1002/bit.24603

Becker, E.W., 2007. Micro-algae as a source of protein. Biotechnol. Adv. 25, 207–10. doi:10.1016/j.biotechadv.2006.11.002

Bernard, O., Rémond, B., 2012. Validation of a simple model accounting for light and temperature effect on microalgal growth. Bioresour. Technol. 123, 520–527. doi:10.1016/j.biortech.2012.07.022

Borowitzka, M.A., 2013. High-value products from microalgae-their development and commercialisation. J. Appl. Phycol. 25, 743–756. doi:10.1007/s10811-013-9983-9

Bosma, R., Miazek, K., Willemsen, S.M., Vermuë, M.H., Wijffels, R.H., 2008. Growth

inhibition of *Monodus subterraneus* by free fatty acids. Biotechnol. Bioeng. 101, 1108–14. doi:10.1002/bit.21963

BP Global, 2009. Sustainability review 2009.

Brennan, L., Owende, P., 2010. Biofuels from microalgae—A review of technologies for production, processing, and extractions of biofuels and co-products. Renew. Sustain. Energy Rev. 14, 557–577. doi:10.1016/j.rser.2009.10.009

Butterwick, C., Heaney, S.I., Talling, J.F., 2005. Diversity in the influence of temperature on the growth rates of freshwater algae , and its ecological relevance. Freshw. Biol. 50, 291–300. doi:10.1111/j.1365-2427.2004.01317.x

Cai, T., Park, S.Y., Li, Y., 2013. Nutrient recovery from wastewater streams by microalgae: Status and prospects. Renew. Sustain. Energy Rev. 19, 360–369. doi:10.1016/j.rser.2012.11.030

Carvalho, A.P., Malcata, F.X., 2003. Kinetic Modeling of the Autotrophic Growth of *Pavlova lutheri* : Study of the Combined Influence of Light and Temperature. Biotechnol. prog. 19, 1128–1135.

Chisti, Y., 2007. Biodiesel from microalgae. Biotechnol. Adv. 25, 294–306. doi:10.1016/j.biotechadv.2007.02.001

Clarens, A.F., Resurreccion, E.P., White, M. a, Colosi, L.M., 2010. Environmental life cycle comparison of algae to other bioenergy feedstocks. Environ. Sci. Technol. 44, 1813–9. doi:10.1021/es902838n

Collet, P., Hélias Arnaud, a., Lardon, L., Ras, M., Goy, R.A., Steyer, J.P., 2011. Life-cycle assessment of microalgae culture coupled to biogas production. Bioresour. Technol. 102,

207–214. doi:10.1016/j.biortech.2010.06.154

Collins, C.D., Boylen, C.W., 1982. Physiological responses of *Anabaena variabilis* (Cyanophyceae) to instant aneous exposure to various combinations of light intensity and temperature. J. Phycol 18, 206–211.

Converti, A., Casazza, A. a., Ortiz, E.Y., Perego, P., Del Borghi, M., 2009. Effect of temperature and nitrogen concentration on the growth and lipid content of *Nannochloropsis oculata* and Chlorella vulgaris for biodiesel production. Chem. Eng. Process. 48, 1146–1151. doi:10.1016/j.cep.2009.03.006

Cordell, D., Drangert, J.O., White, S., 2009. The story of phosphorus: Global food security and food for thought. Glob. Environ. Chang. 19, 292–305. doi:10.1016/j.gloenvcha.2008.10.009

Cornet, J.F., 1992. A Structured Model for Simulation of the Cyanobacterium *Spirulina platensis* in Photobioreactors: I. Coupling Between LIght Transfer and Growth Kinetics. Biotechnol. Bioeng. 40, 817–825.

De Vries, F.W.T.P., Brunsting, A.H.M., Van Laar, H.H., 1974. Products, requirements and efficiency of biosynthesis a quantitative approach. J. Theor. Biol. 45, 339–377. doi:10.1016/0022-5193(74)90119-2

Difusa, A., Talukdar, J., Kalita, M.C., Mohanty, K., Goud, V. V., 2015. Effect of light intensity and pH condition on the growth, biomass and lipid content of microalgae *Scenedesmus* species. Biofuels 6, 37–44. doi:10.1080/17597269.2015.1045274

Droop, M.R., 1968. Vitamin B12 and marine ecology. IV. The kinetics of uptake, growth and inhibition in *Monochrysis lutheri*. J. Mar. Biol. Assoc. United Kingdom 48, 689–733.

Duarte, P., 1995. A mechanistic model of the effects of light and temperature on algal primary

productivity. Ecol. Modell. 82, 151–160.

Edmundson, S.J., Huesemann, M.H., 2015. The dark side of algae cultivation : Characterizing night biomass loss in three photosynthetic algae , *Chlorella sorokiniana* , *Nannochloropsis salina* and *Picochlorum* sp . Algal Researh 12, 470–476. doi:10.1016/j.algal.2015.10.012

Edmundson, S.J., Kruk, R., Huesemann, M.H., n.d. Winter algae crops: characterization of algal strains with cold season production potential. Environ. Exp. Bot.

Eixler, S., Karsten, U., Selig, U., 2006. Phosphorus storage in *Chlorella vulgaris* (Trebouxiophyceae, Chlorophyta) cells and its dependence on phosphate supply. Phycologia 45, 53–60. doi:10.2216/04-79.1

Elser, J., Bennett, E., 2011. Phosphorus cycle: A broken biogeochemical cycle. Nature 478, 29–31. doi:10.1038/478029a

Evers, E.G., 1990. A model for light-limited continous cultures: growth, shading, and maintenance. Biotechnol. Bioeng. 38, 254–259.

Flynn, K.J., 2002. How critical is the critical N:P ratio? J. Phycol. 38, 961–970. doi:10.1046/j.1529-8817.2002.t01-1-01235.x

Forehead, H.I., O'Kelly, C.J., 2013. Small doses, big troubles: Modeling growth dynamics of organisms affecting microalgal production cultures in closed photobioreactors. Bioresour. Technol. 129, 329–334. doi:10.1016/j.biortech.2012.11.082

Galloway, J.N., Townsend, A.R., Erisman, J.W., Bekunda, M., Cai, Z., Freney, J.R., Martinelli, L. a, Seitzinger, S.P., Sutton, M. a, 2008. Transformation of the Nitrogen Cycle: Recent Trends, Questions, and Potential Solutions. Science (80-.). 320, 889–892. doi:10.1126/science.1136674

Geider, R.J., Osborne, B.A., 1989. Respiration and microalgal growth : a review of the quantitative relationship between dark respiration and growth. New Phytol. 112, 327–341.

Global, B., 2017. BP Energy Outlook 2017 edition.

Goldman, J.C., Hole, W., 1979. Outdoor algal mass cultures - II. photosynthetic yield limitations. Water Res. 13, 119–136.

Goldman, J.C., Oswald, W.J., Jenkins, D., 1974. The kinetics of inorganic carbon limited algal growth. J. (Water Pollut. Control Fed. 46, 554–574. doi:10.2307/25038157

Grima, E.M., Acie, F.G., Chisti, Y., 1999. Photobioreactors : light regime , mass transfer , and scaleup. Biotechnology 70, 231–247.

Grobbelaar, J.U., Soeder, C.J., Stengel, E., 1990. Modeling algal productivity in large outdoor cultures and waste treatment systems. Biomass 21, 297–314. doi:10.1016/0144-4565(90)90079-Y

Grover, J.P., 1991a. Dynamics of competition among microalgae in variable environments: experimental tests of alternative models. Oikos 62, 231–243.

Grover, J.P., 1991b. Non-steady state dynamics of algal population growth: experiments with two chlorophytes. J. Phycol. 27, 70–79.

Guterman, H., Vonshak, A., Ben-Yaakov, S., 1990. A Macromodel for Outdoor Algal Mass Production. Biotechnol. Bioeng. 35, 809–819.

Hannon, M., Gimpel, J., Tran, M., Rasala, B., Mayfield, S., 2010. Biofuels from algae: challenges and potential. Biofuels 1, 763–784. doi:10.4155/bfs.10.44

Harris, G.P., Lott, J.N., 1973. Light intensity and photosynthetic rates in phytoplankton. J. Fish.

Res. Board Canada 30, 1771–1778. doi:10.1139/f73-286

Hsieh, C.H., Wu, W.T., 2009. Cultivation of microalgae for oil production with a cultivation strategy of urea limitation. Bioresour. Technol. 100, 3921–3926. doi:10.1016/j.biortech.2009.03.019

Hu, Q., Sommerfeld, M., Jarvis, E., Ghirardi, M., Posewitz, M., Seibert, M., Darzins, A., 2008. Microalgal triacylglycerols as feedstocks for biofuel production: Perspectives and advances. Plant J. 54, 621–639. doi:10.1111/j.1365-313X.2008.03492.x

Huesemann, M., Crowe, B., Waller, P., Chavis, A., Hobbs, S., Edmundson, S., Wigmosta, M., 2016. A validated model to predict microalgae growth in outdoor pond cultures subjected to fluctuating light intensities and water temperatures. Algal Res. 13, 195–206. doi:10.1016/j.algal.2015.11.008

Inderwildi, O.R., King, D.A., 2009. Quo vadis biofuels? Energy Environ. Sci. 2, 343–346. doi:10.1039/b822951c

James, S.C., Boriah, V., 2010. Modeling Algae Growth in an Open-Channel Raceway. J. Comput. Biol. 17, 895–906. doi:10.1089/cmb.2009.0078

Jeon, Y., Cho, C., Yun, Y., 2005. Measurement of microalgal photosynthetic activity depending on light intensity and quality. Biochem. Eng. J. 27, 127–131. doi:10.1016/j.bej.2005.08.017

Kaewkannetra, P., Enmak, P., Chiu, T., 2012. The effect of CO2 and salinity on the cultivation of *Scenedesmus obliquus* for biodiesel production. Biotechnol. Bioprocess Eng. 17, 591–597. doi:10.1007/s12257-011-0533-5

Kamalanathan, M., Gleadow, R., Beardall, J., 2015. Impacts of phosphorus availability on lipid production by *Chlamydomonas reinhardtii*. Algal Res. 12, 191–196.

doi:10.1016/j.algal.2015.08.021

Khozin-Goldberg, I., Didi-Cohen, S., Shayakhmetova, I., Cohen, Z., 2002. Biosynthesis of Eicosapentaenoic Acid (Epa) in the Freshwater Eustigmatophyte *Monodus Subterraneus* (Eustigmatophyceae)1. J. Phycol. 38, 745–756. doi:10.1046/j.1529-8817.2002.02006.x

King, D.L., Novak, J.T., 1974. The kinetics of inorganic carbon limited algal growth. Water Pollu 46, 1812–1816. doi:10.1016/S0262-1762(99)80122-9

Koller, M., Muhr, A., Braunegg, G., 2014. Microalgae as versatile cellular factories for valued products. Algal Res. 6, 52–63. doi:10.1016/j.algal.2014.09.002

Lardon, L., Helias, A., Sialve, B., Steyer, J.-P., Bernard, O., 2009. Life-cycle assessment of biodiesel production from microalgae. Environ. Sci. Technol. 43, 6475–6481.

Lee, H.Y., Erickson, L.E., Yang, S.S., 1987. Kinetics and Bioenergetics of Light-Limited Photoautotrophic Growth of *Spirulina platensis*. Biotechnol. Bioeng. 29, 832–843.

Lemesle, V., Mailleret, L., 2008. A mechanistic investigation of the algae growth "Droop" model. Acta Biotheor. 56, 87–102. doi:10.1007/s10441-008-9031-3

Li, X., Hu, H., Gan, K., Sun, Y., 2010. Effects of different nitrogen and phosphorus concentrations on the growth, nutrient uptake, and lipid accumulation of a freshwater microalga *Scenedesmus* sp. Bioresour. Technol. 101, 5494–5500. doi:10.1016/j.biortech.2010.02.016

Li, Y., Han, F., Xu, H., Mu, J., Chen, D., Feng, B., Zeng, H., 2014. Potential lipid accumulation and growth characteristic of the green alga *Chlorella* with combination cultivation mode of nitrogen (N) and phosphorus (P). Bioresour. Technol. 174, 24–32. doi:10.1016/j.biortech.2014.09.142

Li, Y., Horsman, M., Wang, B., Wu, N., Lan, C.Q., 2008. Effects of nitrogen sources on cell growth and lipid accumulation of green alga *Neochloris oleoabundans*. Appl. Microbiol. Biotechnol. 81, 629–36. doi:10.1007/s00253-008-1681-1

Lincoln, E.P., Hall, T.W., Koopman, B., 1983. Zooplankton control in mass algal cultures. Aquaculture 32, 331–337. doi:10.1016/0044-8486(83)90230-2

Liu, Z., Wang, G., Zhou, B.-C., 2008. Effect of iron on growth and lipid accumulation in *Chlorella vulgaris*. Bioresour. Technol. 99, 4717–4722. doi:10.1016/j.biortech.2007.09.073

Markou, G., Nerantzis, E., 2013. Microalgae for high-value compounds and biofuels production: A review with focus on cultivation under stress conditions. Biotechnol. Adv. doi:10.1016/j.biotechadv.2013.07.011

Marra, J., 1978. Effect of short-term variations in light intensity on photosynthesis of a marine phytoplankter: A laboratory simulation study. Mar. Biol. 46, 191–202. doi:10.1007/BF00390680

Martínez-Fernández, E., Southgate, P.C., 2007. Use of tropical microalgae as food for larvae of the black-lip pearl oyster *Pinctada margaritifera*. Aquaculture 263, 220–226. doi:10.1016/j.aquaculture.2006.09.040

Mata, T.M., Martins, A. a., Caetano, N.S., 2010. Microalgae for biodiesel production and other applications: A review. Renew. Sustain. Energy Rev. 14, 217–232. doi:10.1016/j.rser.2009.07.020

Menger-Krug, E., Niederste-Hollenberg, J., Hillenbrand, T., Hiessl, H., 2012. Integration of microalgae systems at municipal wastewater treatment plants: Implications for energy and emission balances. Environ. Sci. Technol. 46, 11505–11514. doi:10.1021/es301967y

Milledge, J.J., 2010. Commercial application of microalgae other than as biofuels: a brief review. Rev. Environ. Sci. Bio/Technology 10, 31–41. doi:10.1007/s11157-010-9214-7

Monod, J., 1949. The growth of bacterial cultures. Annu. Rev. Microbiol. 3, 371–394.

Moreno-Garrido, I., Cañavate, J.P., 2000. Assessing chemical compounds for controlling predator ciliates in outdoor mass cultures of the green algae *Dunaliella salina*. Aquac. Eng. 24, 107–114. doi:10.1016/S0144-8609(00)00067-4

Naguib, Y.M.A., 2000. Antioxidant activities of astaxanthin and related carotenoids. J. Agric. Food Chem. 48, 1150–1154. doi:10.1021/jf991106k

Naik, S.N., Goud, V. V., Rout, P.K., Dalai, A.K., 2010. Production of first and second generation biofuels: A comprehensive review. Renew. Sustain. Energy Rev. 14, 578–597. doi:10.1016/j.rser.2009.10.003

Nigam, P.S., Singh, A., 2011. Production of liquid biofuels from renewable resources. Prog. Energy Combust. Sci. 37, 52–68. doi:10.1016/j.pecs.2010.01.003

Novak, J.T., Brune, D.E., 1985. Inorganic carbon limited growth kinetics of some freshwater algae. Water Res. 19, 215–225. doi:10.1016/0043-1354(85)90203-9

Packer, A., Li, Y., Andersen, T., Hu, Q., Kuang, Y., Sommerfeld, M., 2011. Growth and neutral lipid synthesis in green microalgae: a mathematical model. Bioresour. Technol. 102, 111–7. doi:10.1016/j.biortech.2010.06.029

Panwar, N.L., Kaushik, S.C., Kothari, S., 2011. Role of renewable energy sources in environmental protection: A review. Renew. Sustain. Energy Rev. 15, 1513–1524. doi:10.1016/j.rser.2010.11.037

Patil, V., Tran, K.Q., Giselrød, H.R., 2008. Towards sustainable production of biofuels from

microalgae. Int. J. Mol. Sci. 9, 1188–1195. doi:10.3390/ijms9071188

Pérez-López, P., González-García, S., Jeffryes, C., Agathos, S.N., McHugh, E., Walsh, D., Murray, P., Moane, S., Feijoo, G., Moreira, M.T., 2014. Life cycle assessment of the production of the red antioxidant carotenoid astaxanthin by microalgae: From lab to pilot scale. J. Clean. Prod. 64, 332–344. doi:10.1016/j.jclepro.2013.07.011

Pulz, O., Gross, W., 2004. Valuable products from biotechnology of microalgae. Appl. Microbiol. Biotechnol. 65, 635–48. doi:10.1007/s00253-004-1647-x

Quinn, J., de Winter, L., Bradley, T., 2011. Microalgae bulk growth model with application to industrial scale systems. Bioresour. Technol. 102, 5083–92. doi:10.1016/j.biortech.2011.01.019

Ranga Rao, a, Ravishankar, G. a, Sarada, R., 2012. Cultivation of green alga *Botryococcus braunii* in raceway, circular ponds under outdoor conditions and its growth, hydrocarbon production. Bioresour. Technol. 123, 528–33. doi:10.1016/j.biortech.2012.07.009

Rhee, G.-Y., 1972. Competition between an alga and an aquatic bactrium for phosphate. Limnol. Ocean. 17, 505–514.

Rippka, R., Deruelles, J., Waterbury, J.B., Herdman, M., Stanier, R.Y., 1979. Generic assignments, strain histories and properties of pure cultures of cyanobacteria. J. Gen. Microbiol. 111, 1–61. doi:10.1099/00221287-111-1-1

Roessler, P.G., 1990. Environmental Control of Glycerolipid Metabolism in Microalgae: Commercial Implications and Future Research Directions. J. Phycol. doi:10.1111/j.0022-3646.1990.00393.x

Rogers, J.N., Rosenberg, J.N., Guzman, B.J., Oh, V.H., Elena, L., Ghassemi, A., Betenbaugh,

M.J., Oyler, G.A., Donohue, M.D., 2014. A critical analysis of paddlewheel-driven raceway ponds for algal biofuel production at commercial scales. Algal Res. 4, 76–88. doi:10.1016/j.algal.2013.11.007

Slade, R., Bauen, A., 2013. Micro-algae cultivation for biofuels: Cost, energy balance, environmental impacts and future prospects. Biomass and Bioenergy 53, 29–38. doi:10.1016/j.biombioe.2012.12.019

Sommer, U., 1991. A comparison of the Droop and the Monod models of nutrient limited growth applied to natural populations of phytoplankton. Funct. Ecol. 5, 535–544.

Sorokin, C., Krauss, R.W., 1958. The effects of light intensity on the growth rates of green algae. Plant Physiol. 33, 109–13. doi:10.2307/4259285

Spolaore, P., Joannis-Cassan, C., Duran, E., Isambert, A., 2006. Commercial applications of microalgae. J. Biosci. Bioeng. 101, 87–96. doi:10.1263/jbb.101.87

Suh, I.S., Lee, S.B., 2003. A light distribution model for an internally radiating photobioreactor. Biotechnol. Bioeng. 82, 180–189. doi:10.1002/bit.10558

Tam, N.F.Y., Wong, Y.S., 1989. Wastewater nutrient removal by *Chlorella pyrenoidosa* and *Scenedesmus* sp. Environ. Pollut. 58, 19–34. doi:10.1016/0269-7491(89)90234-0

Tantanasarit, C., Englande, A.J., Babel, S., 2013. Nitrogen, phosphorus and silicon uptake kinetics by marine diatom *Chaetoceros calcitrans* under high nutrient concentrations. J. Exp. Mar. Bio. Ecol. 446, 67–75. doi:10.1016/j.jembe.2013.05.004

Teles, I., Cabanelas, D., Ruiz, J., Arbib, Z., Alexandre, F., Garrido-pérez, C., Rogalla, F., Andrade, I., Perales, J.A., 2013. Comparing the use of different domestic wastewaters for coupling microalgal production and nutrient removal. Bioresour. Technol. 131, 429–436.

doi:10.1016/j.biortech.2012.12.152

Thompson, G.A., 1996. Lipids and membrane function in green algae. Biochim. Biophys. Acta 1302, 17–45. doi:10.1016/0005-2760(96)00045-8

Tingem, M., Rivington, M., 2009. Adaptation for crop agriculture to climate change in Cameroon: Turning on the heat. Mitig. Adapt. Strateg. Glob. Chang. 14, 153–168. doi:10.1007/s11027-008-9156-3

Tischner, R., Lorenzen, H., 1979. Nitrate uptake and nitrate reduction in synchronous *Chlorella*. Planta 146, 287–292. doi:10.1007/BF00387800

Torzillo, G., Sacchi, a., Materassi, R., Richmond, a., 1991. Effect of temperature on yield and night biomass loss in *Spirulina platensis* grown outdoors in tubular photobioreactors. J. Appl. Phycol. 3, 103–109. doi:10.1007/BF00003691

Turpin, D.H., 1991. Effects of Inorganic N Availability on Algal Photosynthesis and Carbon Metabolism. J. Phycol. doi:10.1111/j.0022-3646.1991.00014.x

United Nations, 2008. Biofuel production technologies: status, prospects and implications for trade and development, United Nations Conference on Trade and Development.

Unkefer, C.J., Sayre, R.T., Magnuson, J.K., Anderson, D.B., Baxter, I., Blaby, I.K., Brown, J.K., Carleton, M., Cattolico, R.A., Dale, T., Devarenne, T.P., Downes, C.M., Dutcher, S.K., Fox, D.T., Goodenough, U., Jaworski, J., Holladay, J.E., Kramer, D.M., Koppisch, A.T., Lipton, M.S., Marrone, B.L., McCormick, M., Molnár, I., Mott, J.B., Ogden, K.L., Panisko, E.A., Pellegrini, M., Polle, J., Richardson, J.W., Sabarsky, M., Starkenburg, S.R., Stormo, G.D., Teshima, M., Twary, S.N., Unkefer, P.J., Yuan, J.S., Olivares, J.A., 2017. Review of the algal biology program within the National Alliance for Advanced Biofuels and

Bioproducts. Algal Res. 22, 187–215. doi:10.1016/j.algal.2016.06.002

Wijffels, R.H., Barbosa, M.J., 2010. An outlook on microalgal biofuels. Science 329, 796–799. doi:10.1126/science.1189003

Yamaguchi, K., 1997. Recent advances in microalgal bioscience in Japan, with special reference to utilization of biomass and metabolites: a review. J. Appl. Phycol. 8, 487–502. doi:10.1007/BF02186327

Yoshimura, T., Okada, S., Honda, M., 2013. Culture of the hydrocarbon producing microalga Botryococcus braunii strain Showa: Optimal CO2, salinity, temperature, and irradiance conditions. Bioresour. Technol. 133, 232–239. doi:10.1016/j.biortech.2013.01.095

Appendix A Incorporation of the effects of salinity, nitrogen stress, and shading into an algae growth model and evaluation in the ARID raceway

Song Gao[a], Peter Waller[a], George Khawan[a], Said Attalah[a], Michael Huesemann[b], Kimberly Ogden[c]

[a] Department of Agricultural and Biosystems Engineering, The University of Arizona, Tucson, AZ 85721, USA

[b] Pacific Northwest National Laboratory,Marine Sciences Laboratory, Sequim,WA 98382, USA

[c] Department of Chemical Engineering, The University of Arizona, Tucson, AZ 85721, USA

Journal: Algal Research (under review)

Abstract

The Huesemann Algae Biomass Growth (HABG) model predicts microalgae biomass growth in outdoor raceways as a function of water temperature and incident light intensity. The model over-predicted growth in several Regional Algal Feedstock Testbed (RAFT) experiments. Inspection of the culture conditions suggested that salinity stress, nutrient limitation, and shading reduced growth, which were not included in the original model. Laboratory experiments were carried out to measure growth response of *S. obliquus* to high salinity and limited nitrogen. In addition, the shading effect was estimated based on raceway geometry, solar angle, albedo and measured light intensity data. In this study, the improvement of model performance is presented step by step as each growth limiting factor is incorporated into the model. The new salinity, shading, and nitrogen stress factors remove most of the over-prediction of the original model. Comparison of the model

with observed data indicated that ignoring the lag phase also resulted in overprediction. Delaying the start of the simulation until the end of the lag phase and inclusion of stress factors lowered model inaccuracy from 90% over-prediction to within ±10% in six out of seven batches.

Key Words: Huesemann algae biomass growth model, ARID raceway, salinity, nitrogen, shading

1. Introduction

Many algae growth models have input parameters such as light, temperature, and nutrient concentration (Bannister, 1979; Cornet and Dussap, 2009; Quinn et al., 2011; Yuan et al., 2014). Some models are designed to incorporate reduced growth rates under conditions such as low nitrogen concentration or limiting light intensity (Goldman and Hole, 1979; James and Boriah, 2010; Packer et al., 2011). The Huesemann Algae Biomass Growth (HABG) model requires light and temperature as input variables (Huesemann et al., 2016). Growth rate coefficients were measured over a range of light intensities and temperature in the laboratory experiments. The model was thus able to predict the biomass productivity under conditions of daily fluctuating water temperature and incident light intensity in outdoor algae raceways (Huesemann et al. 2016). Because the model assumes that all conditions other than temperature and light are optimal, it must be adjusted in cases when other parameters are not optimal.

Some high salinity adapted algal strains such as *Dunaliella* can be maintained as monoculture in open raceway ponds with high salinity (Rao et al., 2012). In the U.S. Department of Energy RAFT (Regional Algal Feedstock Testbed) project, increasing culture salinity has been proposed as a method to control contamination by organisms that have low tolerance for salinity, and was tested in several experiments. However, high salinity inhibits the growth of many algal species, particularly freshwater algal strains (Mohammed and Shafea, 1992; Rao et al., 2007).

Kaewkannetra et al. (2012) found that salinity of 0.05M (1.42 g/L) sodium chloride stressed *S. obliquus* and caused a significant decrease in growth rate., Simulation of these experiments with the growth model without considering salinity effect will result in large error.

Nitrogen is one of the major algae nutrient requirements, and nitrogen status in the culture has a strong impact on biomass productivity (Converti et al., 2009; Hsieh and Wu, 2009; Wijffels and Barbosa, 2010). It is also one of the major costs in microalgal biomass production (Rogers et al., 2014). In RAFT project, researchers also attempted to reduce nitrogen fertilization rate in order to reduce cost and environmental impact, but in the process caused intermittent nitrogen stress in the culture. Thus, to realistically simulate algal growth in these experiments, it was necessary to quantify the effect of nitrogen stress on algal growth.

Algal growth rate is highly sensitive to light intensity (Difusa et al., 2015; Sorokin and Krauss, 1958; Yoshimura et al., 2013). Although not commonly an issue in large outdoor raceways, many experimental raceways have significantly reduced light intensity due to shading from walls. The HABG model assumes unshaded conditions and was originally validated with indoor and outdoor pond data where shading was minimal. The model must be adjusted for shading in order to obtain accurate prediction of algae growth in shaded experimental raceways.

The goal of the current research was to introduce stress effects such as salinity, nitrogen limitation, and shading to the HABG model and to simulate *S. obliquus* growth rate in outdoor raceway experiments with measured water temperature and light intensity data in the ARID (Algae Raceway Integrate Design) raceway (Waller et al., 2012). The simulations were evaluated against experimental data to evaluate the consecutive modifications to HABG model.

2. Materials and Methods

2.1 Outdoor culture system

The ARID open pond raceway is located at Campbell Avenue Agriculture Center, the University of Arizona, Tucson, AZ (32° 16' 49" N / 110° 56' 45" W). This version of the ARID raceway used in this study is 16 m in length and 5 m in width, consisting of 22 shallow channels and one deep canal (Figure A1). Channels were separated by plastic baffles. The baffles are 15 cm in height and the channels are 45 cm in width. The canal shape is a 1.5 m deep inverted rectangular frustum. The top area is 5 m by 3.6 m rectangle, and the bottom area is 2 m by 0.6 m rectangle. The side slope is 45°.

During daytime, water flowed through a labyrinth of east-west channels by gravity from north to south. Culture was circulated from the last lower channel and the canal to the upper channel using pumps driven by solar energy. Daytime culture depth was maintained at 0.1 m in the channels and 0.3 m in the canal. The total culture volume is approximately 5800 L. During night, the culture drains entirely into the canal. Thermal insulation in the canal protects algae from adverse environmental conditions, such as low temperature. When the sun rises in the morning, the pump starts circulating the water through the raceway.

There were only two *S. obliquus* experiments conducted in ARID raceway with the above-mentioned configuration in RAFT project, RAFT06 and RAFT07. They were conducted from 7th January to 2nd March 2015 and from 16th March to 30th April 2015, respectively. In both experiments, the pH was controlled by on-demand periodic CO_2 injection and was maintained at 8.0. Electric conductivity (EC) was used to measure salinity, and a calibration curve was obtained prior to the experiment to determine the relationship between salinity and EC reading.

In this study, salinity was expressed as equivalent to g-NaCl/L. Nutrients were added to the culture multiple times in both experiments. The chemical constituents of each nutrient addition were 50 mg urea/L, 10 mg ammonium diphosphate/L, and 12 mg magnesium sulfate/L. Other micronutrients were added according to the BG-11 nutrient recipe (Rippka et al., 1979). Harvests took place in both experiments. In each harvest, approximately half of the biomass and two thirds of the culture media were removed from the raceway. After each harvest, the raceway was replenished with water to the original volume, and nutrients were added. In the model, the initial biomass concentration for simulations was reset to measured biomass concentration after harvest dilution.

Operation conditions in the two experiments differed mainly on salinity and nutrients. RAFT06 experiment started with freshwater, and the salinity remained low during the experiment, whereas RAFT07 experiment started with higher salinity (5 g-NaCl/L), and the salinity remained at higher level by adding NaCl. Nutrients were added on day of year (DOY) 7, 20, 33, 41, 44, 46, 51 and 58 in RAFT06 experiment, and on DOY77, 80, 84, 90, 92, 100, 110 and 112 in RAFT07 experiment. However, there was only one harvest in RAFT06 (DOY46) and three harvests in RAFT07 (DOY 92, 100 and 112). Although same amount of nitrogen was added in the two experiments, RAFT07 produced more biomass, thus nitrogen stress is likely to be more intense in RAFT07. Because this study was to evaluate salinity stress and nitrogen stress in algal growth modeling, we focused more on growth simulation of RAFT07 experiment.

Figure A.1 The ARID (Algae Raceway Integrated Design) raceway used in this experiment

2.2 Data collection and biomass concentration measurement

Temperature, pH and EC were recorded with a Campbell Scientific CR3000 datalogger. Readings from sensors were averaged every 5 seconds and recorded every 10 minutes. Optical density (OD) was measured manually using a spectrophotometer (Spectronic Genesys^{TM} 5, Thermo Fisher Scientific Inc. Waltham, MA, USA) at 750 nm, at 9:00 am after refilling the pond with water to the initial volume. Biomass concentration was then converted from OD to AFDW. AFDW was measured by filtering, drying at 75 ℃ overnight and ashing the sample at 550 ℃ for 4 hours. Correlation of OD and AFDW (g/L) was found to be linear, following Equation 1.

$$AFDW = 0.5023 * OD_{750} \ (R^2 = 0.98) \quad (1)$$

Solar radiation was obtained from Arizona Meteorological Network (AZMET), measured with LI-COR LI-200 silicon cell pyranometer. Solar radiation data (MJ/m^2/hr) reported by the weather station was converted to Photosynthetically Active Radiation (PAR) (μmole/m^2-s). The following equation was used for the conversion (Thimijan and Heins, 1983):

$$\left(\frac{MJ}{hr\ m^2}\right) = 581.4\ \frac{\mu mole}{s\ m^2}(PAR) \quad (2)$$

2.3 Theoretical development of stress factors

The specific growth rate of *S. obliquus* as a function of light intensity and water temperature was measured by Edmundson et al. (n.d.) (Equation 3).

$$\mu = \mu(T, I) \quad (3)$$

Where, T is water temperature (°C), I is light intensity (μmol/m^2-s)

Growth rate reduction caused by salinity stress, nitrogen stress, and shading effect were represented by three factors in the model, namely, salinity factor, nitrogen factor and shading factor. Each factor, ranging from 0 to 1, is a multiplier in the growth rate calculation equation (Equation 4). The factor is 0 if the corresponding stress is severe enough to prevent any growth, between 0 and 1 if the stress lowers the growth rate but does not completely stop growth, and 1 if the stress has insignificant effect on growth. This section describes how stress factors were determined as a function of the salinity, nitrogen, and shading status.

$$\mu = F_S F_N \mu(T, R_Z I) \quad (4)$$

Where F_S is salinity factor, F_N is nitrogen factor, R_Z is shading factor

2.3.1 Measurement of the specific growth rate as a function of salinity

The specific growth rate of *S. obliquus* as a function of salinity was determined at room temperature in shaker flask cultures containing BG-11 media amended with different concentrations of Instant OceanTM. The incident light intensity was above 400 μmol/m^2-s and the cultures were kept sufficiently thin to ensure that all cells received above saturating light intensity (>200 μmol/m^2-s) and thus were growing exponentially at their maximum specific growth rate. The cultures were sparged with CO_2-enriched air to maintain an equilibrium pH of 7.5. The specific growth rate, μ_s, at different salinities was determined from the slope of $\ln(OD_{750})$ versus time (Van Wagenen et al., 2014).

The maximum specific growth rate, $\mu_{max\text{-}s}$, is expected below the salinity threshold. Growth rate μ_s, decreases with increasing salinity up to the point that growth is zero. The growth rate fraction ($\mu_s/\mu_{max\text{-}s}$) is the salinity factor (F_s).

2.3.2 Measurement of specific growth rate as a function of nitrogen availability

In a previous study (Gao et al. n.d.), *S. obliquus* was cultured in a flat-panel photobioreactor in the laboratory at room temperature, provided with CO_2-enriched air, and an incident light intensity of 360 μmol/m^2-s with 12h light:12 h dark. Cellular nitrogen content was used as a measure of nitrogen stress intensity. The alga was first cultured in nitrogen-replete medium (BG-11), where maximum cellular nitrogen content and maximum growth rate were obtained. The alga was then cultured in semi-continuous batches using nitrogen-depleted BG-11 medium, and cellular nitrogen content decreased from batch to batch. At the beginning of light period in each batch, the culture was diluted to the same biomass concentration, approximately 0.32 g-dry mass/L, in order to normalize light attenuation effect on growth. The specific growth rate (μ_N) as

a function of cellular nitrogen content was determined from ln(dry mass concentration) versus time during the light period in each batch. The experiment continued until no growth was observed during the light period. The maximum specific growth rate ($\mu_{max\text{-}N}$) was obtained above a threshold cellular nitrogen content, and minimum cellular nitrogen content was measured when there was no growth ($\mu_N \leq 0$). The relationship between specific growth rate and cellular nitrogen content can be described by Droop equation (Equation 5; Droop, 1968). The parameters, μ'_m and k_{NA}, were determined by non-linear regression on experimental data.

$$\mu_N = \mu'_m - \left(k_q \mu'_m\right)\frac{1}{Q} \tag{5}$$

Where μ_N is specific growth rate, Q is nutrient quota, k_q is subsistence quota, μ'_m is specific growth rate at infinite Q;

Because cellular nitrogen was not tracked in the outdoor raceway experiments, to apply the laboratory-experiment based theory, we introduced the concept of nitrogen availability (N_A), the ratio of total added nitrogen in fertilizer to accumulated biomass. We assumed that the cell can consume all the available nitrogen, and cellular nitrogen can be maintained at maximum level if media nitrogen is available. With these assumptions, if media nitrogen is depleted, N_A is simply cellular nitrogen. If media nitrogen is not depleted, because cellular nitrogen is maintained at maximum level, media nitrogen has only minimal effect. Therefore, we replaced Droop's cell quota (Q), the internal available nitrogen per biomass, with nitrogen availability (N_A), the total available nitrogen per biomass (Equation 6).

$$\mu_N = \mu'_m - \left(k_q \mu'_m\right)\frac{1}{Q} = \mu'_m - \left(k_{NA} \mu'_m\right)\frac{1}{N_A} \tag{6}$$

Where N_A is nitrogen availability (g/g); μ_m' is growth rate at infinite N_A; k_{NA} is the minimum N_A at zero growth rate;

The nitrogen factor (F_N) was the fraction of growth rate at a certain N_A to the maximum growth rate observed in the laboratory experiment ($\mu_N/\mu_{max\text{-}N}$). Therefore, F_N was calculated by dividing Equation 6 with $\mu_{max\text{-}N}$ (Equation 7). In the outdoor raceway experiments, total available nitrogen was the amount of applied nitrogen fertilizer. At each harvest, we assumed that the fraction of nitrogen removal was the same as the fraction of culture volume harvested. The remaining nitrogen plus added fertilizer was the initial N_A for the next batch culture run.

$$F_N = \frac{\mu_N}{\mu_{max-N}} = \frac{\mu_m' - (k_{NA}\mu_m')\frac{1}{N_A}}{\mu_{max-N}} \quad (7)$$

2.3.3 Shading effect estimation

In outdoor cultivation systems, shading can significantly reduce the average light to the system. The ARID raceway version used in this study was a set of rectangular channels separated by baffles oriented in the East-West direction (Figure A1). Shade on the north side of the board, especially in winter when solar angle is low, reduces average light to the culture. A solar path model was incorporated into the model to calculate solar angles for calculating shading change throughout the day.

To estimate the reduced incident light due to shading, two factors were considered, the area covered by shade and light intensity in the shade. Part of the incident light is reflected at the surface (albedo) and the rest enters the water at the refracted angle. Light reflection (1 – albedo) was calculated with the Fresnel equations. Figure A2(a) shows the light beam at the edge of the shaded area. The zenith angle (θ_1) and azimuth angle (A) (from North, clockwise) were

calculated at each time step. The refractive angle (θ_2) was calculated with Snell's Law. The refractive index of algae culture was measured manually with a refractometer (RF20, Extech), and was the same as that of water. Shade width (w) from the board to the edge of the shade at depth (z) was calculated with Equations 8 and 9.

$$w_z = -(H - D)\tan(\theta_1)\cos(A) - z\cot(\theta_2)\cos(A) \quad (8)$$

$$\theta_2 = \sin^{-1}(n_1 \sin\theta_1 / n_2) \quad (9)$$

where

w_z = shade width (board to edge of shade) at depth z (m)

H = board height (m)

D = culture depth (m)

θ_1 = zenith angle

θ_2 = refractive angle

A = azimuth angle (from North, clockwise)

z = depth (m)

n_1 = refractive index of air

n_2 = refractive index of water

Light intensity in shaded regions is not zero but is a fraction of the unblocked incident light, which we call the light ratio. We measured light intensity, I_{zx}, as a function of depth z and distance x from the board using a LI-250A light meter and LI-COR LI-190R quantum sensor facing vertically up (Figure A2b). Meanwhile, light intensity at the same depth within the unshaded area was measured and denoted as I_{z0}. The light ratio at this point is expressed by Equation 10:

$r_{zx} = I_{zx} / I_{z0}$ (10)

where

I_{zx} = light intensity at point at distance x and depth z (μmol/m^2-s)

I_{z0} = light intensity in unshaded area at depth z (μmol/m^2-s)

For the entire layer at depth z, cumulative light received within the shaded area is calculated by Equation 11 and total light received within the unshaded area is calculated by Equation 12. Total light received by layer z is the sum of these two values and represented by I_z as shown by Equation 13. Due to high flow rate and mixing, we averaged sun light exposure in shaded and unshaded areas at each depth. Therefore, I_z in Equation 10 is the average light received in shaded and unshaded areas by the culture at depth z. The original HABG model doesn't include the shading effect, and calculates the total light at each depth as $I_{z0}L$.

$$I_{z-shaded} = \int_0^{w_z} I_{z0} r_{zx} d_x \quad (11)$$

$$I_{z-unshaded} = I_{z0}(L - w_z) \quad (12)$$

$$I_z = \int_0^{w_z} I_{z0} r_{zx} d_x + I_{z0}(L - w) \quad (13)$$

where

I_z = light received by layer z

I_{z0} = light intensity within unshaded area at depth z

L = channel width (m)

r_{zx} = light ratio of point at distance x, depth z

w_z = shade width at depth z (m)

$$R_Z = \frac{\int_0^{wz} I_0 r_{zx} d_x + I_{z0}(L-w)}{I_{z0} L} \quad (14)$$

Dividing Equation 13 by $I_{z0}L$ calculates the fraction of light with shading over the light without considering shading. This is shown by Equation 14 and yields the shading factor, R_z, at each depth. The product of shading factor and Beer-Lambert light intensity at each layer is the average light intensity at that layer. The geometry of the canal is slightly more complicated than the channels since the canal has sloping sides, but the decreasing area with depth was accounted for in the algorithm, and the same integration method was applied to calculate light intensity in the canal.

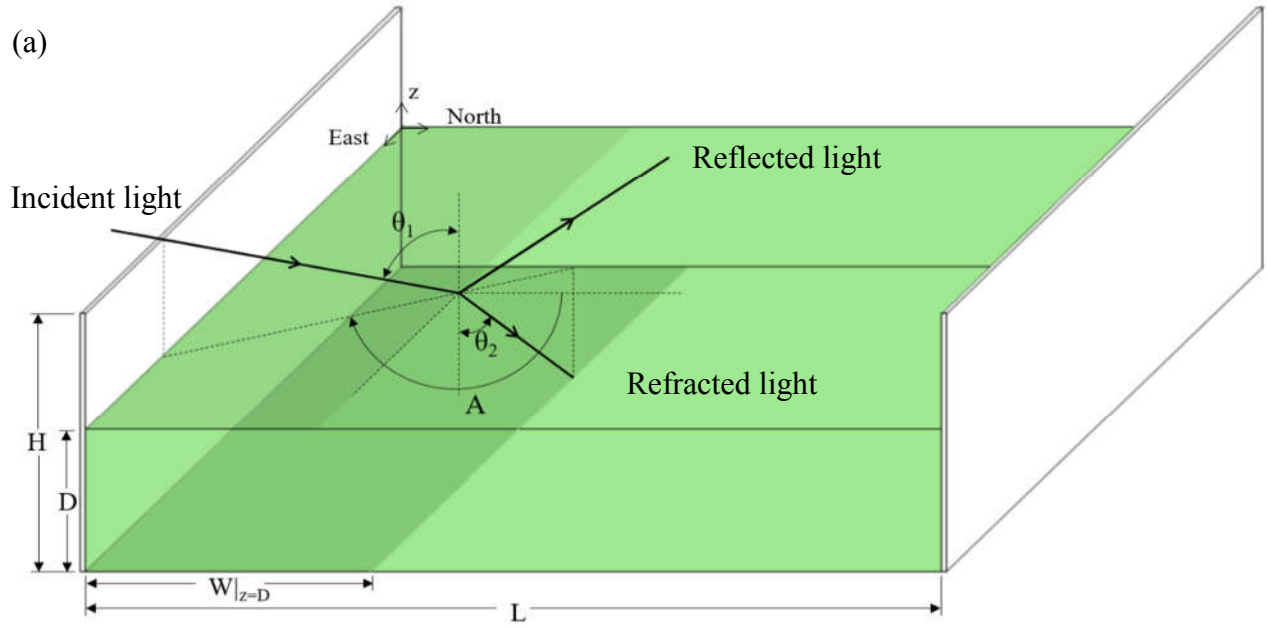

(b)

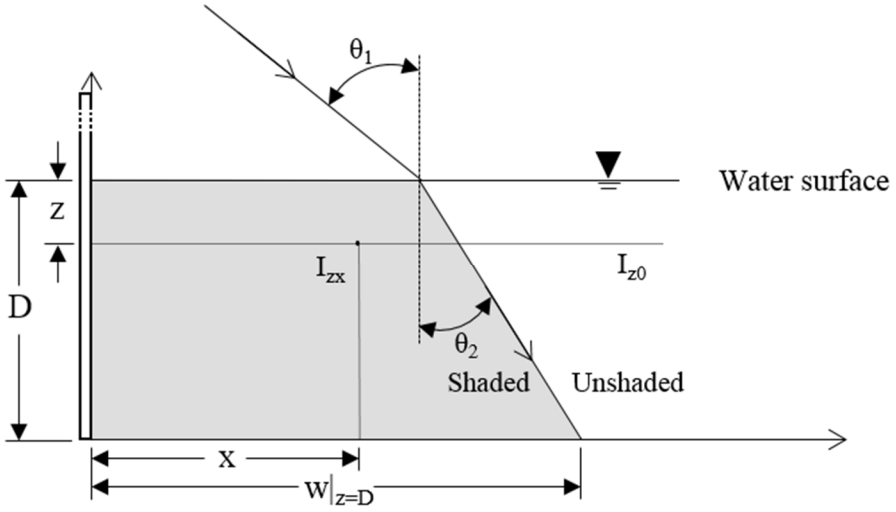

Figure A.2 (a) Dark area represents shaded area; *L* is channel width; w is shade length, *H* is board height; *D* is culture depth; θ_1 is zenith angle; θ_2 is refractive angle; *A* is azimuth angle (from north, clockwise) (b) Side view of raceway channel. I_{zx} is light intensity at depth *z* and distance x; I_{z0} is light intensity in unshaded area at depth *z*

2.4 Simulation parameters and other assumptions

The simulation time steps were set to be the same as the datalogger recording frequency (10 mins). Due to low residence time, we assumed that temperature and salinity were uniformly distributed in the raceway. Growth was calculated in 100 vertical layers in both the channel culture and canal culture. Biomass concentration was averaged at each time step by numerically combining the volumes of the channel culture and canal culture. EC can vary largely because of operations and weather such as harvest, water addition, evaporation and precipitation. In the simulation, EC was averaged daily for salinity calculation.

The effect of salinity and nitrogen on dark respiration during day and night has not been quantified in experiments. In this study, we assumed that night dark respiration rate was not affected by salinity or nitrogen stress factors. However, daytime dark respiration was adjusted by

the salinity and nitrogen factors because it was part of the total culture growth rate that was adjusted during the day. Further research is required for verifying this assumption.

Although the setpoint of pH in the raceway experiments was 8.0, fluctuation occurred. The average pH was approximately 7.8 throughout the experiments. The difference from the pH at which the growth coefficients in the HABG model were determined in laboratory experiments (7.5) was small, thus we assumed the growth coefficients were applicable to the raceway experiments.

2.5 Statistical analysis

Model performance can be evaluated by comparing observed growth and predicted growth. We evaluated the root mean square error (RMSE) between simulated and experimental biomass concentration. To quantify over-prediction, we used the bias factor (BF), a concept proposed by Ross (1996), modified by Baranyi et al. (Baranyi et al., 1999) and used for microbial growth model evaluation (López et al., 2004; te Giffel and Zwietering, 1999). Perfect prediction yields a BF value of 1. A BF value greater than 1 represents over-prediction, and vice-versa. The hypothesis of this study is that quantifying the effects of salinity, nitrogen stress and shading in the algae culture will improve the agreement between observed culture data and model predictions (lowered BF value).

3. Results and discussion

In this section, the successive incorporation of salinity, nitrogen and shading factors into the HABG model is discussed. The simulation results were compared to experimental data from the RAFT07 ARID experiment. Then, we compared the modified model with all factors to

experimental data collected in the RAFT06 experiment, which experienced less salinity and nitrogen stress.

3.1 Original model

In this section, the original growth model predictions were compared to observed data from RAFT 07. Four consecutive batch culture runs were separated by three harvests (Figure A3). The saw-tooth shaped curve in the simulation line was caused by biomass accumulation during daytime due to photosynthesis, and biomass loss during night due to dark respiration. The comparison of observed data and the simulation showed significant over-prediction with the original HABG model. The RMSE was 0.62, and 1.90 BF means that over-prediction averaged 90% for the four successive batch culture runs.

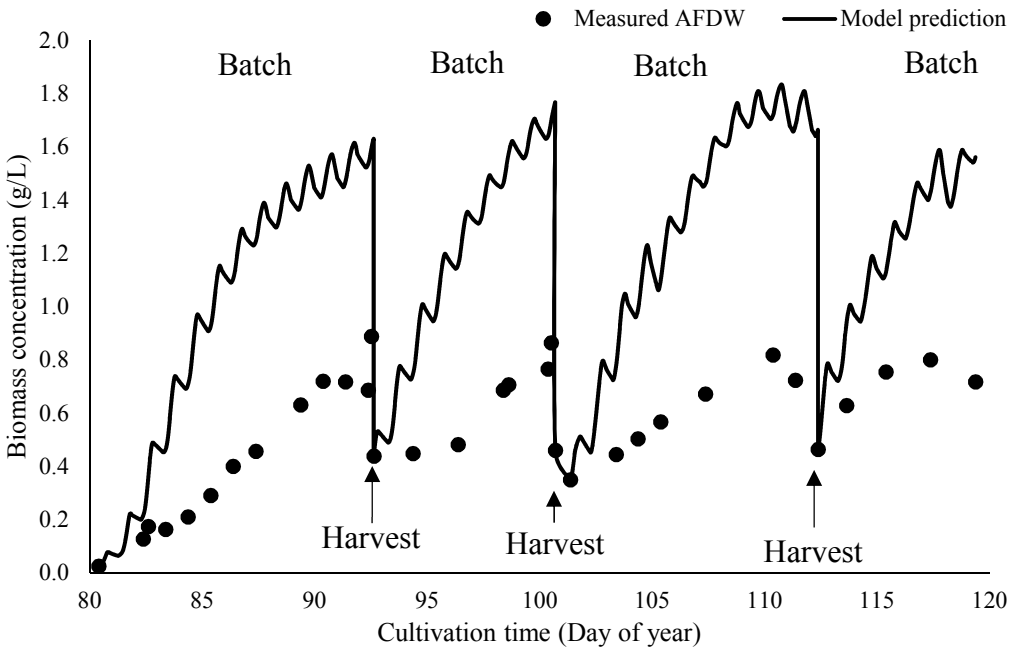

Figure A.3 Measured and predicted biomass concentration over time. Three harvests divided the experiment into 4 successive batch culture runs. The initial biomass concentration for growth simulation was set to the respective measured biomass concentration in each run. $RMSE_1 = 0.62$, $BF_1 = 1.90$

3.2 Incorporation of salinity factor

In laboratory experiments, the growth response of *S. obliquus* to salinity was quantified within the salinity range of 0 to 40 g/L (Figure A4). The curve can be divided into three sections (Equation 11). Between salinity 0 and 1 g/L, there was no growth rate reduction, thus F_S is 1. From 1 g/L to 30 g/L, the specific growth rate decreased linearily with increasing salinity. F_s was obtained by linear interpolation within this range. Salinity greater than 30 g/L prevented any growth, thus F_s is 0.

$$F_S = \begin{cases} 1 & (S \leq 1) \\ -0.035S + 1.2045 & (1 < S < 30) \\ 0 & (S \geq 30) \end{cases} \quad (15)$$

where S = salinity (g/L).

In the raceway experiment, salinity decreased from 3-4 g/L in the first two batch culture runs to 1-2 g/L in the latter ones (Figure A5). Consequently, the F_S was lower (higher salinity stress) in early culture runs than in latter ones (Figure A6). After adjustment for salinity effect, the average over-prediction was reduced from 90% to 57% (BF = 1.57).

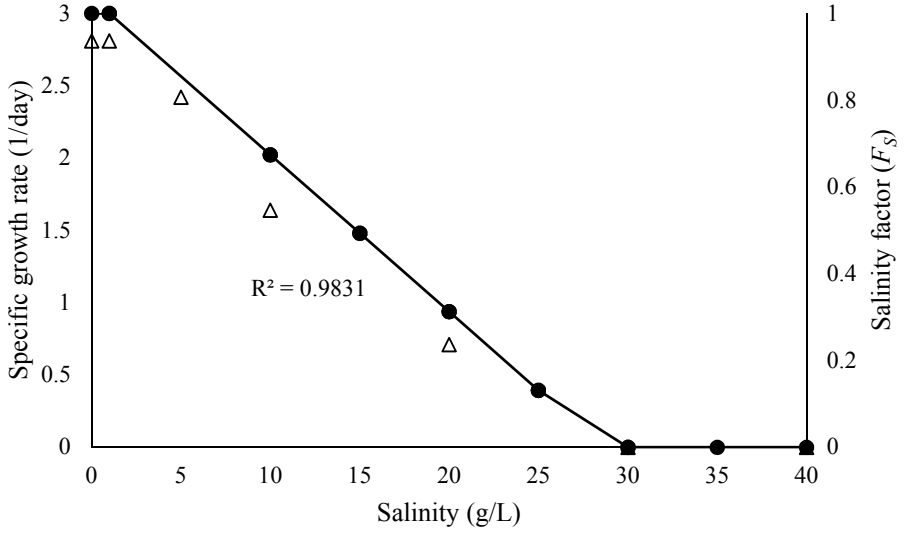

Figure A.4 Specific growth rate (△) and salinity factor (●, μ_s/μ_{max}) as a function of salinity (equivalent to g-NaCl/L) for *S. obliquus* in laboratory culture

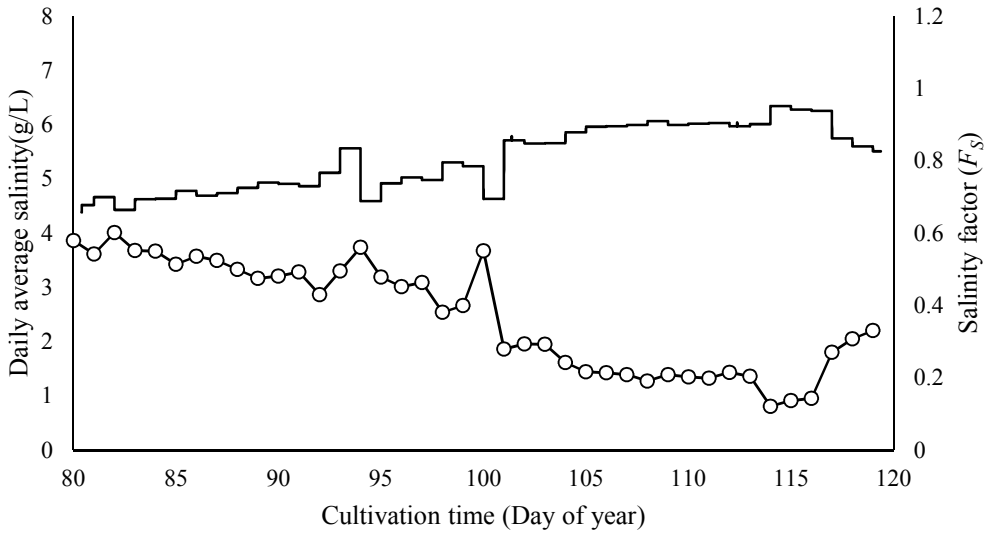

Figure A.5 Daily average salinity (○) and corresponding salinity factor F_S (—) during RAFT07 ARID raceway experiment

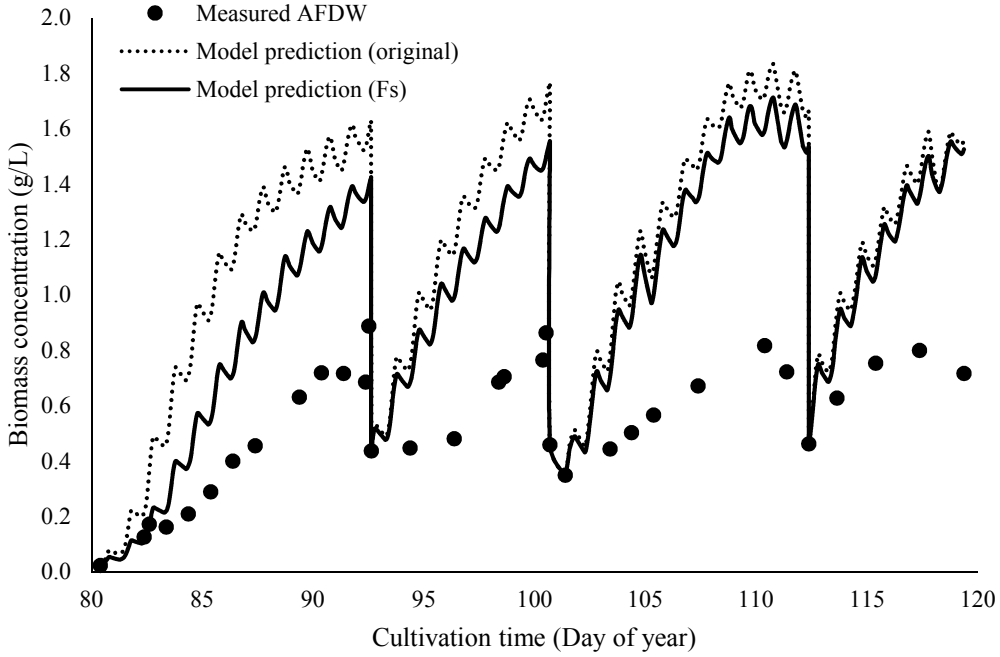

Figure A.6 Measured biomass concentration, original growth model prediction and *Fs* - adjusted model prediction ($RMSE_2$ = 0.47, BF_2 = 1.57)

3.3. Incorporation of nitrogen factor

Figure A7 shows measured specific growth rate and nitrogen factor (F_N) as a function of nitrogen availability (N_A). With measured specific growth rates and their corresponding N_A, the two model parameters were determined (μ_m' = 1.27, k_{NA} = 0.02). Equation 16 was obtained by substituting the parameters into Equation 7 and was used to calculate F_N. It is represented by the solid line in Figure A7.

$$F_N = \frac{\mu_N}{\mu_{max-N}} = \frac{\mu_m' - (k_{NA}\mu_m')\frac{1}{N_A}}{\mu_{max-N}} = 1.33(1 - 0.022/N_A) \quad (16)$$

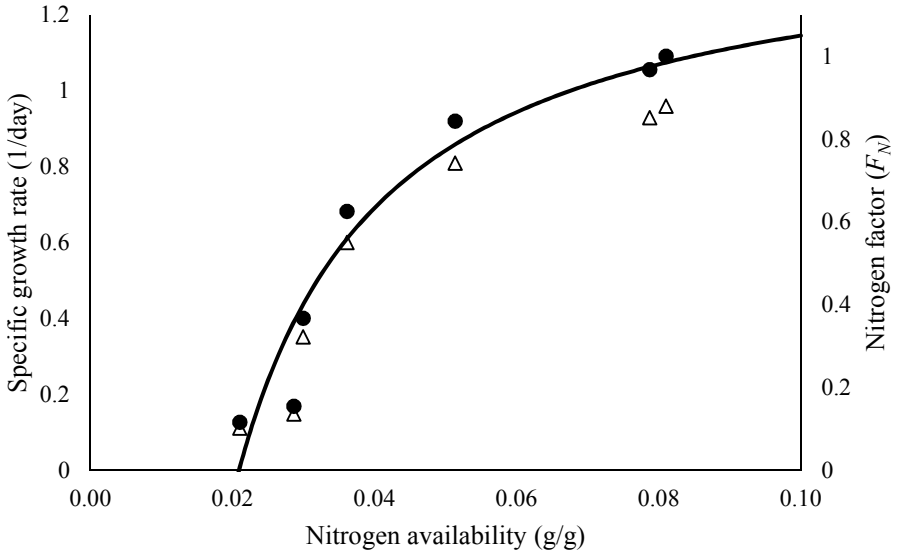

Figure A.7 Specific growth rate (μ_N, △) and nitrogen factor ($\mu_N/\mu_{max\text{-}N,}$ ●) as a function of nitrogen availability for *S. obliquus* in laboratory culture.

During the outdoor raceway experiment, there were several fertilizer additions. At each addition, nitrogen was added to the total available nitrogen (Figure A8). The total available nitrogen was then divided by biomass concentration at each time step. In the early culture, N_A was maintained at a high level; thus, there was no significant nitrogen stress, and F_N was maintained at or close to 1. With biomass accumulation, N_A decreased rapidly. Although nitrogen was added to the culture several times (as shown by arrow in Figure A8), the amount was not enough to prevent growth rate reduction. During most of the experiment, F_N was below 1, indicating that the pond operational practices that were intended to minimize fertilizer cost provided insufficient nitrogen supply. After accounting for nitrogen stress, over-prediction was lowered from 57% to 33% (Figure A9).

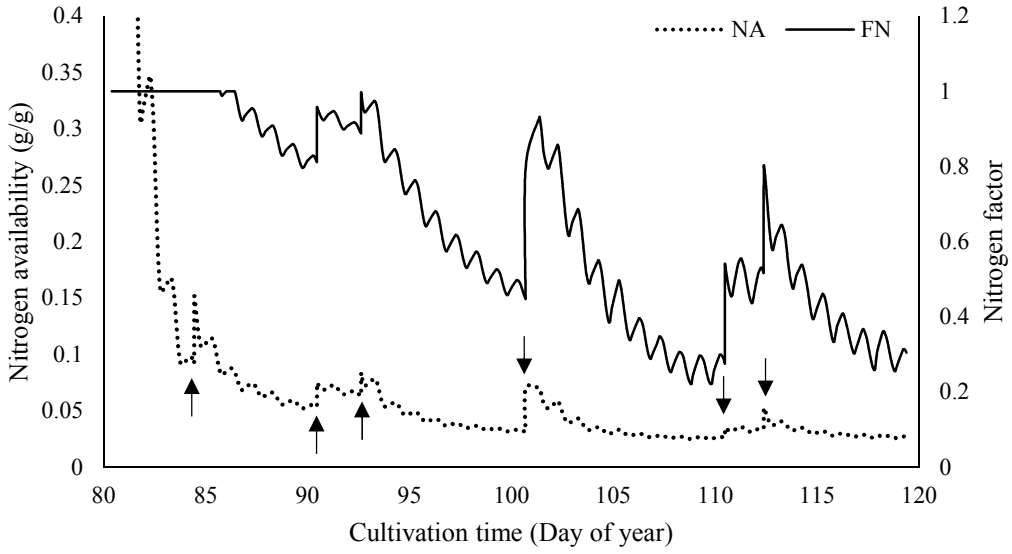

Figure A.8 Nitrogen availability (N_A) and nitrogen factor (F_N) as a function of time during RAFT07 experiment. N_A increases due to nutrient addition (↑)

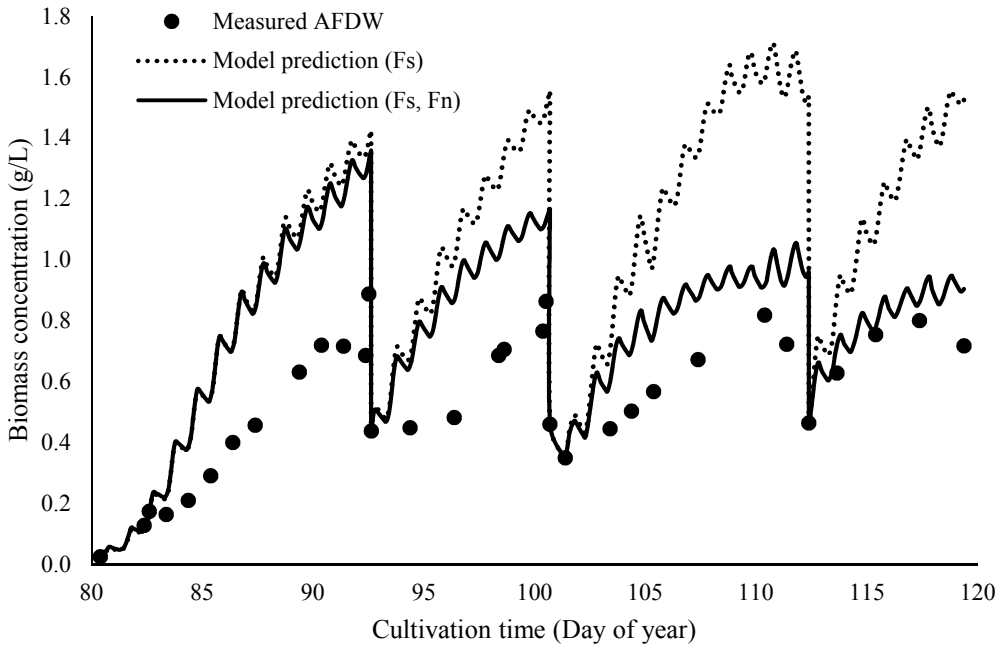

Figure A.9 Measured biomass concentration, F_S - adjusted model prediction, and $F_S F_N$ - adjusted model prediction. RMSE3 = 0.30 and BF3 = 1.33

3.4 Adjustment of the model for shading effect

The measured light intensity ratio (r_{zx}) vs. distance (x) from the baffle at each depth (z) is shown in Figure A10. A linear relationship was found between light ratio and distance from the board at each depth. Light ratios at the edge of shade were close to 30% at all depths. The change of light ratio from 30% in the shade to 100% in the sun takes place within a short distance (< 1cm). Thus, we assumed that the light ratio increased from 30% in the shade to 100% in the sun. The furthest point with the light ratio less than 100% was defined as the edge of shade. Because of the size of sensor, it was impossible to practically measure light intensity at $x = 0$. This value was estimated based on the linear change with distance. The light ratios at the board were within the range of 10% to 14% with average value 12% and standard deviation 1%. The two boundary conditions for r_{zx} were then determined as, $x = 0$, $r_{zx} = 12\%$ and $x = w$, $r_{zx} = 30\%$. Therefore,

$$r_{zx} = 0.18x/w_z + 0.12 \quad (18)$$

Following the procedure described in Theoretical Development, light ratio R_z was calculated.

Case 1, shade at layer z doesn't cover the entire channel ($wz < L$). Equation 6 can be applied directly to find Rz. Substitute Equation 5 into Equation 9 and simplify.

$$R_z = (L\text{-}0.7w_z)/L. \quad (19)$$

Case 2, shade at layer z covers the entire channel ($w_z \geq L$). In this case, there will be no unshaded area; thus, $I_{z\text{-unshaded}} = 0$. The upper limit for the integral (Equation 6) is no longer w_z, but L. Substitute Equation 5 into Equation 9.

$$R_z = \frac{\int_0^L I_{z0} r_{zx} d_x}{I_{z0} L} = 0.09L/w_z + 0.12 \quad (20)$$

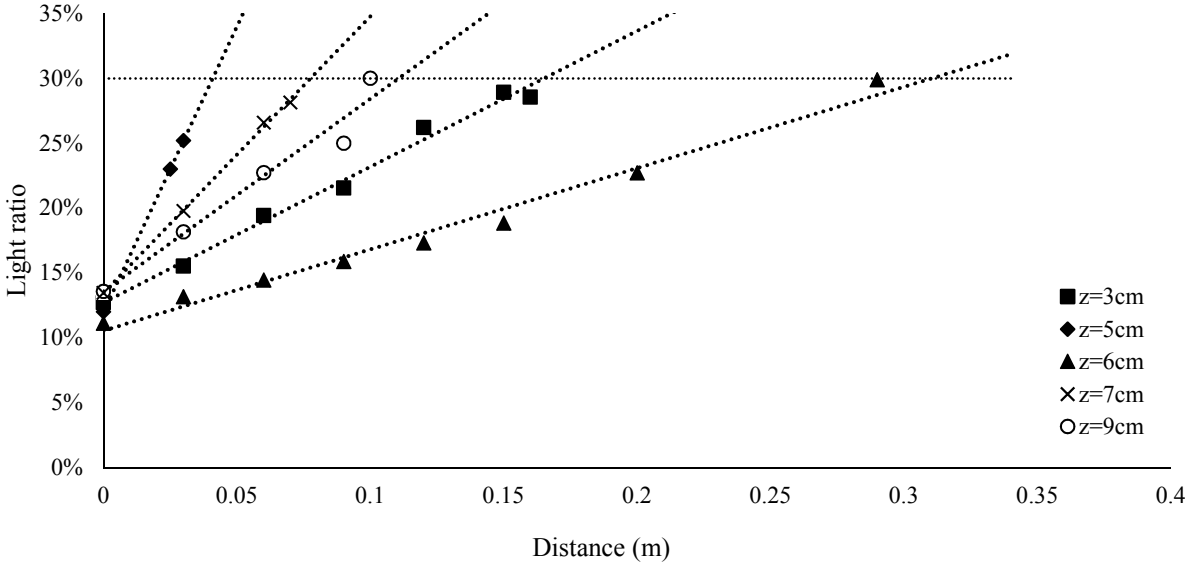

Figure A.10 Light intensity ratio (r_{zx}) as a function of distance from board (x) at different depths (z)

Equation 15 and 16 calculates shading factor R_Z in each layer at depth z. The total shading effect in the culture was expressed as average light ratio, using weighted average of R_Z for the 100 layers. As the experiment approached summer, solar angle increased and led to a higher average light ratio (Figure A11a). Within one day, shade width in early morning and late afternoon is shorter than it in the mid-day within the experimental period; thus, the overall shading effect reaches its maximum at mid-day. Figure A11b is an example of the overall shading effect variation within DOY100. In general, less than 10% of the light was blocked by shading during this experiment. Incorporation of shading effect lowered model over-prediction from 33% to 22% (Figure A12). In this experiment, shading exhibited less impact than salinity and nitrogen stress, but in winter or a higher latitude area, its significance would be larger. Cultivation system geometry also has a direct impact on shading effect. For most commercial scale raceways with wide channels and short or sloping berms, shading effect is not significant, but for many smaller scale research raceways, shading may have a significant impact on growth. In these systems, including shading helps to achieve a more accurate and realistic simulation in outdoor raceways.

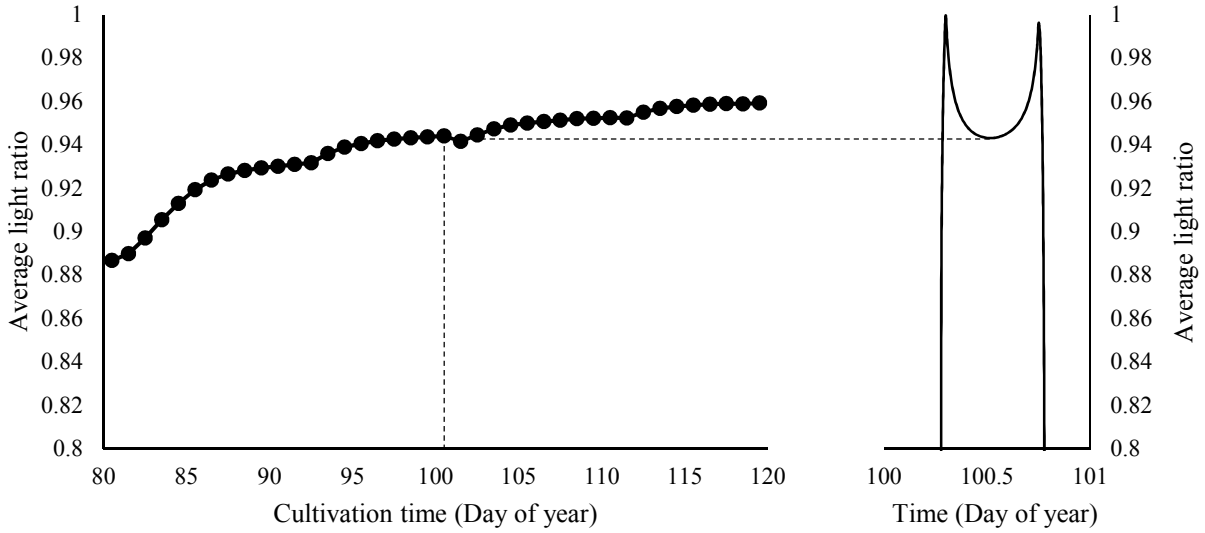

Figure A.11(a) Average light ratio at mid-day during the experiment. (b) Average light ratio variation within DOY 100. Before sunrise, average light ratio was set to 0. After sunrise, average light ratio increased from 0 to 100% at 7:17 AM, decreased to 94% at 12:33 PM, increased to 100% at 6:00 PM, and decreased to 0 at sunset

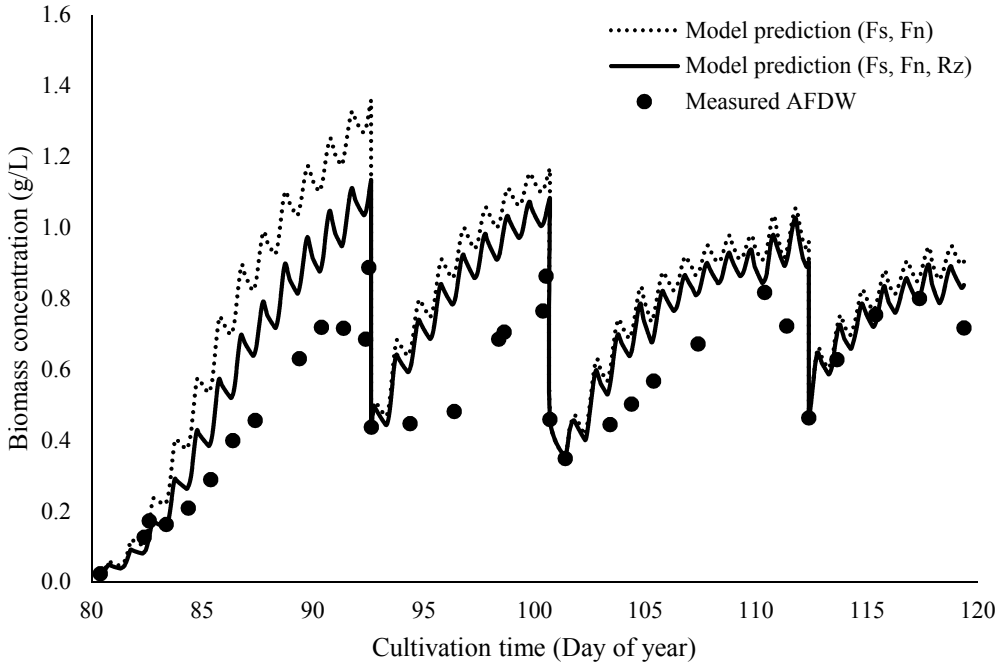

Figure A.12 Measured biomass concentration, $F_S F_N$ - adjusted model prediction, and F_S F_N Rz- adjusted model prediction. $RMSE_4 = 0.21$, $BF_4 = 1.22$

Comparison of the modified model (with all three factors) and RAFT 06 experimental data is shown in Figure A13. The growth rate in the first batch culture run was lower than expected, unfortunately, the cause was unknown. An examination of the growth conditions indicated that the reduced growth was not due to weather or contaminants. Both the original model and modified model provided relative good prediction of biomass growth during the second batch culture run, where the experiment was conducted with freshwater and sufficient nutrient supply.

The influence of the above described model modification was not significant due to the absence of salinity or nitrogen stress. The assumptions for the original model were satisfied. Overall, the model provided an accurate estimate of growth rate in later two cultural batch runs (BF = 0.92).

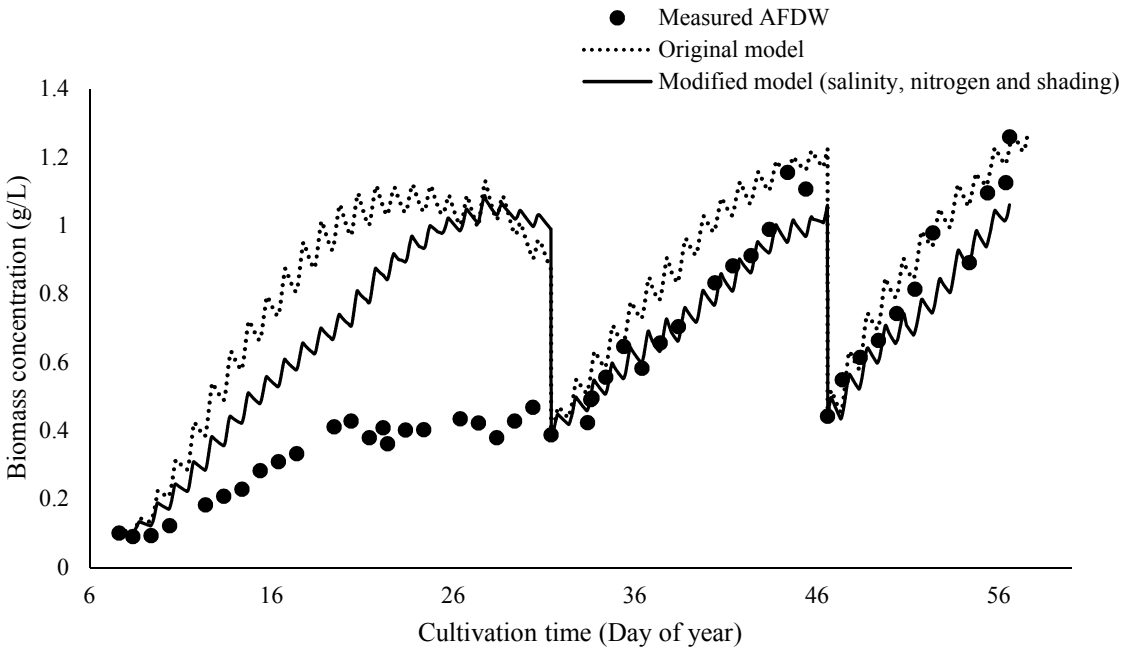

Figure A.13 Comparison of measured biomass growth, original growth model prediction, and modified growth model prediction in RAFT06, ARID raceway *Scenedesmus obliquus* experiment. Biomass concentration was reset on DOY 31

3.5 Lag phase

In newly inoculated cultures, physiological adaption to the altered conditions usually causes a significantly lower growth rate than in the exponential growth phase (Becker, 1994). During this experiment and many others, we observed that there is a somewhat unpredictable lag phase before exponential growth takes place. Harvesting and culture media replenishment may also alter growth conditions and cause reoccurrence of an adaption period. The HABG model, however, only simulates the exponential growth phase and stationary phase. Thus, growth during

the lag phase or adaption to new conditions is not predicted by the model. The simulations presented so far started directly after each harvest without considering lag phase. In Figure A14, the dashed line represents simulated growth without removing the lag phase from the simulation, showing much higher over-prediction. Delaying the simulation by 4, 4 and 2 days in batch cultures 1, 2 and 3, respectively, lowered over-prediction from 22% to 10%.

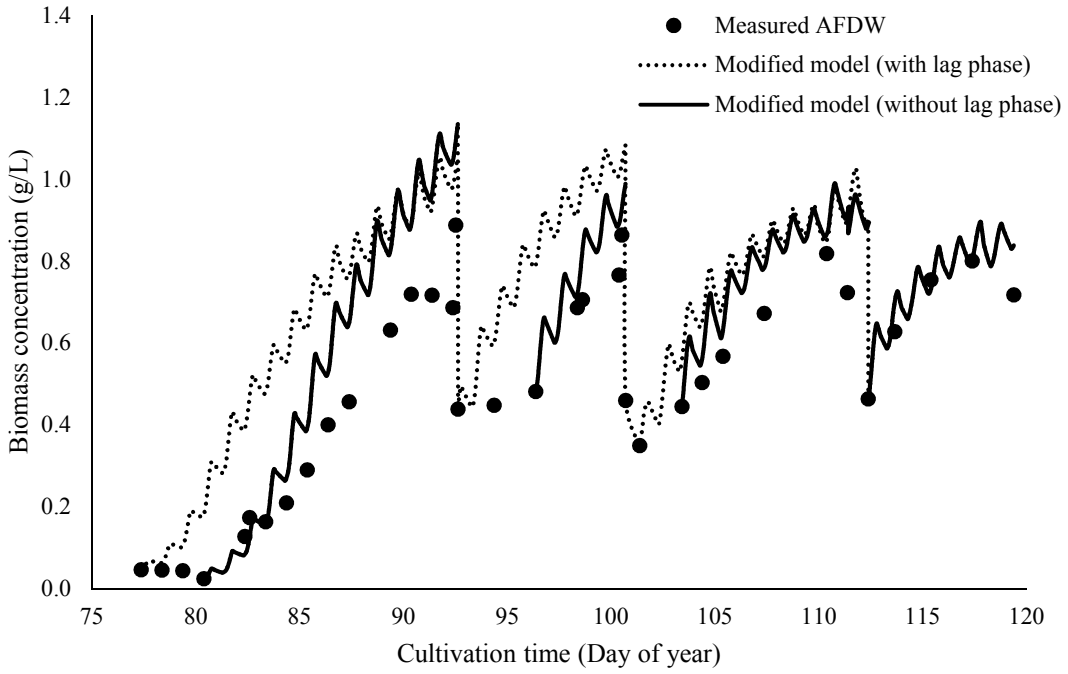

Figure A.14 Comparison of F_S F_N Rz - adjusted model predictions with and without lag phase. $RMSE_5$ = 0.16, BF_5 = 1.10 for lag phase excluded simulation

4. Conclusions

In this study, we improved the HABG model by adding factors correcting for salinity and nitrogen stress, as well as for shading. For the experiment with high salinity and limited nitrogen supply, the modification greatly improved model prediction. Over-prediction reduced from 90% in the original model to 13% in the modified model, and 10% if lag phase is excluded. For the

experiment with fresh water and sufficient nitrogen supply, stress factors were not significant, and both the original model and modified model provided good growth prediction.

5. Acknowledgement

This study was supported by the U.S. Department of Energy and Regional Algal Feedstock Testbed (RAFT) project, University of Arizona, for which the authors are grateful.

6. References

Bannister, T.T., 1979. Quantitative description of steady state , algal growth , including adaptation. Limnol. Oceanogr. 24, 76–96.

Baranyi, J., Pin, C., Ross, T., 1999. Validating and comparing predictive models. Int. J. Food Microbiol. 48, 159–166. doi:10.1016/S0168-1605(99)00035-5

Becker, E.W., 1994. Microalgae: Biotechnology and Microbiology. Cambridge University Press, Cambridge, UK.

Converti, A., Casazza, A. a., Ortiz, E.Y., Perego, P., Del Borghi, M., 2009. Effect of temperature and nitrogen concentration on the growth and lipid content of *Nannochloropsis oculata* and *Chlorella vulgaris* for biodiesel production. Chem. Eng. Process. 48, 1146–1151. doi:10.1016/j.cep.2009.03.006

Cornet, J.-F., Dussap, C.-G., 2009. A simple and reliable formula for assessment of maximum volumetric productivities in photobioreactors. Biotechnol. Prog. 25, 424–435. doi:10.1021/bp.138

Difusa, A., Talukdar, J., Kalita, M.C., Mohanty, K., Goud, V. V., 2015. Effect of light intensity and pH condition on the growth, biomass and lipid content of microalgae *Scenedesmus* species. Biofuels 6, 37–44. doi:10.1080/17597269.2015.1045274

Droop, M.R., 1968. Vitamin B12 and Marine Ecology. IV. The kinetics of uptake, growth and Inhibition in *Monochrysis lutheri*. J. Mar. Biol. Assoc. United Kingdom 48, 689–733.

Edmundson, S.J., Kruk, R., Huesemann, M.H., n.d. Winter algae crops: characterization of Algal Strains with cold season production potential. Environ. Exp. Bot.

Goldman, J.C., Hole, W., 1979. Outdoor Algal Mass Cultures - II. Photosynthetic Yield Limitations. Water Res. 13, 119–136.

Hsieh, C.H., Wu, W.T., 2009. Cultivation of microalgae for oil production with a cultivation strategy of urea limitation. Bioresour. Technol. 100, 3921–3926. doi:10.1016/j.biortech.2009.03.019

Huesemann, M., Crowe, B., Waller, P., Chavis, A., Hobbs, S., Edmundson, S., Wigmosta, M., 2016. A validated model to predict microalgae growth in outdoor pond cultures subjected to fluctuating light intensities and water temperatures. Algal Res. 13, 195–206. doi:10.1016/j.algal.2015.11.008

James, S.C., Boriah, V., 2010. Modeling Algae Growth in an Open-Channel Raceway. J. Comput. Biol. 17, 895–906. doi:10.1089/cmb.2009.0078

Kaewkannetra, P., Enmak, P., Chiu, T., 2012. The effect of CO2 and salinity on the cultivation of *Scenedesmus obliquus* for biodiesel production. Biotechnol. Bioprocess Eng. 17, 591–597. doi:10.1007/s12257-011-0533-5

López, S., Prieto, M., Dijkstra, J., Dhanoa, M.S., France, J., 2004. Statistical evaluation of mathematical models for microbial growth. Int. J. Food Microbiol. 96, 289–300. doi:10.1016/j.ijfoodmicro.2004.03.026

Mohammed, A.A., Shafea, A.A., 1992. Growth and some metabolic activities of *Scenedesmus obliquus* cultivated under different NaCl concentrations. Biol. Plant. 34, 423–430.

Packer, A., Li, Y., Andersen, T., Hu, Q., Kuang, Y., Sommerfeld, M., 2011. Growth and neutral lipid synthesis in green microalgae: a mathematical model. Bioresour. Technol. 102, 111–7. doi:10.1016/j.biortech.2010.06.029

Quinn, J., de Winter, L., Bradley, T., 2011. Microalgae bulk growth model with application to industrial scale systems. Bioresour. Technol. 102, 5083–92. doi:10.1016/j.biortech.2011.01.019

Ranga Rao, a, Ravishankar, G. a, Sarada, R., 2012. Cultivation of green alga *Botryococcus braunii* in raceway, circular ponds under outdoor conditions and its growth, hydrocarbon production. Bioresour. Technol. 123, 528–33. doi:10.1016/j.biortech.2012.07.009

Rao, A.R., Dayananda, C., Sarada, R., Shamala, T.R., Ravishankar, G.A., 2007. Effect of salinity on growth of green alga *Botryococcus braunii* and its constituents. Bioresour. Technol. 98, 560–564. doi:10.1016/j.biortech.2006.02.007

Rippka, R., Deruelles, J., Waterbury, J.B., Herdman, M., Stanier, R.Y., 1979. Generic assignments, strain histories and properties of pure cultures of cyanobacteria. J. Gen. Microbiol. 111, 1–61. doi:10.1099/00221287-111-1-1

Rogers, J.N., Rosenberg, J.N., Guzman, B.J., Oh, V.H., Elena, L., Ghassemi, A., Betenbaugh, M.J., Oyler, G.A., Donohue, M.D., 2014. A critical analysis of paddlewheel-driven raceway

ponds for algal biofuel production at commercial scales. Algal Res. 4, 76–88. doi:10.1016/j.algal.2013.11.007

Ross, T., 1996. Indices for performance evaluation of predictive models in food microbiology. J. Appl. Bacteriol. 81, 501–508. doi:10.1111/j.1365-2672.1996.tb03539.x

Sorokin, C., Krauss, R.W., 1958. The effects of light intensity on the growth rates of green algae. Plant Physiol. 33, 109–13. doi:10.2307/4259285

te Giffel, M.C., Zwietering, M.H., 1999. Validation of predictive models describing the growth of *Listeria monocytogenes*. Int. J. Food Microbiol. 46, 135–49. doi:10.1016/S0168-1605(98)00189-5

Thimijan, R.W., Heins, R.D., 1983. Photometric, radiometric, and quantum light units of measure: a review of procedures for interconversion. HortScience 18, 818–822.

Van Wagenen, J., Holdt, S.L., De Francisci, D., Valverde-Pérez, B., Plósz, B.G., Angelidaki, I., 2014. Microplate-based method for high-throughput screening of microalgae growth potential. Bioresour. Technol. 169, 566–572. doi:10.1016/j.biortech.2014.06.096

Waller, P., Ryan, R., Kacira, M., Li, P., 2012. The algae raceway integrated design for optimal temperature management. Biomass and Bioenergy 46, 702–709. doi:10.1016/j.biombioe.2012.06.025

Wijffels, R.H., Barbosa, M.J., 2010. An outlook on microalgal biofuels. Science 329, 796–799. doi:10.1126/science.1189003

Yoshimura, T., Okada, S., Honda, M., 2013. Culture of the hydrocarbon producing microalga *Botryococcus braunii* strain Showa: Optimal CO2, salinity, temperature, and irradiance conditions. Bioresour. Technol. 133, 232–239. doi:10.1016/j.biortech.2013.01.095

Yuan, S., Zhou, X., Chen, R., Song, B., 2014. Study on modelling microalgae growth in nitrogen-limited culture system for estimating biomass productivity. Renew. Sustain. Energy Rev. 34, 525–535. doi:10.1016/j.rser.2014.03.032

Appendix B Nutrient recipes used in RAFT algae cultivation

The following is a summary of chemical composition in different culture media. Most of the *Chlorella sorokiniana* experiments used PECOS 07+, and most of the *Scenedesmus obliquus* experiments used PECOS 09+. Some of the experiments were designed for nutrient studies and the recipes are listed in the nutrient experiments column.

Chemical (g/L)	BG11	PECOS 07 Recipes			PECOS 09 Recipes		
	BG11	PE07-SG[a]	PE-07[b]	PE-07+[c]	PE09-SG[a]	PE-09[b]	PE-09+[c]
Urea		0.1	0.1	0.1	0.05	0.05	0.05
$NaNO_3$	1.496						
$NH_4H_2PO_4$		0.035	0.035	0.035	0.01	0.01	0.010
KH_2PO_4	0.038						
Potash $K_2O + SO_4$			0.175	0.175		0.175	0.175
Potash KCl		0.175			0.175		
$MgSO_4*7H_2O$	0.007	0.012	0.012	0.075	0.012	0.012	0.075
NaCl	0	0	0	0		0	0
Citraplex 20% Iron		0.005423	0.005423	0.005423	0.00315	0.005423	0.005423
Ammonium Ferric Citrate	0.00524						
$FeCl_3$							
H_3BO_3	0.00286	0.002853	0.002860	0.00286	0.002853	0.002860	0.00286
$MnCl_2•4H_2O$	0.00181	0.001268	0.001810	0.00181	0.001268	0.001810	0.00181
$ZnSO_4•7H_2O$	0.00022	0.000137	0.000137	0.00022	0.000137	0.000137	0.00022
$Na_2MoO_4•2H_2O$	0.000391	0.000391	0.000390	0.00039	0.000391	0.000390	0.00039
$CuSO_4•5H_2O$	0.000079	0.000079	0.000079	0.000079	0.000079	0.000079	0.000079
$Co(NO_3)_2•6H_2O$	0.00005	0.000055	0.000055	0.0000494	0.000055	0.000055	0.0000494
$NiCl_2•6H_2O$			0.000100	0.0001		0.000100	0.0001
Na_2CO_3	0.01907802	0.02					
$Na_2EDTA*2H_2O$	0.00074448	0.00436			0.00545		
Citric Acid * H_2O	0.00630372						
Vitamin Soln. B_{12}, B_1, H (mL/L)				0.005			0.005

	Chemical (g/L)	Nutrient Experiments			
		P-[d]	P+[d]	N-[d]	N+[d]
N	Urea				
	$NaNO_3$	0.075	0.845	0.075	0.845
P	$NH_4H_2PO_4$	0.009	0.095	0.038	0.038
	KH_2PO_4				
K	Potash $K_2O + SO_4$				
	Potash KCl	0.175	0.175	0.175	0.175
Mg	$MgSO_4*7H_2O$	0.075	0.075	0.075	0.075
NaCl	NaCl	0.000	0.000	0.000	0.000
Fe	Citraplex 20% Iron				
	Ammonium Ferric Citrate				
	FeCl3	0.005423	0.005423	0.005423	0.005423
Micro	H_3BO_3	0.00286	0.00286	0.00286	0.00286
	$MnCl_2•4H_2O$	0.00181	0.00181	0.00181	0.00181
	$ZnSO_4•7H_2O$	0.00022	0.00022	0.00022	0.00022
	$Na_2MoO_4•2H_2O$	0.000391	0.000391	0.000391	0.000391
	$CuSO_4•5H_2O$	0.000079	0.000079	0.000079	0.000079
	$Co(NO_3)_2•6H_2O$	0.00005	0.00005	0.00005	0.00005
	$NiCl_2•6H_2O$				
Buffer	Na2CO3				
	$Na_2EDTA*2H_2O$				
	Citric Acid * H_2O				
Vitamin	Vitamin Soln. B_{12}, B_1, H (mL/L)				

[a] Modified PECOS media based on laboratory nutrient yield experiments
[b] Original PECOS media
[c] Original PECOS media amended with BG11 Mg/micronutrients and Vitamins
[d] Recipes used for nutrient experiments

Appendix C Nitrogen and phosphorus yields in *Scenedesmus obliquus* cultivation

Song Gao[a], Peter Waller[a*], Renhe Qiu[b], Kimberly Ogden[b],

[a] Department of Agricultural and Biosystems Engineering, The University of Arizona, Tucson, AZ 85721, USA

[b] Department of Chemical Engineering, The University of Arizona, Tucson, AZ 85721, USA

Journal: TBD

Abstract

The application of nitrogen and phosphorus fertilizers is the one of the major costs in algae production. This study investigated algae growth and nutrient biomass yields under different nutrient levels for better control fertilizer usage. Cultures with large and small internal nutrient storage resulted in severalfold of variation both nitrogen and phosphorus biomass yields. In this study, nitrogen and phosphorus yields were maximized (44 g dry biomass/g N and 805 g dry biomass/g P) simultaneously at atomic N/P ratio of 36.7. A larger scale photobioreactor operated under different culture conditions tested and confirmed the results from flask experiments. In comparison, repeated outdoor raceway experiments had lower nutrient biomass yields than that in indoor experiments. However, compare to earlier RAFT experiments, phosphorus fertilizer was used more efficiently without lowering biomass productivity or lipid content, showing large potential for resources usage improvement.

1. Introduction

Increases in climate variability and the desire by some countries to limit greenhouse gas emissions, supports research to find alternative sustainable energy sources. Biofuel production is one of the most strategically important energy technologies that converts atmospheric CO_2 into biomass (Chisti, 2007; Nigam and Singh, 2011). Microalgae have long been recognized as a promising biofuel feedstock, for its advantages of rapid growth, high lipid content, and high areal productivity (Chisti, 2007).

Nitrogen and phosphorus are the major nutrient inputs for algal fuel production (Wijffels and Barbosa, 2010). In paddlewheel-driven raceway systems, urea is one of top cost drivers (Rogers et al., 2014). Global reserves of phosphate rock are finite, and the price of phosphorus fertilizer increased drastically in the past, spiking by 700% in 2007 to 2008 (Elser and Bennett, 2011). Life cycle assessment of biodiesel production indicates the necessity of decreasing fertilizer consumption (Lardon et al., 2009). Moreover, intensive energy and greenhouse gas emissions are associated with producing fertilizer (Clarens et al., 2010). The value of biofuel as an energy source and its advantage of carbon neutrality are inhibited by the use of fertilizer. Therefore, efficient fertilizer use is an economic and environmental necessity and is an important factor in determining whether algal biofuel production is sustainable.

Studies have found that many algae have the ability to store nutrients intracellularly (Elgavish et al., 1980; McGlathery et al., 1996). Only part of the nutrient absorbed by the cell is used for biomass production, and the rest is stored in the intracellular nutrient pool. The size of the intracellular nutrient pool is proportional to the ambient nutrient concentration and varies greatly (Saxton et al., 2012). Keeping a high nutrient concentration in culture media increases the amount

of stored nutrient, which lowers the efficiency of fertilizer. Therefore, quantification of the nutrient demand of algae is necessary to avoid unnecessary fertilizer usage.

Various environmental conditions affect lipid content, including nutrient depletion, iron concentration, salinity, and light intensity (Gordillo et al., 1998; Li et al., 2008; Liu et al., 2008; Zhila and Kalacheva, 2011). Among them, nutrient limitation is the most common method to increase lipid content. Controlling fertilizer application influences nutrient status of the culture, and consequently cell lipid content. An ideal scenario for fertilizing the culture is that high fertilizer efficiency and high lipid content are realized at the same time.

The present study determines the maximum yields of the two major nutrients, nitrogen and phosphorus, for growing *Scenedesmus obliquus*, an algae strain that holds potential as a biofuel feedstock (Mandal and Mallick, 2009). The optimal N/P ratio was determined based on biomass yields of each element. The results were evaluated in outdoor raceway experiments.

2. Materials and methods

2.1 Algae strain and culture conditions

Scenedesmus obliquus was isolated as part of the National Alliance for Biofuels and Bioproducts (NAABB) project by Dr. Juergen Polle (Unkefer et al., 2017). The bench-scale experiment was conducted by culturing algae in 1000 ml glass flasks (Fisher Scientific). Nutrients were removed from the inoculum by removing the supernatant after centrifugation. Fluorescent light tubes (AgroBrite, T5 54W 6400K) were used as a light source. The output photosynthetically active radiation (PAR) was measured by a quantum sensor (LI-190R) at 120 μmol/m^2-s. The light and dark cycle was 12 h:12 h. All flasks were placed on a shaker for mixing. Ambient temperature in the room was consistently 22 ℃. Air was injected with 5% CO_2 (v/v), and air flow rate was

maintained at 1 liter/minute both day and night. Samples were collected every day at the same time (in the first few minutes of the dark cycle) for monitoring algal growth and nutrient uptake.

2.2 Experiment design

The experiment was a two by two factorial design consisting of two levels of initial nitrogen (TN) and phosphorus (TP) using $NaNO_3$ and KH_2PO_4: low and high, denoted as - and +. For the low level, nutrient concentration in the media was non-detectable at the end of the experiment. For the high level, final nutrient concentrations remained several folds higher than detection levels (Detection levels, TN: 0.8 mg/L; TP: 0.5 mg/L). Cultures were maintained until all treatments with a low level of nutrient reached stationary phase. The idea is based on Liebig's Law that the biomass yield only depends upon the most limiting nutrient. The assumption is that the limited nutrient is completely used for producing biomass, thus the maximum nutrient yield is realized. The four treatments are N-P- (TN: 15 mg/L TP: 2 mg/L), N-P+ (TN: 15 mg/L TP:22 mg/L), N+P- (TN: 140 mg/L; TP: 2 mg/L), and N+P+ (TN: 140 mg/L TP: 22 mg/L). TN and TP concentration of BG-11 (Rippka et al., 1979) is also provided for reference. A pre-test of system carrying capacity was carried out by providing a continuous nutrient supply, in order to make sure that the stationary phase in the latter part of the experiment was caused by nutrient availability, rather than other conditions such as light limitation. Other nutrients were added following Jia et al (2015) with one modification. Citraplex was replaced by ferric chloride with an equivalent amount of iron.

Validation experiments were conducted in a flat plate photobioreactor (PBR) and two outdoor paddlewheel reactors. The PBR was operated at the same temperature and light cycle but with stronger light intensity (360 μmol/m^2 -s) and a larger volume (30 liter) than in the bench-scale experiments. There were two sets of outdoor experiments carried out in two side-by-side paddlewheel raceways. Nitrogen were provided excessively in both two raceways, and phosphorus

had high and low levels, with concentrations approximately the same as the P+ and P- conditions in flask experiments. In both PBR and raceway experiments, the cultures were kept until no growth can be obtained.

2.3 Nutrient measurement

TN and TP were measured using ion chromatography (Dionex ICS-5000; Dionex Corporation, Sunnyvale, CA, USA). The column was a Dionex IonPac AS18 (2 × 250mm), and the sample injection size was 10 μL. Flow rate of KOH eluent was set at 0.38 mL/min, and the operating temperature was 30 ℃. Ion peak detection was undertaken by suppressing conductivity measurements at 22 mA. The spectra were analyzed using Chromeleon provided by Dionex.

2.4 Determination of biomass concentration and nutrient yields

Biomass concentration was measured as ash free dry weight (AFDW g/L). Each of treatment started at approximated 0.02 g-AFDW/L, and the accumulation of AFDW was used to calculate nutrient biomass yield. It was measured by filtering culture samples onto a pre-dried and pre-weighted GF/C grade Whatman glass microfiber filter and drying at 75℃ over 24 hours, and ashing for 4 hours at 540 ºC. Biomass concentration was measured by re-weighting the filter and taking the weight difference. Nutrient biomass yields (Y, g biomass/g nutrient) were calculated via:

$$Y = \Delta B / \Delta S$$

where, ΔB is change in biomass for a given time period (g/L); and ΔS is the corresponding amount of nutrient (g/L) removed from the liquid.

2.5 Estimation of nutrient storage

Intracellular nutrients storage was usually measured as g-nutrient/cell or g-nutrient/g-C. In this study, biomass carbon contents in each treatment are close (average 51.43%, standard deviation

2%). Therefore, the ratio of absorbed nutrient to AFDW is equivalent to g-nutrient/g-C and was used to show nutrient storage variation during the experiment. The nutrient content of accumulated biomass, $Q_{n,}$ on day n is calculated as:

$$Q_n = (N_0 - N_n) / C_n \quad (1)$$

where, N_0 is the initial media nutrient concentration; N_n is the media nutrient concentration on day n; and C_n is AFDW on day n.

2.6 Lipid content measurement

Total lipids were extracted by the method of Bligh and Dyer (Bligh and Dyer, 1959) with modifications. Samples were dried overnight after centrifugation. Biomass was pulverized before mixing with chloroform and methanol (2:1, v/v) and held at room temperature for at least 2 hours. Samples were then subjected to microwave treatment using a CEM Microwave Accelerated Reaction System (MARS, CEM Corp., Matthews, NC, USA). The suspensions were heated to 70 ^{o}C and held for 60 min. The treated samples were filtered, and the chloroform layer was transferred into a pre-weighted glass tube. Organic solvent was then evaporated by a nitrogen evaporator (N-Evap 112, Organomation Association Inc., Berlin, MA, USA) to obtain dry lipid. After weighting the glass tube again, lipid content can be calculated from known weight of the dry biomass (weight of lipid / weight of biomass, x %).

2.7 Statistical analysis

For each treatment, three replicates were used for data collection (not including outdoor raceway experiments). Multivariate analysis of variance (MANOVA) was used to evaluate whether nitrogen and phosphorus have strong effects on algae growth. For analysis of nutrient effects on lipid contents, a two-way analysis of variance (ANOVA) were applied. All analysis was carried

out using JMP (JMP Pro 11.2.1, SAS Institute Inc., Cary, NC). Variables were reported as significant at 95% confidence (p-value less than or equal to 0.05).

3. Results and discussion

3.1 Growth under different culture conditions

Prior to implementing the design of experiments to determine the minimum amount of nitrogen and phosphorus required for cell growth, the carrying capacity of the culture was determined for the given light and temperature conditions with continuous sufficient nutrient supply (solid line in Figure C1). The culture denoted as N+P+ could reach this cell density given sufficient time. The highest biomass concentration achieved in all treatments was less than the carrying capacity, thus nutrient availability was the primary growth limiting factor. All treatments were started with the same biomass concentration, and all N- and P- cultures reached stationary phase at the end of the experiment (Figure C1).

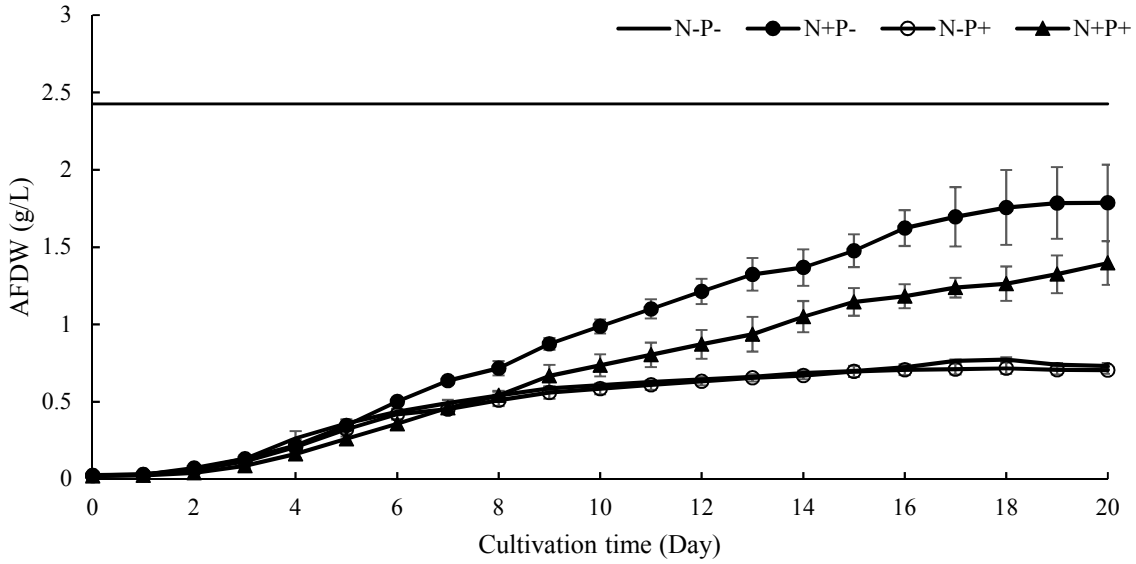

Figure C.1 Growth curve of *S. obliquus* under different conditions. Solid line (—) on the top represents system carrying capacity under nutrient-rich condition. Data are given as mean ± standard deviation of triplicates

3.1.1 Nitrogen

In the first 5 days, all treatments had similar growth. After that, the growth rate of the algae with N- treatments became lower than that of algae with N+ treatments, indicating nitrogen stress. Because the other P-limited (N+P-) cultures grew the best, lowered growth rate of N-P- cultures was presumably caused by nitrogen stress.

Different nitrogen levels had a strong effect on culture growth (p-value < 0.0001). Average growth of N+ cultures was 2.6 times as that of N- cultures, regardless of their phosphorus levels. This is especially clear in N- cultures with almost the same growth curve for both P treatments. Apparently, the growth is more sensitive to nitrogen availability. Improved growth is usually associated with higher nitrogen input (Converti et al., 2009; Hsieh and Wu, 2009). Our results also suggest that

sufficient nitrogen supply is of great importance in obtaining higher biomass productivity in algal biomass production.

3.1.2 Phosphorus

As opposed to the high sensitivity of growth to nitrogen, phosphorus had little impact on growth in this study (p-value > 0.1). The amount of phosphorus input in P+ cultures (22 mg/L) was 11 times as that in P- cultures (2 mg/ L). However, elevated phosphorus concentration didn't improve growth rate (Figure C1). N-P+ had identical growth as N-P-, whereas N+P+ had even less growth than N+P-. Different from nitrogen, growth effect of phosphorus is not consistent in the literature. Ruangsomboon et al. (2013) and Li et al. (2010) observed a strong impact of phosphorus on *Scenedesmus* biomass productivity, whereas Wu et al. (2012) observed insignificant phosphorus impact on growth. Results from this work agreed with the later study.

Final biomass concentration of N+P- cultures was greater than that of N+P+ cultures. Higher concentration of phosphorus appeared to inhibit the algal growth under nitrogen-rich conditions. Similar results were observed in repeated experiments. In agricultural activities, crop productivity is reduced by excessive application of phosphorus fertilizers. The reduction is caused by the interaction between concentrated phosphorus and micronutrients, which immobilizes micronutrients and makes them less available (Fageria, 2001; Gianquinto et al., 2000; Murphy et al., 1981). The same mechanism might be responsible for lowered growth in N+P+ cultures in this study. An experiment was conducted to verify the hypothesis. N+P+ and N+P- treatment were repeated with the same amount of micronutrients, denoted as N+P+M and N+P-M. Another treatment started with the same nutrient condition but received extra micronutrient every three days denoted as N+P+M+. The result is presented in Figure C2. The small p-value (< 0.0001) suggested that adding micronutrients brought about significant growth difference among the

cultures. It supported the above-mentioned hypothesis. Such inhibition was not observed in N- cultures due to the early occurrence of nitrogen stress which dominated the growth.

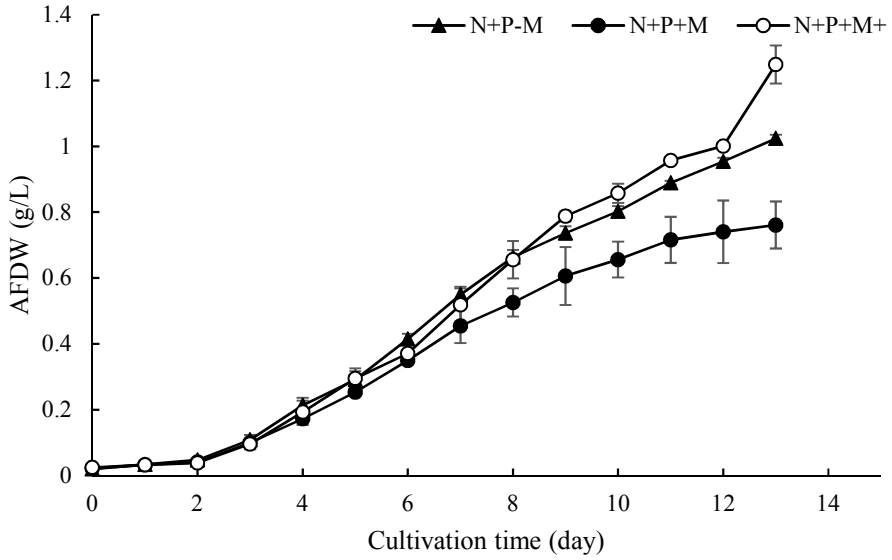

Figure C.2 Growth curve of different phosphorus and micronutrient concentrations. Culture conditions are represented by P-M (low P), P+M (high P) and P+M+ (high P with micronutrients addition). Data are given as mean ± standard deviation of triplicates

The minimum phosphorus of no growth rate reduction was not identified based on the results, however, keeping phosphorus concentration high in culturing algae is not recommended. Excessive application of phosphorus fertilizer may not enhance biomass production, instead, it may induce a negative impact on growth.

3.2 Nutrient uptake

Figure C3 depicts nitrogen concentration (a) and phosphorus concentration (b) in culture media during the experiment. Full consumption of nitrogen in N- cultures occurred within 5 days, and

that of phosphorus in P- cultures occurred within 3 days. For N+ and P+ cultures, nutrient uptake rate decreased as the culture entered the stationary phase.

By comparing the growth and nutrient uptake between the two levels of the same nutrient, it is easy to visualize excess nutrient uptake in N+ and P+ cultures. N+ cultures accumulated about 3 times as much biomass as N- groups, but consumed more than 6 times as much nitrogen. N-P- and N-P+ cultures had identical growth, but the later treatment consumed almost 5 times as much phosphorus. The phosphorus uptake was 9 times greater in the N+P+ cultures compared to the N+P- cultures. This phenomenon of excessive nutrient uptake was reported in a number of phytoplankton studies and is known as "luxury uptake" (Levin and Shapiro, 1965; Powell et al., 2011). The presence of luxury uptake means that excessive nutrients can be consumed without producing more biomass or higher productivity.

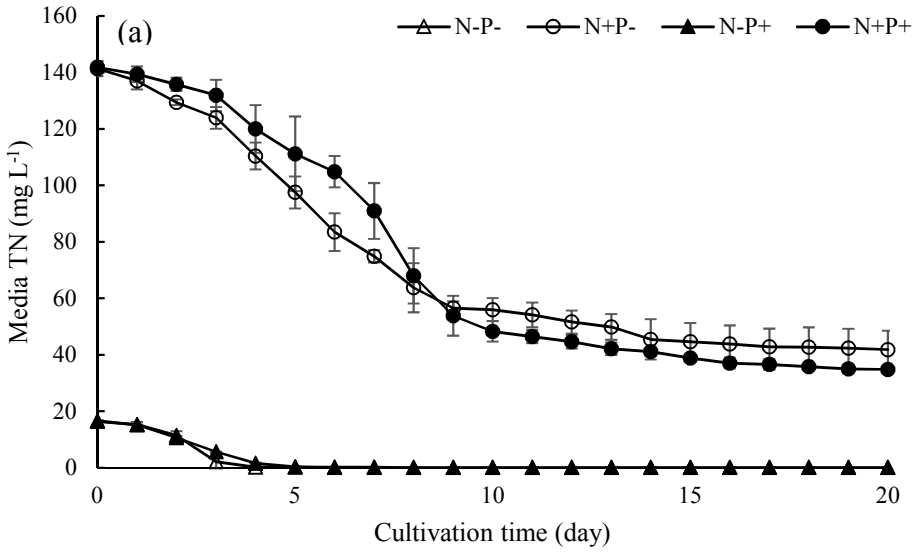

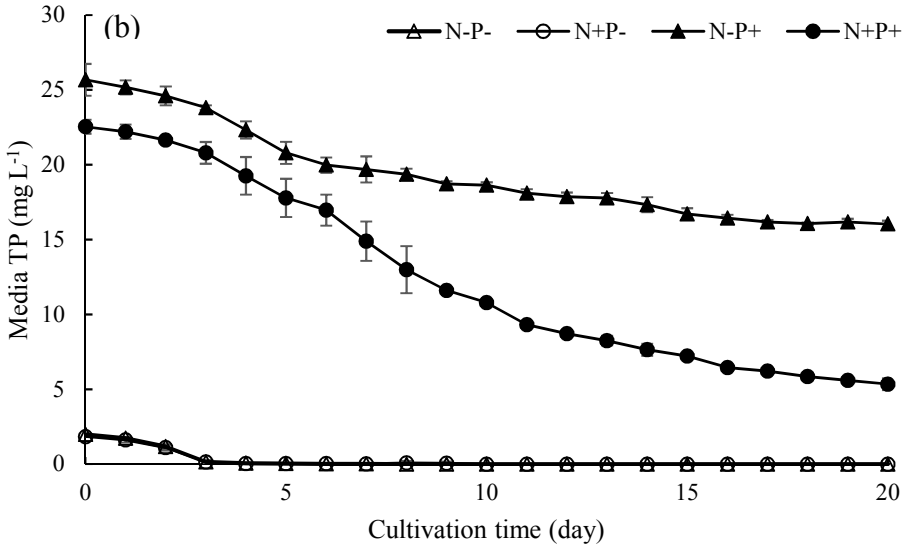

Figure C.3 Total nitrogen (TN) concentration in media (a) and total phosphorus (TP) concentration in media (b) under different culture conditions during the experiment. Data are given as mean ± standard deviation of triplicates

3.3 Nutrient storage

Intracellular nutrient storage has been found in many algal species and supports growth when external nutrients are limited or unavailable (Li et al., 2008; Tantanasarit et al., 2013). Based on mass balance, the ratio of absorbed nutrients to accumulated biomass was calculated via Equation 1 and were presented in Figure C4. The calculated nutrient contents were much higher at the beginning and decreased with time. Nutrient contents in early culture were unbelievably high and were not reliable because that growth was negligible during lag phase and slight decrease of nutrient concentration can result in large nutrient content. Usually, the microalgal biomass nitrogen content is between 2% to 10% (Adams et al., 2013, Gao et al. n.d.). Phosphorus content can vary from almost 0 to more than 3% (Powell et al., 2011). At the end, nitrogen content in accumulated biomass varied from 2.4% (N-P+) to 7.8% (N+P+), and phosphorus content varied from 0.1% (N+P-) to 1.4% (N-P-). Unlike nitrogen, higher phosphorus content didn't improve biomass

productivity. Such large variation indicates large variation in phosphorus fertilizer efficiency. This is tested in outdoor raceway experiments and is discussed in section 3.6.

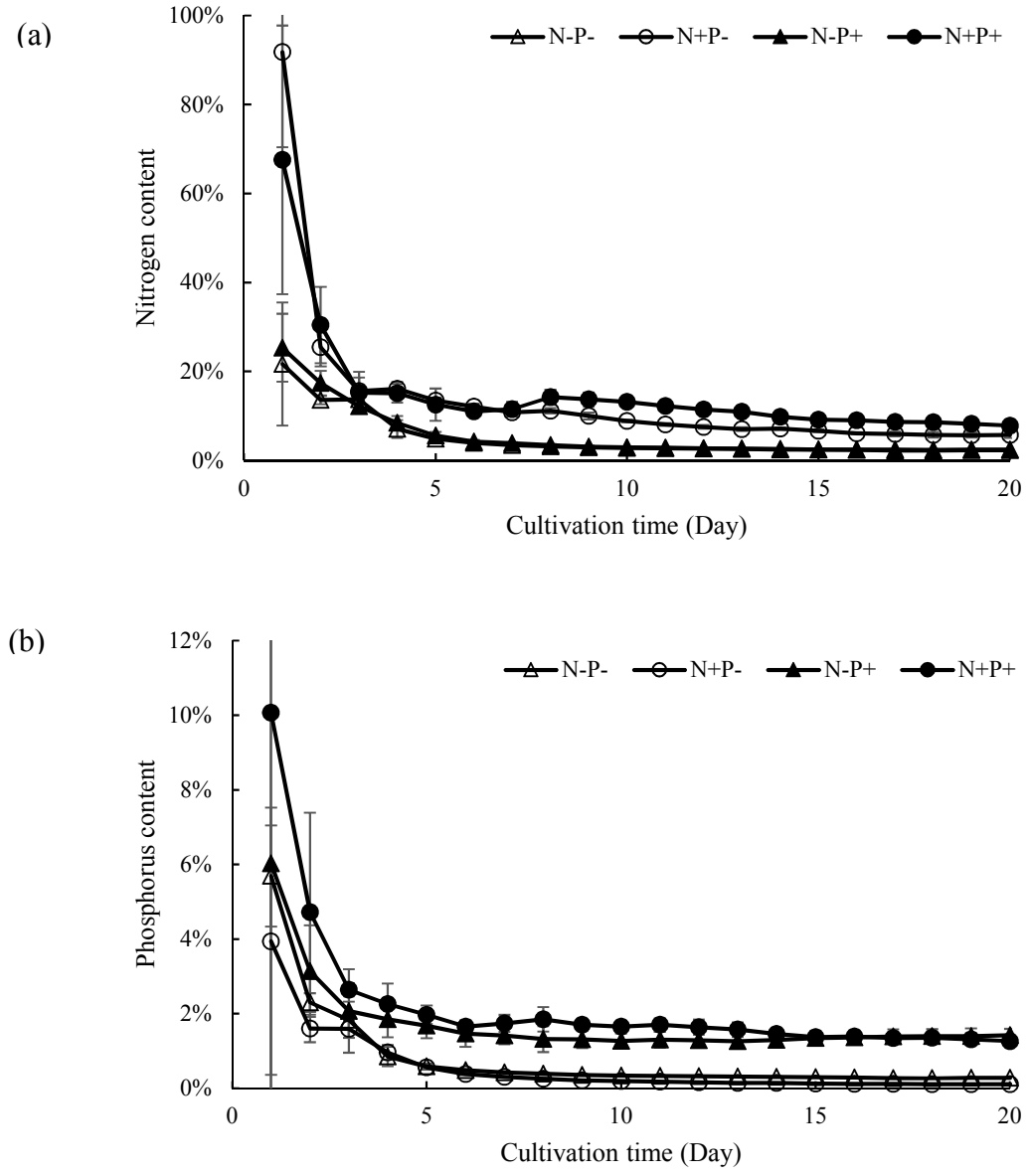

Figure C.4 Calculated nutrient content with the assumption of negligible initial nutrient storage: (a) nitrogen (p-value < 0.0001); (b) phosphorus (p-value = 0.019). Data are given as mean ± standard deviation of triplicates. Both nutrient contents have significant difference among different treatments.

3.4 Nutrient biomass yields and optimal N/P ratio

In flask experiments, nitrogen yield varied from 13 to 49 g-dry biomass/g-N, and phosphorus yield varied from 74 to 813 g-dry biomass/g-P. The result is summarized in Table 2. These results indicated that, for producing a given amount of biomass, nitrogen input can vary by a factor of 4 and phosphorus input can vary by a factor of 11. The large variation resulted from the large variation in the internal nutrient storage. Under limited conditions, internal nutrient storage of the corresponding nutrient was minimized, and most of the nutrient is converted to biomass, thus higher nutrient biomass yield is achieved.

To realize maximum yields of nitrogen and phosphorus simultaneously, an appropriate N/P ratio is required. If both yields were maximized at the same time, based on the maximum yields, the optimal N/P can be calculated, which is 36.7 (mol/mol), or 16.6 (g/g). Both yields were obtained from the stationary phase where growth rate (μ) is 0, and quotas of nitrogen and phosphorus were at a minimum. It agrees with the concept of an optimal N/P ratio proposed by Rhee and Gotham (Rhee and Gotham, 1980). Commonly used culture media may contain N/P ratios far away from this value, and consequently, one of the nutrients is limited on the efficiency. For instance, N/P ratio of BG-11 medium (Rippka et al., 1979) is 80, which may result in large intracellular nitrogen storage, and lower nitrogen yield. On the contrary, Bristol medium (Bold, 1949) has low N/P ratio of 1.7, which may lead to large intracellular phosphorus storage, and lower phosphorus yield. This result was tested in PBR experiments.

3.5 PBR experiment

The PBR tests were done under stronger light conditions to test the hypothesis of using an optimal N/P ratio for obtaining simultaneous maximum yields. Initial TN concentration was designed to

be 15 mg/L, same as in N- treatments. Following the N/P ratio of 36.7 (mol/mol) suggested by the bench-scale experiments, the initial TP concentration was set to 0.9 mg/L.

The growth curve, total nitrogen and phosphorus concentrations during the experiments is shown in Figure C.5. The growth last approximately 13 days, and most of the biomass accumulated after nutrient depletion in the media. The average nitrogen and phosphorus biomass yields were 44 g dry biomass/g-N and 812 g dry biomass/g-P, respectively. The results were within the variation of N yield in N- cultures and within the experimental error of P yield in P- cultures, suggesting that the nutrient yields can be maximized by using N/P ratio 36.7 (mol/mol).

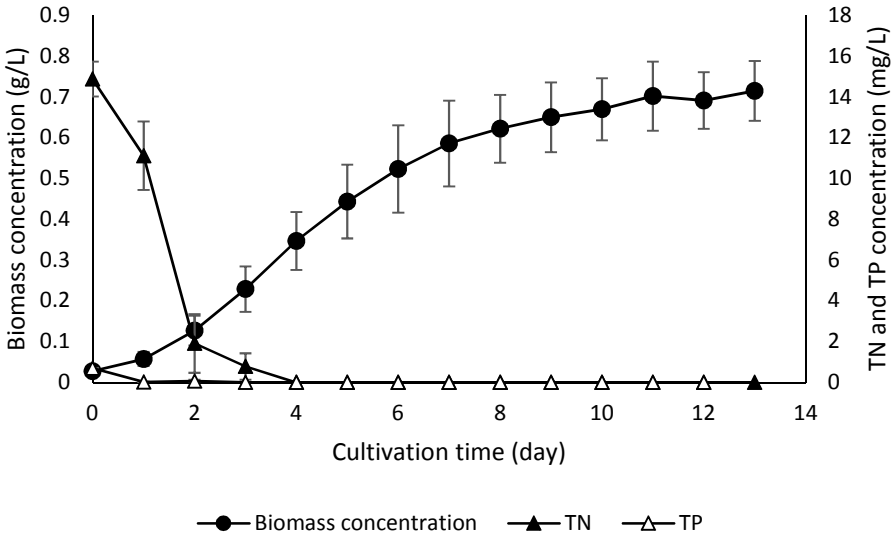

Figure C.5 Biomass concentration, total nitrogen concentration and total phosphorus concentration in the PBR experiment. Data are given as mean ± standard deviation of triplicates.

3.6 Outdoor raceway test

Outdoor raceway experiments were carried out to verify the large potential of improving phosphorus fertilizer usage in microalgae cultivation and potential maximum phosphorus yield under outdoor conditions. In our several attempts of testing nitrogen yield and optimal N/P ratio

with outdoor raceways, cultures crashed before any conclusive results can be reached, probably due to nitrogen stress. Nitrogen seems not only closely related to growth rate, but also the robustness of the culture. Providing the culture with sufficient nitrogen is critical to biomass productivity and culture health.

The two raceway experiments on phosphorus yields experiments were shown in Figure C5. Similar to observation in indoor experiments, microalgal growth was similar in high phosphorus and low phosphorus treatments (crash period excluded, p-value = 0.72 > 0.05). In RAFT30, the culture with higher phosphorus level even crashed earlier (Figure C5b). Phosphorus yields obtained in these experiments varied from 30.5 to 546.7 g-AFDW/g-P (Table 1), and biomass productivities were the same in the two raceways. Outdoor phosphorus biomass yield was lower than that achieved in indoor experiments, and this is not unexpected because the culture was exposed to more complicated environmental conditions. Variation of light intensity, water temperature, as well as contamination could post stresses that indoor culture didn't experience. However, compared to the average of phosphorus yield in other RAFT experiments (158 g-AFDW/g-P), maximum phosphorus yield obtained in this study by limiting phosphorus supply was more than three times higher (Figure C6). The result indicated that there is still a large space for optimizing phosphorus fertilizer usage.

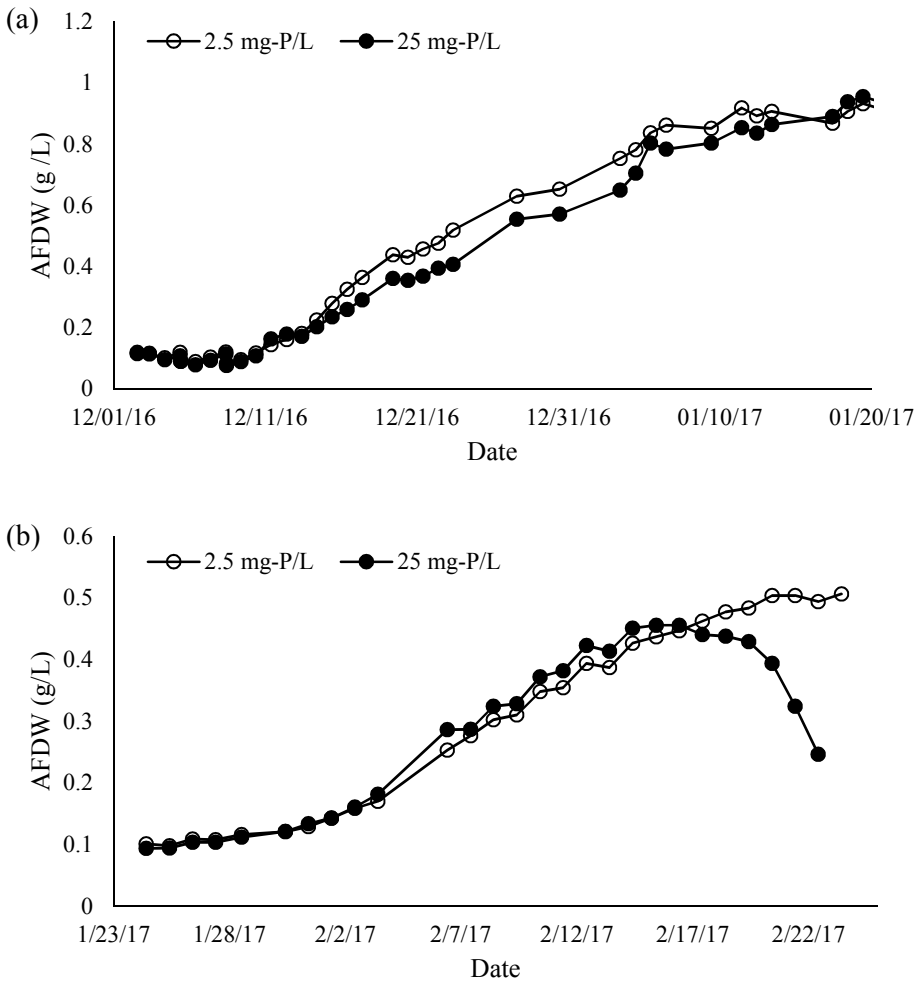

Figure C.6 Growth curve of outdoor raceway experiments. RAFT29 (a) and RAFT30 (b) are experiments for comparing phosphorus biomass yields

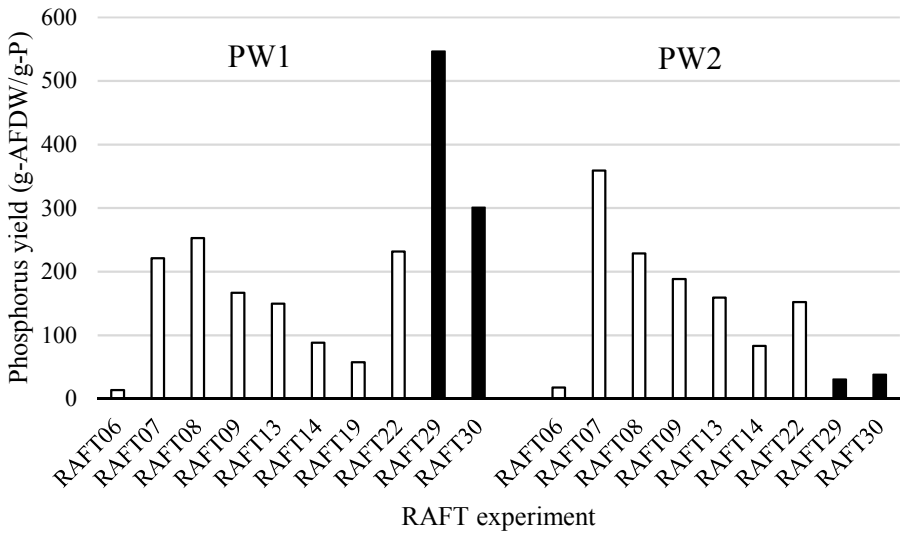

Figure C.7 Phosphorus biomass yield of *S. obliquus* in RAFT experiments. The columns in black represent the two experiments for phosphorus yield test. PW1: 2.5 mg-P/L; PW2: 25 mg-P/L

Table C.1 Nutrient yields of each treatment and validation test[a]

Treatment	N-P-	N+P-	N-P+	N+P+	PBR (N/P = 36.7)	Outdoor raceway
Nitrogen yield[b]	49 ± 2	28 ± 2	42 ± 1	13 ± 1	44 ± 6	n.a.
Phosphorus yield[b]	404 ± 16	813 ± 142	74 ± 10	78 ± 10	805 ± 9	30.5 – 546.7

[a] Data are expressed as mean ± standard deviation of triplicates

[b] The unit of yields is g-dry biomass/g-element

3.7 Lipid content

Lipid contents of cultures under different culture conditions were presented in Figure C7. Nutrient stress has long been recognized as an effective trigger to increase lipid content in algal cells (Feng et al., 2011; Li et al., 2008). *S. obliquus* was reported to accumulate lipid more than 35% of the

dry biomass under nitrogen-deficient conditions (Breuer et al., 2012). Similar results were observed in this study. Nitrogen stress exhibited strong impact on biomass lipid content (p-value < 0.0001). In comparison, phosphorus stress had insignificant effect on lipid content (p-value = 0.95 > 0.05). However, phosphorus stress was reported to stimulate triacylglycerol (TAG) production and increases lipid content in other microalgae species (Kamalanathan et al., 2015; Khozin-Goldberg et al., 2002). In indoor experiments, N+P- cultures had higher lipid content than N+P+ cultures, but in outdoor raceway experiments, P- cultures had lower lipid content than P+ cultures. Due to the more complicated outdoor growth condition, lipid content could be affected by other factors. It is not clear if the conflict between indoor and outdoor culture lipid contents was caused phosphorus concentration difference.

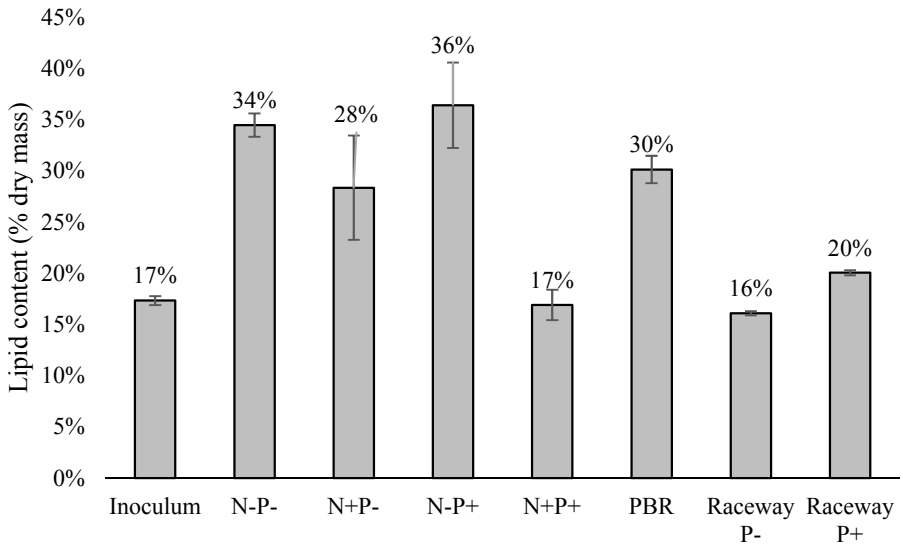

Figure C.8 Final lipid contents under different culture conditions. All the treatments started with the same inoculum. Data are given as mean ± standard deviation of triplicates

4. Conclusions

In this study, nitrogen and phosphorus biomass yields for *S. obliquus* were studied using indoor and outdoor reactors. Both yields varied greatly among different culture conditions, and their maximums were obtained under limited conditions. Based on the ratio of the maximum nitrogen and phosphorus yields, the optimal N/P ratio was determined (36.7 mol/mol) to maximize both yields simultaneously, and was verified by indoor PBR experiments. Maximum phosphorus yield achieved in outdoor raceway experiments was lower than that achieved in indoor experiments possibly due to stressors that didn't exist under indoor condition. However, considering phosphorus yields in previous RAFT outdoor experiments, as well as insignificant impact on growth and lipid content, we have shown that by limiting phosphorus input, fertilizer can be used much more efficiently without decreasing biomass productivity or lipid content in outdoor large-scale production.

5. References

Adams, C., Godfrey, V., Wahlen, B., Seefeldt, L., Bugbee, B., 2013. Understanding precision nitrogen stress to optimize the growth and lipid content tradeoff in oleaginous green microalgae. Bioresour. Technol. 131, 188–194. doi:10.1016/j.biortech.2012.12.143

Bligh, E.G., Dyer, W.J., 1959. A rapid method of total lipid extraction and purification. Can. J. Biochem. Physiol. 37, 911–917. doi:dx.doi.org/10,1139/cjm2014-0700

Bold, H.C., 1949. The Morphology of *Chlamydomonas chlamydogama*, Sp. Nov. Bull. Torrey Bot. Club 76, 101–108.

Breuer, G., Lamers, P.P., Martens, D.E., Draaisma, R.B., Wijffels, R.H., 2012. The impact of nitrogen starvation on the dynamics of triacylglycerol accumulation in nine microalgae

strains. Bioresour. Technol. 124, 217–226. doi:10.1016/j.biortech.2012.08.003

Chisti, Y., 2007. Biodiesel from microalgae. Trends Biotechnol. 26, 126–131. doi:10.1016/j.tibtech.2007.12.002

Clarens, A.F., Resurreccion, E.P., White, M. a, Colosi, L.M., 2010. Environmental life cycle comparison of algae to other bioenergy feedstocks. Environ. Sci. Technol. 44, 1813–9. doi:10.1021/es902838n

Converti, A., Casazza, A. a., Ortiz, E.Y., Perego, P., Del Borghi, M., 2009. Effect of temperature and nitrogen concentration on the growth and lipid content of *Nannochloropsis oculata* and *Chlorella vulgaris* for biodiesel production. Chem. Eng. Process. 48, 1146–1151. doi:10.1016/j.cep.2009.03.006

Elgavish, A., Elgavisd, G.A., Berman, T., 1980. Intracellular phosphorus pools in intact algal cells. FEBS Lett. 117, 137–142.

Elser, J., Bennett, E., 2011. Phosphorus cycle: A broken biogeochemical cycle. Nature 478, 29–31. doi:10.1038/478029a

Fageria, V.D., 2001. Nutrient Interactions in Crop Plants. J. Plant Nutr. 24, 1269–1290. doi:10.1081/PLN-100106981

Feng, P., Deng, Z., Hu, Z., Fan, L., 2011. Lipid accumulation and growth of *Chlorella zofingiensis* in flat plate photobioreactors outdoors. Bioresour. Technol. 102, 10577–84. doi:10.1016/j.biortech.2011.08.109

Gianquinto, G., Abu-rayyan, A., Tola, L. Di, Piccotino, D., Pezzarossa, B., 2000. Interaction effects of phosphorus and zinc on photosynthesis , growth and yield of dwarf bean grown in two environments. Plant Soil 220, 219–228. doi:10.1023/A:1004705008101

Gordillo, F.J.L., Goutx, M., Figueroa, F.L., Niell, F.X., 1998. Effects of light intensity , CO 2 and nitrogen supply on lipid class composition of *Dunaliella viridis*. J. Appl. Phycol. 10, 135–144.

Hsieh, C.H., Wu, W.T., 2009. Cultivation of microalgae for oil production with a cultivation strategy of urea limitation. Bioresour. Technol. 100, 3921–3926. doi:10.1016/j.biortech.2009.03.019

Jia, F., Kacira, M., Ogden, K.L., 2015. Multi-wavelength based optical density sensor for autonomous monitoring of microalgae. Sensors 15, 22234–22248. doi:10.3390/s150922234

Kamalanathan, M., Gleadow, R., Beardall, J., 2015. Impacts of phosphorus availability on lipid production by *Chlamydomonas reinhardtii*. Algal Res. 12, 191–196. doi:10.1016/j.algal.2015.08.021

Khozin-Goldberg, I., Didi-Cohen, S., Shayakhmetova, I., Cohen, Z., 2002. Biosynthesis of Eicosapentaenoic Acid (Epa) in the Freshwater Eustigmatophyte *Monodus Subterraneus* (Eustigmatophyceae)1. J. Phycol. 38, 745–756. doi:10.1046/j.1529-8817.2002.02006.x

Lardon, L., Helias, A., Sialve, B., Steyer, J.-P., Bernard, O., 2009. Life-Cycle Assessment of Biodiesel Production from Microalgae. Environ. Sci. Technol. 43, 6475–6481.

Levin, G. V, Shapiro, J., 1965. Metabolic uptake of phosphorus by wastewater organisms. Water Pollut. Control Fed. 37, 800–821.

Li, X., Hu, H., Gan, K., Sun, Y., 2010. Effects of different nitrogen and phosphorus concentrations on the growth, nutrient uptake, and lipid accumulation of a freshwater microalga *Scenedesmus* sp. Bioresour. Technol. 101, 5494–5500. doi:10.1016/j.biortech.2010.02.016

Li, Y., Horsman, M., Wang, B., Wu, N., Lan, C.Q., 2008. Effects of nitrogen sources on cell growth and lipid accumulation of green alga *Neochloris oleoabundans*. Appl. Microbiol. Biotechnol. 81, 629–36. doi:10.1007/s00253-008-1681-1

Liu, Z., Wang, G., Zhou, B.-C., 2008. Effect of iron on growth and lipid accumulation in *Chlorella vulgaris*. Bioresour. Technol. 99, 4717–4722. doi:10.1016/j.biortech.2007.09.073

Mandal, S., Mallick, N., 2009. Microalga *Scenedesmus obliquus* as a potential source for biodiesel production. Appl. Microbiol. Biotechnol. 84, 281–291. doi:10.1007/s00253-009-1935-6

McGlathery, K.J., Pedersen, M.F., Borum, J., 1996. Changes in Intracellular Nitrogen Pools and Feedback Controls on Nitrogen Uptake in *Chaetomorpha Linum* (Chlorophyta)1. J. Phycol. 32, 393–401. doi:10.1111/j.0022-3646.1996.00393.x

Murphy, L.S., Ellis, R., Adriano, D.C., 1981. Phosphorus-micronutrient interaction effects on crop production. J. Plant Nutr. 3, 593–613. doi:10.1080/01904168109362863

Nigam, P.S., Singh, A., 2011. Production of liquid biofuels from renewable resources. Prog. Energy Combust. Sci. 37, 52–68. doi:10.1016/j.pecs.2010.01.003

Powell, N., Shilton, A.N., Pratt, S., Chisti, Y., 2011. Factors influencing luxury uptake of phosphorus by microalgae in waste stabilization ponds. Environ. Sci. Technol. 64, 704–709. doi:10.1021/es703118s

Rhee, G.-Y., Gotham, I.J., 1980. Optimum N:P Ratios and Coexistence of Planktonic Algae. J. Phycol. doi:10.1111/j.1529-8817.1980.tb03065.x

Rippka, R., Deruelles, J., Waterbury, J.B., Herdman, M., Stanier, R.Y., 1979. Generic Assignments, Strain Histories and Properties of Pure Cultures of cyanobacteria. J. Gen.

Microbiol. 111, 1–61. doi:10.1099/00221287-111-1-1

Rogers, J.N., Rosenberg, J.N., Guzman, B.J., Oh, V.H., Elena, L., Ghassemi, A., Betenbaugh, M.J., Oyler, G.A., Donohue, M.D., 2014. A critical analysis of paddlewheel-driven raceway ponds for algal biofuel production at commercial scales. Algal Res. 4, 76–88. doi:10.1016/j.algal.2013.11.007

Ruangsomboon, S., Ganmanee, M., Choochote, S., 2013. Effects of different nitrogen, phosphorus, and iron concentrations and salinity on lipid production in newly isolated strain of the tropical green microalga, *Scenedesmus dimorphus* KMITL. J. Appl. Phycol. 25, 867–874. doi:10.1007/s10811-012-9956-4

Saxton, M.A., Arnold, R.J., Bourbonniere, R.A., McKay, R.M.L., Wilhelm, S.W., 2012. Plasticity of total and intracellular phosphorus quotas in *Microcystis aeruginosa* cultures and Lake Erie algal assemblages. Front. Microbiol. 3, 1–9. doi:10.3389/fmicb.2012.00003

Tantanasarit, C., Englande, A.J., Babel, S., 2013. Nitrogen, phosphorus and silicon uptake kinetics by marine diatom *Chaetoceros calcitrans* under high nutrient concentrations. J. Exp. Mar. Bio. Ecol. 446, 67–75. doi:10.1016/j.jembe.2013.05.004

Unkefer, C.J., Sayre, R.T., Magnuson, J.K., Anderson, D.B., Baxter, I., Blaby, I.K., Brown, J.K., Carleton, M., Cattolico, R.A., Dale, T., Devarenne, T.P., Downes, C.M., Dutcher, S.K., Fox, D.T., Goodenough, U., Jaworski, J., Holladay, J.E., Kramer, D.M., Koppisch, A.T., Lipton, M.S., Marrone, B.L., McCormick, M., Molnár, I., Mott, J.B., Ogden, K.L., Panisko, E.A., Pellegrini, M., Polle, J., Richardson, J.W., Sabarsky, M., Starkenburg, S.R., Stormo, G.D., Teshima, M., Twary, S.N., Unkefer, P.J., Yuan, J.S., Olivares, J.A., 2017. Review of the algal biology program within the National Alliance for Advanced Biofuels and

Bioproducts. Algal Res. 22, 187–215. doi:10.1016/j.algal.2016.06.002

Wijffels, R.H., Barbosa, M.J., 2010. An outlook on microalgal biofuels. Science 329, 796–799. doi:10.1126/science.1189003

Wu, Y.H., Yu, Y., Li, X., Hu, H.Y., Su, Z.F., 2012. Biomass production of a *Scenedesmus* sp. under phosphorous-starvation cultivation condition. Bioresour. Technol. 112, 193–198. doi:10.1016/j.biortech.2012.02.037

Zhila, N.O., Kalacheva, G.S., 2011. Effect of salinity on the biochemical composition of the alga *Botryococcus braunii* Kütz IPPAS H-252. J. Appl. Phycol. 23, 47–52. doi:10.1007/s10811-010-9532-8

Appendix D Nitrogen stress and health indicator in microalgae cultures

Song Gao [a], Renhe Qiu[b], Lydia Toscano-Palomar[b], Peter Waller*[a], Kimberly Ogden[b]

[a] Department of Agricultural and Biosystems Engineering, the University of Arizona, Tucson, AZ 85721, U.S.

[b] Department of Chemical Engineering, The University of Arizona, Tucson, AZ 85721, U.S.

Journal: Algal Research (under review)

Abstract

Many microalgae have internal nitrogen storage, which can be utilized when environmental nitrogen is limited. Storage introduces complexity in evaluating culture nitrogen status. In this study, three microalgae species were cultured in nitrogen depleted media, and the cellular nitrogen concentration, growth rate, lipid content, and nitrogen stress index were observed over time. Cellular nitrogen decline did not result in immediate growth reduction. Instead, growth rate vs. cellular nitrogen concentration followed the cell quota model. Lipid accumulation rate in response to nitrogen stress varied between species. However, lipid unsaturation degree decreased with nitrogen stress in all species. By taking advantage of the strong correlation between chlorophyll content and cellular nitrogen status, as well as the light absorbance feature of chlorophyll, an optical density based to quantify nitrogen/health status of the culture.

Keywords: *Chlorella sorokiniana*, *Scenedesmus obliquus*, *Monoraphidium minutum*, growth rate, lipid content, stress index

1. Introduction

Microalgae have been recognized as a competitive candidate for biofuel feedstock for their rapid growth, high lipid content, carbon neutrality and other advantages over land plant biomass (Chisti, 2007). They are also widely cultured for other purposes such as nutraceuticals, pharmaceuticals, food supplements, and animal feed (Vigani et al., 2015).

Nitrogen is an important nutrient in microalgal cultivation. It is in numerous biochemical compounds in the cell such as proteins, pigments, genetic materials, and energy transfer molecules (Cai et al., 2013). Sufficient nitrogen is a prerequisite to a healthy culture and maximizing biomass productivity (Converti et al., 2009; Mostert and Grobbelaar, 1987). Because chemical nitrogen addition is among the highest operating costs in microalgal cultivation (Rogers et al., 2014), it is imperative to quantify nitrogen requirements.

Cellular nitrogen status is not necessarily correlated with media nitrogen concentration. The cause of such variation is microalgae's capability of storing a large amount of nitrogen intracellularly. Thus, growth continues after nitrogen depletion in culture media. A variety of compounds, including nitrate, ammonium, amino acids, protein, RNA and pigments can serve as intracellular nitrogen pools and can support growth when external nitrogen is insufficient (DeManche et al., 1979; Dortch et al., 1984; Lourenço et al., 2004). However, internal nitrogen is not commonly tracked in large scale algal cultivation practices due to the complexity of analysis.

Under nitrogen limited conditions, most of nitrogen containing compounds in microalgae cells decline greatly (Dortch et al., 1984). Proteins and pigments are among the reduced synthesized compounds and decrease drastically with limited nitrogen accessibility (Yilancioglu et al., 2014).

Thus, nitrogen stress reduces growth rate. On the contrary, lipid content increases in the absence of nitrogen (Hu et al., 2008). With nitrogen deficiency, excess carbon is diverted to storage compounds such as lipids and starch when carbon fixation rate exceeds carbon demand for nitrogen assimilation (Turpin, 1991). Since photosynthesis cannot be shut down completely, lipid synthesis also works as a protective mechanism for siphoning off ATP and NAD(P)H, and prevents photodamage (Roessler, 1990). Restricting nitrogen can double lipid content in some green algae (Thompson, 1996). Cultivation techniques such as two-phase culture have been suggested (Rodolfi et al., 2009) to improve lipid productivity, in which nitrogen stress is introduced in the second phase to increase lipid content at the expense of growth rate.

In order to better understand the relationship between growth rate, lipid accumulation and nitrogen status, three microalgae were cultured under nitrogen-deplete conditions, with a range of nitrogen stress. Growth rate, cellular nitrogen, chlorophyll content, and lipid content, as well as fatty acid composition were monitored as growth rate diminished due to nitrogen limitation. By taking advantage of the high sensitivity of chlorophyll content to nitrogen stress, optical density, a common and simple measurement technique, can be used to evaluate nitrogen status in microalgae culture. The result was compared to outdoor raceway experiments in RAFT (Regional Algal Feedstock Testbed) project.

2. Materials and Methods

2.1 Microalgae culture conditions and sampling procedure

Three species, *Scenedesmus obliquus*, *Chlorella sorokiniana*, *Monoraphidium minutum*, were used in this study. *Scenedesmus obliquus* and *Chlorella sorokiniana* were isolated as part of the National Alliance for Biofuels and Bioproducts (NAABB) project by Dr. Juergen Polle (Unkefer

et al., 2017). *Monoraphidium minutum* was obtained from Texas A&M University and classified by 18S rDNA phylogenetic analysis in Dr Judith Brown's laboratory in the University of Arizona. The experiments were conducted in a flat plate bioreactor with height 60 cm, width 7.8 cm and breadth 60 cm. The culture volume was approximately 25 L. Fluorescent light tubes (AgroBrite, T5 54W 6400K) provided an average light intensity of 360 μmol m^{-2} s^{-1}, measured by a LI-COR LI-190R quantum sensor (LI-COR, Inc., Lincoln, Nebraska) at the bioreactor surface. The photoperiod was 12 h : 12 h (light : dark). The experiment was operated at ambient temperature 22 ℃, and culture was mixed by CO_2-enriched air (5%, v:v).

The control batch for each species was initially cultured in BG-11 media at optical density (750nm, OD_{750}) 0.5 ± 0.05, The corresponding dry mass concentration for *S. obliquus*, *C. sorokiniana*, and *M. minutum* were approximately 0.32, 0.18 and 0.27 g-dry mass/L, respectively. The specific growth rate obtained in control batch was the maximum growth rate (μ_m) achievable under the experimental conditions for each species. Before inoculation, the culture media was removed by centrifugation (8000 rpm, 10 minutes), and biomass was resuspended in nitrogen-excluded BG-11 media. The suspension was kept in the dark with aeration for 12 hours. The first culture batch after nitrogen removal started at a biomass concentration 0.5 ± 0.05 (OD_{750}) by diluting with nitrogen-excluded BG-11 media. After a 12h light period, the light was turned off, and the culture was kept in the dark for another 12 h. Every 24 hours, a new batch was started by diluting the culture to the same biomass concentration (OD_{750} = 0.5 ± 0.05) using nitrogen-excluded BG-11 medium following the same light cycle. This technique was used in order to reduce the nitrogen concentration and minimize the light difference (varying average light intensity) among batches. This cultural cycle continued until no growth was observed ($\mu \leq 0$).

Samples were taken at the beginning and at the end of the light period for each batch to determine the dry mass concentration. Biochemical composition analysis was conducted at the beginning of the light period to evaluate the initial chlorophyll and lipid status for each batch. The result was presented by average and standard deviation of measurements from three replicates for each species.

2.2 Growth rate and kinetic model

In order to ensure that dark respiration did not interfere with growth rate calculation, only biomass accumulation during the light period was used to estimate growth rate. Biomass concentration was measured by being rinsed with distilled water, filtered onto a pre-dried and pre-weighted GC/F grade Whatman glass microfiber filter, and dried at 75 ℃ for 24 hours. Specific growth rate was calculated as,

$$\mu = \frac{ln(DM_f) - ln(DM_i)}{\Delta t} \quad (1)$$

Where, DM_i is the initial dry mass concentration of the light period, DM_f is the final dry mass concentration of the light period, and Δt is the time interval between the two sampling points (0.5 day).

Because nitrogen was removed from the culture media, microalgal growth was fully supported by intracellular nitrogen storage. The relationship between internal nitrogen status and growth rate is expected to follow cell quota model (Droop, 1968). For each species, by setting the initial biomass concentration the same for each batch, light attenuation caused by self-shading was normalized among batches. Considering that the cultures were not dense, and the light path was short, light attenuation was assumed insignificant. After obtaining the specific growth rate (μ)

and cellular nitrogen content, model parameters were determined by fitting the experimental data to the cell quota model.

$$\mu = \mu'_m(1 - \frac{k_q}{Q}) \quad (2)$$

Where, μ is specific growth rate, k_q is the subsistence quota, Q is nitrogen quota, μ_m' is maximum specific growth rate at infinite Q.

2.3 Measurements of chlorophyll content, light absorbance spectrum, and cellular nitrogen content

Chlorophyll content was measured as described by Pancha et al. (2014). The extraction process was conducted in the dark, and samples were incubated in glass centrifuge tubes at 50 ℃ for 48 hours. Light absorbencies were measured using a spectrometer (Spectronic GenesysTM 5, Thermo Fisher Scientific Inc. Waltham, MA, USA). Based on dry mass concentration, chlorophyll content was converted to percentage of dry mass. The chlorophyll content was expressed as the sum of chlorophyll a and chlorophyll b. Using the same spectrometer, the light absorbance spectra of the raw sample were scanned, covering the major region of chlorophyll light absorption (400 – 800 nm).

Biomass samples were dried and ground to fine powder prior to elemental analysis. Cellular nitrogen content was measured by ECS 4010 CNS analyzer (Costech Analytical Technologies, Valencia, CA, USA) at ALEC (Arizona Laboratory for Emerging Contaminants, Tucson, AZ, U.S.).

2.4 Lipid content and fatty acid composition

Lipids were extracted by the method of Bligh and Dyer (1959) with modifications. Dried biomass was pulverized before mixing with chloroform and methanol (2:1, v/v) and held at room

temperature for at least 2 hours. Samples were then subjected to microwave treatment using a CEM Microwave Accelerated Reaction System (MARS, CEM Corp., Matthews, NC, USA). The suspensions were heated to 70 ºC and held for 60 min. The treated samples were filtered, and the chloroform layer was transferred into a pre-weighted glass tube. Organic solvent was then evaporated by a nitrogen evaporator (N-Evap 112, Organomation Association Inc., Berlin, MA, USA) to obtain dry lipid. After weighing the glass tube again, the lipid content was calculated from the known weight of the dry biomass (weight of lipid / weight of biomass, x %).

Fatty acid composition was measured by gas chromatography mass spectrum (GCMS). Extracted lipids were converted to fatty acid methyl esters (FAMEs) through a transesterification reaction [37, 38]. The FAMEs were solubilized in dichloromethane and analyzed with an Agilent 7890A gas chromatograph (GC) coupled to an Agilent 5975C inert XL mass selective detector (MSD) with Triple-Axis Detector (Agilent Technologies, Santa Clara, CA). A fused silica capillary column (Omegawax 250, Supelco, Bellefonte, L × I.D. 30 m × 0.25 mm, d_f 0.25 μm) was used for compound separation. The oven temperature was set to 90 °C at 2 min, increased at 3 °C min^{-1} to 240 °C in 50 mins, and maintained for 15 minutes. The carrier gas, helium, was injected at 1.0 mL min^{-1} constantly. Temperature for the mass spectrometry source, quadrupole and transfer line were set to 230 °C, 150 °C and 180 °C, respectively. Spectra were acquired in positive (70 eV) full scan model from 50 to 600 m/z at 1.4 spectra/s scan speed.

2.4 Statistical analysis

Data was collected from three replicates for each species. Parameters for the cell quota model were determined by linearizing the equation and fit with experimental data. R^2 was used to express the goodness of fit.

3. Results and Discussion

Cellular nitrogen is a direct measure of nitrogen status in the culture. Its relationship with growth rate, lipid content, and chlorophyll content were analyzed successively. During the experiment, chlorophyll content decreased drastically with decreasing cellular nitrogen content. By using light absorbance features of chlorophyll, we propose a method, using optical density, as a quick solution for evaluating nitrogen status.

3.1 Cellular nitrogen content and specific growth rate

Figure D1 shows the decrease in cellular nitrogen content over time. The first point in each of the graphs represents cellular nitrogen content before nitrogen removal. Sufficient external nitrogen allowed the cells to accumulate a large amount of intracellular nitrogen storage. The maximum cellular nitrogen in *C. sorokiniana* accounted for almost 10% of the total dry biomass. Cellular nitrogen in *S. obliquus* and *M. minutum* were approximately 8%.

Without external nitrogen, microalgae continued growing for 8 to 9 days while cellular nitrogen decreased by approximately two-thirds to 2.0%, 2.7% and 2.3% for *S. obliquus*, *C. sorokiniana*, and *M. minutum,* respectively. Because there was no growth at the end of the experiment ($\mu \approx 0$), the final nitrogen percentages are the minimum nitrogen requirements for supporting growth. Lower nitrogen contents were reported in other studies (Adams et al., 2013; Richardson et al., 1969). Considering that growth rates have already decreased to zero or below, further decreases in cellular nitrogen would cause biomass loss.

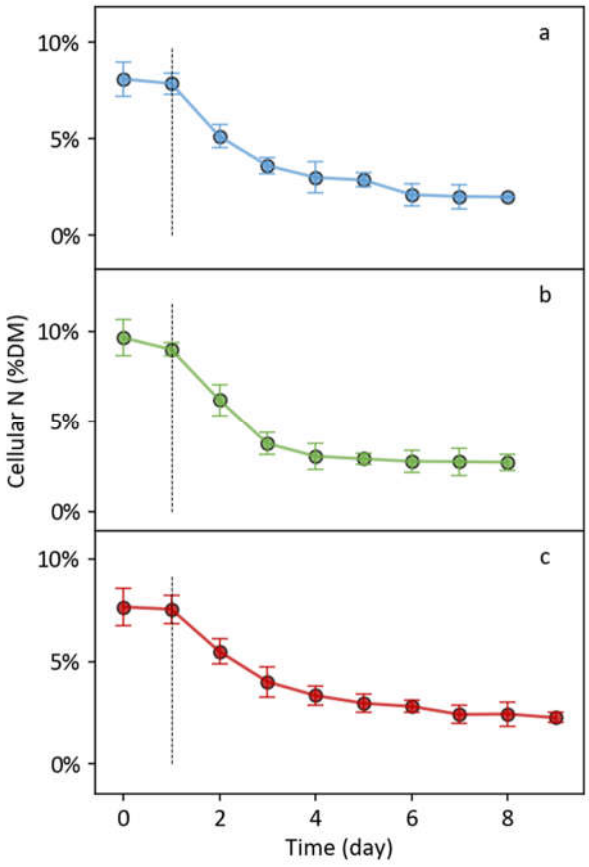

Figure D.1 Cellular nitrogen content at the beginning of each culture batch (day) during the experiment for *Scenedesmus obliquus* (a), *Chlorella sorokiniana* (b), and *Monoraphidium minutum* (c). The first point in each graph stands for cellular nitrogen content of nitrogen-rich culture. The dashed line marks the first culture batch after removing nitrogen. Data are given as mean ± standard deviation of triplicates

Specific growth rates were plotted against cellular nitrogen content in Figure D2. Due to the high internal nitrogen content at the beginning after nitrogen removal, the cultures didn't experience significant growth rate reduction. They maintained more than 80% of their maximum growth rates during the first two days. At lower cellular nitrogen range, approximately 4%, growth rate decreased faster with decreasing nitrogen content.

The relationship between specific growth rate and cellular nitrogen content is described by the cell quota model (Equation 2) and is presented by the solid lines in Figure D2. Fitted model parameters were k_q = 2.1%, μ_m' = 1.27 for *S. obliquus*, k_q = 2.6%, μ_m' = 1.49 for *C. sorokiniana,* k_q = 2.3%, μ_m' = 0.93 for *M. minutum.* Based on the results, when cellular nitrogen decreased to approximately 2%, microalgae had no growth ($\mu \leq 0$). At this point, all the remaining nitrogen is likely to be in structural materials that are inaccessible as nitrogen sources for growth. On the other hand, cellular nitrogen at 6-8% and above only caused minimal growth rate reduction ($\mu \geq 90\%\mu_m$).

In commercial scale cultivation, nitrogen fertilizer application is easy to track. Because algae cells consume most of the available nitrogen, the ratio between applied nitrogen fertilizer/biomass produced, which we call nitrogen availability, can provide an estimate of cellular content. Based on the results, with slight variance among species, nitrogen availability between 6 to 10% can avoid significant growth rate reduction as well as over-fertilization.

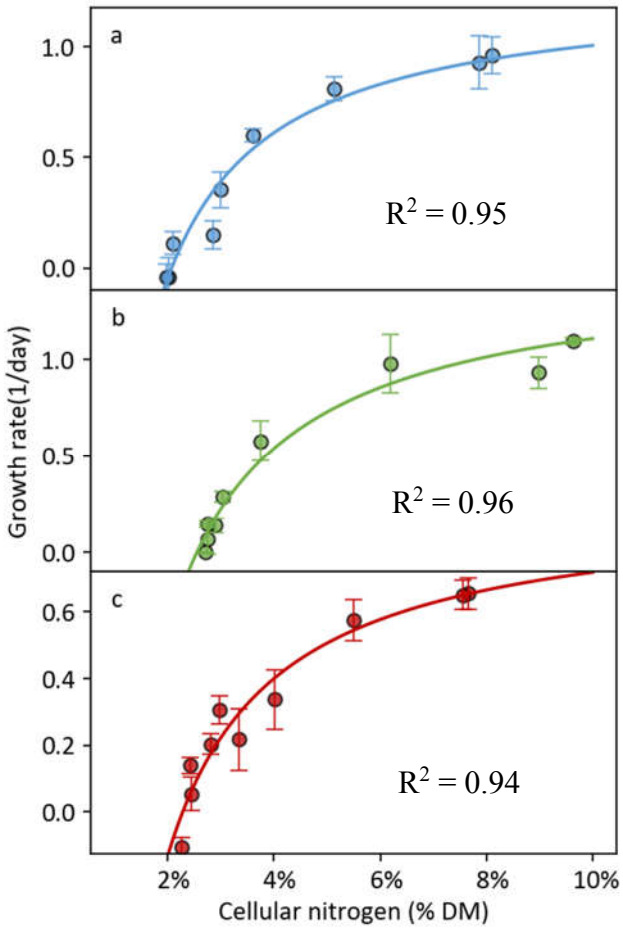

Figure D.2 Plot of specific growth rates (dots) and the cell quota model (solid lines) as a function of cellular nitrogen for *Scenedesmus obliquus* (a), *Chlorella sorokiniana* (b), and *Monoraphidium minutum* (c). Data are given as mean ± standard deviation of triplicates

3.2 Lipid content, lipid productivity and fatty acid composition

While it limits microalgal growth rates, nitrogen stress increases biomass lipid content (Converti et al., 2009; Rodolfi et al., 2009). Lipid contents of *S. obliquus*, *C. sorokiniana*, and *M. minutum* were increased from 19%, 19% and 24%, to 27%, 35% and 43 % (Figure D3) as internal nitrogen was depleted. Lipid increase for *S. obliquus* and *C. sorokiniana* was minimal above 3-4% cellular nitrogen but then increased rapidly with nitrogen stress. Other studies have also

observed that an increase in lipid synthesis took place when cellular nitrogen was below approximately 3% of dry weight (Richardson et al., 1969). Adams et al. (2013) found that the trigger point of lipid synthesis varied between species, and ranged from 3 to 7.5 % cellular nitrogen. In comparison to the previous two species, lipid content in *M. minutum* began to increase at the high end of this range, approximately 7% cellular nitrogen. The lowest cellular nitrogen obtained in this study was approximately 2%. We did not investigate whether the trend of lipid accumulation would continue with increasing nitrogen stress. However, given the fact that an elongated stationary phase could substantially increase lipid content (Zhang and Hong, 2014), and higher lipid content was reported in some algae (Mandal and Mallick, 2009; Zhang and Hong, 2014; Zhao et al., 2016), lower cellular nitrogen could potentially stimulate more lipid synthesis.

The downside of increasing lipid content using nitrogen stress is the diminishing biomass production (Rodolfi et al., 2009). In Fig. 4, growth rate was also plotted against cellular nitrogen for each species, showing the tradeoff between lipid content and growth rate. Under the experimental and operational conditions in this study, the net lipid accumulation (only during light period) were maximized at cellular nitrogen concentrations of 7.9% (67 mg/L/day), 6.2% (53 mg/L/day), and 7.6% (47 mg/L/day) for *S. obliquus*, *C. sorokiniana*, and *M. minutum*, respectively. However, microalgal growth and lipid accumulation are also affected by other environmental conditions such as light intensity, pH, temperature, salinity, and iron concentration (Álvarez-Díaz et al., 2014; Converti et al., 2009; Difusa et al., 2015; Kaewkannetra et al., 2012; Liu et al., 2008) . Determination of optimal nitrogen stress for maximization of lipid productivity should be made with consideration of actual growth conditions, operation conditions and reactor type.

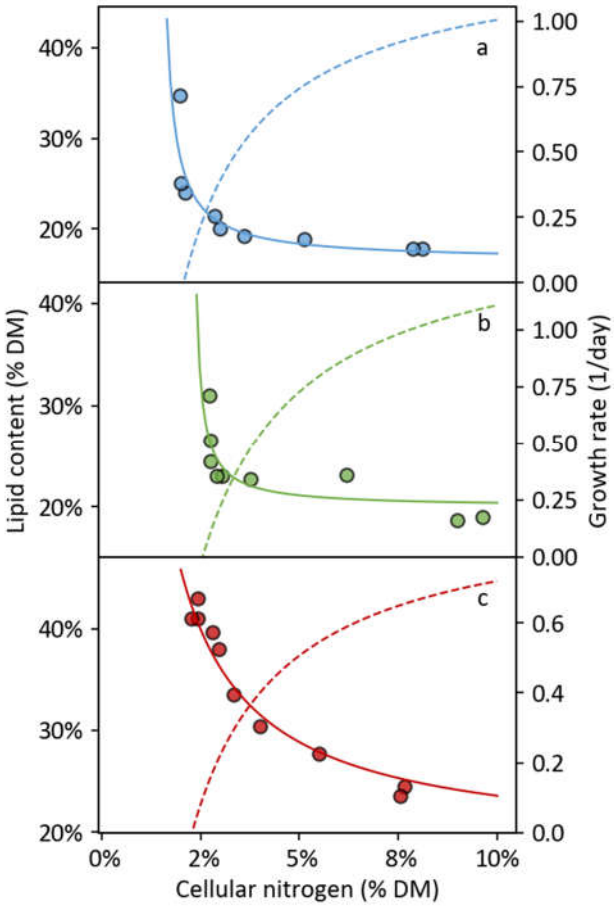

Figure D.3 Lipid content as a function of cellular nitrogen for *Scenedesmus obliquus* (a), *Chlorella sorokiniana* (b), and *Monoraphidium minutum* (c). Solid line represents the trend of lipid accumulation at different cellular nitrogen contents. Dashed line represents growth rate as a function of cellular nitrogen, obtained from the section 3.1

Lipids were mostly C16 and C18 fatty acids (90 to 98%). The degree of lipid unsaturation was inversely proportional to cellular nitrogen (Figure D.4). With nitrogen stress, saturated fatty acids (SFA) and mono-unsaturated fatty acids (MUFA) increased as poly-unsaturated fatty acids (PUFA) decreased. This result is in agreement with previous studies (An et al., 2017; Hu et al., 2015; Ramanna et al., 2014). The extent of unsaturation degree varied between species.

Compared to the starting levels, maximum increase of SFA and MUFA was observed in *S. obliquus* cultures, and largest decrease of PUFA was observed in *M. minutum* cultures. During nutrient deficiency with sufficient light and CO_2, microalgae cells divert fatty acids into triacylglyceride (TAG) synthesis as growth diminishes and membrane compounds become less (Sharma et al., 2012). SFA and MUFA are the primary components of TAG (Roessler, 1990), hence the degree of unsaturation shifted towards SFA and MUFA as TAG accumulated. High nitrogen stress may be favorable if the biomass is cultivated for biodiesel conversion because low SFA and PUFA improve oxidative stability and low temperature operability of biodiesel (Hoekman et al., 2012). Other applications of biomass such as human and animal diets may prefer higher PUFA content (Adarme-Vega et al., 2012).

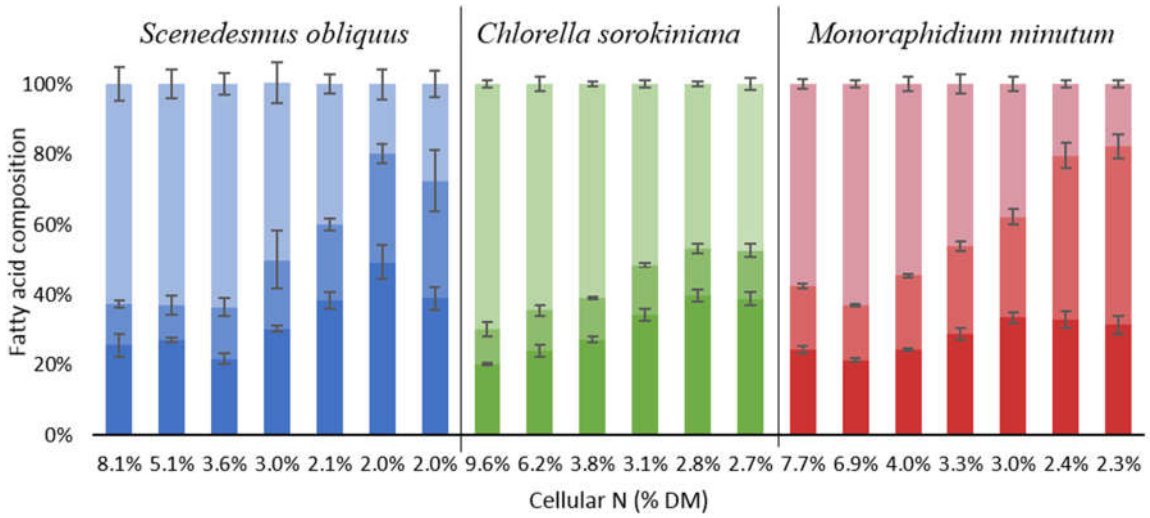

Figure D.4 Lipid compositions of *Scenedesmus obliquus*, *Chlorella sorokiniana*, and *Monoraphidium minutum* at different cellular nitrogen contents. Sections in each column represent PUFA (top), MUFA (middle), and SFA (bottom). Data are given as mean ± standard deviation of triplicates

3.3 Chlorophyll content

As a structural element of chlorophyll molecules, nitrogen is critical to chlorophyll synthesis (Geider et al., 1998). Chlorophyll content declined rapidly as nitrogen was depleted (Figure D.5a, 5b, 5c). Chlorophyll is one of the most accessible internal nitrogen pool in microalgae cells (Li et al., 2008). Lowered external nitrogen accessibility is usually followed by immediate and drastic decrease of chlorophyll content (Cakmak et al., 2012; Yilancioglu et al., 2014). During the experiments, chlorophyll content of the microalgae decreased almost linearly with the decreasing cellular nitrogen content, indicating the potential of using features associated with chlorophyll content as a measurement of cellular nitrogen status (Figure D.5d).

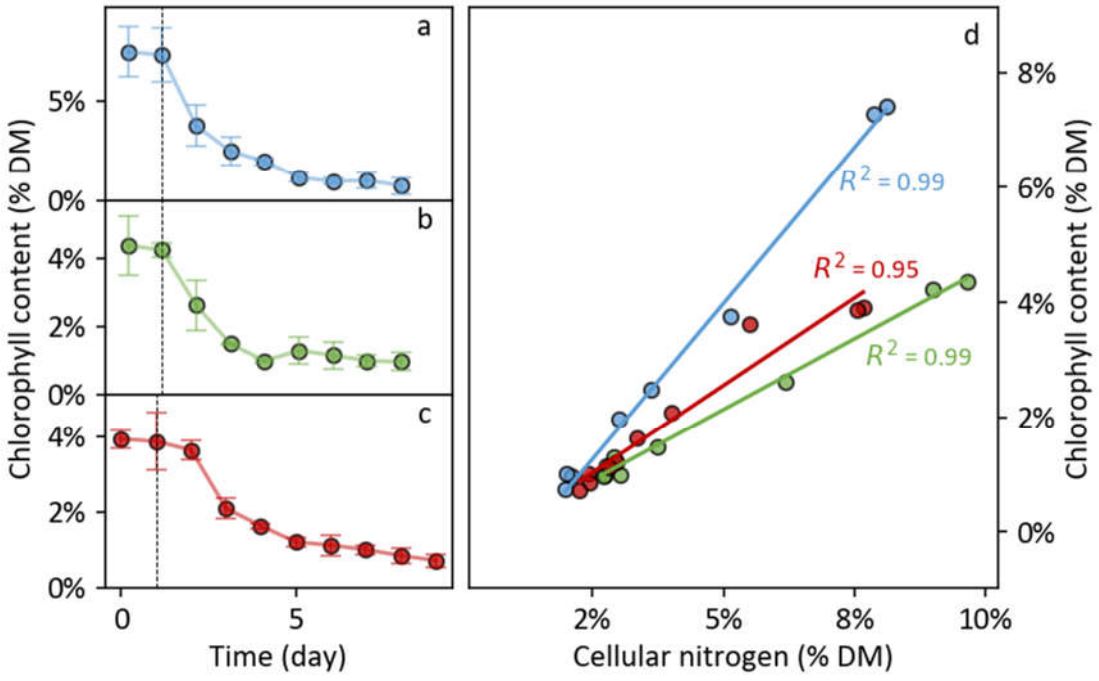

Figure D.5 Chlorophyll contents of *Scenedesmus obliquus* (a), *Chlorella sorokiniana* (b), and *Monoraphidium minutum* (c) decreased with culture time. (d) shows the linear relationship between

chlorophyll content and cellular nitrogen in *S. obliquus* (blue), *C. sorokiniana* (green), and *M. minutum* (red) cultures. Data are given as mean ± standard deviation of triplicates

3.4 Nitrogen stress index

Optical density (OD) is a quick and convenient measure of microalgal biomass concentration (Havlik et al., 2013; Santos-ballardo et al., 2015). The OD at wavelengths within chlorophyll light absorbance spectrum, such as 680 nm, is sensitive to chlorophyll content, whereas OD at wavelengths outside the region, such as 750 nm, is more representative of biomass concentration (Griffiths et al., 2011). Therefore, comparison of chlorophyll sensitive OD and chlorophyll insensitive OD can be used to evaluate chlorophyll content in biomass, which strongly correlates with nitrogen status. Figure 7 shows normalized OD at 400 nm to 800 nm to OD_{750} (OD/OD_{750}, Figure D.6). With increasing nitrogen stress, normalized OD decreased with chlorophyll content. The largest variation occurred at 680 nm in the three species, thus we selected normalized OD_{680} as the nitrogen stress index.

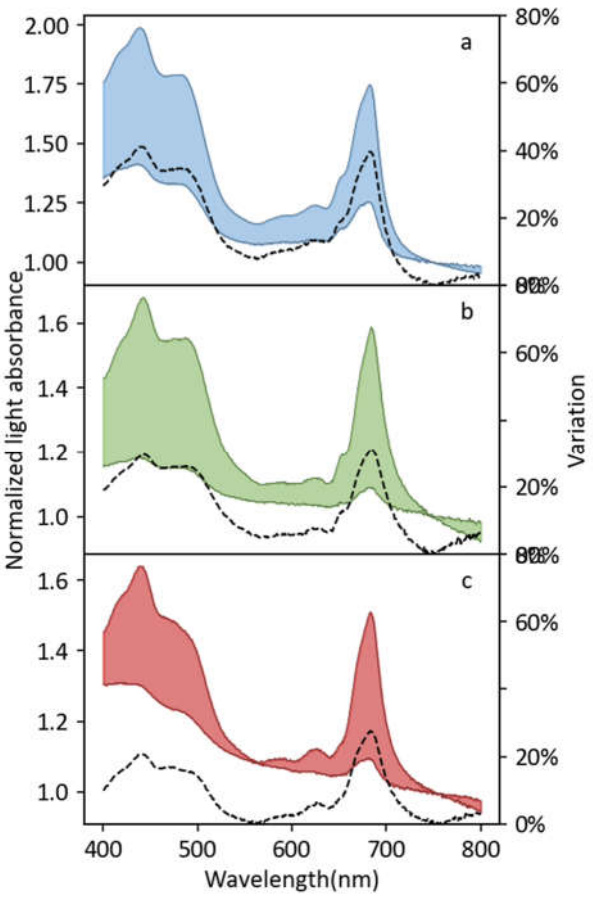

Figure D.6 Normalized light absorbance within 400 - 800 nm (nitrogen status index, OD/OD_{750}) decreased with increasing nitrogen stress of *Scenedesmus obliquus* (a), *Chlorella sorokiniana* (b) and *Monoraphidium minutum* (c). Colored area shows the variation of normalized light absorbance between first batch ($\mu = \mu_m$, upper bound) and the last batch ($\mu \leq 0$, lower bound). Dashed line indicates the variation of the index at each wavelength from the beginning to the end of the experiment

The stress index was closely related to cellular nitrogen content for all species (Figure D.7). Thus, growth rate and biomass chemical composition can be predicted by the index. For instance, an index value of 1.6 for *C. sorokiniana* culture indicates approximately 10% cellular nitrogen, at which nitrogen concentration the maximum growth rate was achieved. Whereas an

index value below 1.08 indicates severe nitrogen stress and no growth is observed. An index value 1.17 in *S. obliquus* culture corresponds to 3% cellular nitrogen, which triggers rapid lipid accumulation.

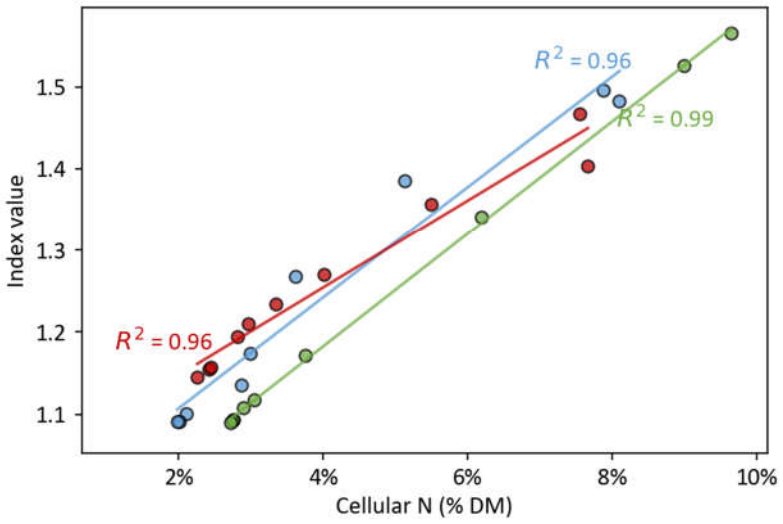

Figure D.7 Relationship between nitrogen status index and cellular nitrogen content was found in *Scenedesmus obliquus* (blue), *Chlorella sorokiniana* (green), and *Monoraphidium minutum* (red). The equations of index value (I) is shown as a function of cellular nitrogen (N) are placed at the right bottom corner

During the experiments, culture appearance was altered greatly with increasing nitrogen stress. Figure D8 presents the dried biomass, stress index value, and corresponding cellular nitrogen content. The degree of greenness of the biomass decreased with decreasing chlorophyll content. The culture turned from dark green to light green with increasing nitrogen stress, resulting in a declining index value. Mild nitrogen stress in early culture may not be easily noticed by microscopic or bare eye examination. However, the index value can reflect the intensity of nitrogen stress in the slightly stressed range.

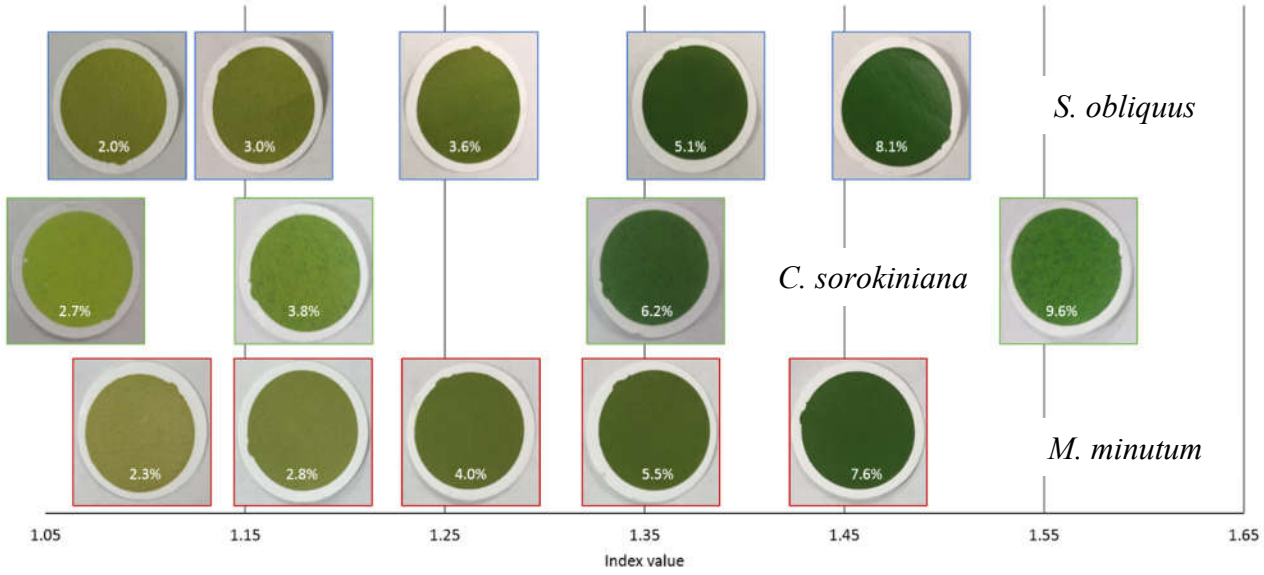

Figure D.8 Dried biomass versus nitrogen status index value. *Scenedesmus obliquus*, *Chlorella sorokiniana*, and *Monoraphidium minutum* are presented in top, middle and bottom row, respectively. Percentage in white is the corresponding cellular nitrogen content of the sample. All the values presented are the average of triplicates used in previous figures.

Because the index is based on chlorophyll content, multiple sources of stress can cause the same effect. For example, other nutrients, such as magnesium and iron, are also essential for chlorophyll synthesis, and shortage of these nutrients can cause a lowered index value. Contamination is a common problem in open culture systems (Brennan and Owende, 2010; Rashid et al., 2014). Invasion of non-photosynthetic contaminants is expected to lower chlorophyll content in biomass, which lowers the index value. In such cases, an index value in the stress range indicates presence of other stress, and analysis might be needed to determine the source.

Figure D9 shows an example from outdoor raceway experiments for each species. Although the index range of the three species in outdoor experiments is lower than that in laboratory experiments, nitrogen addition usually leads to increasing index value. Actively growing outdoor culture usually has an index value greater than 1.3 for all three microalgae, and stressed or crashing culture usually has an index below 1.2. In Figure D9c, the index value decreased after nitrogen addition on day 55. Microscopic examination of the culture identified severe contamination by ciliates and flagellates.

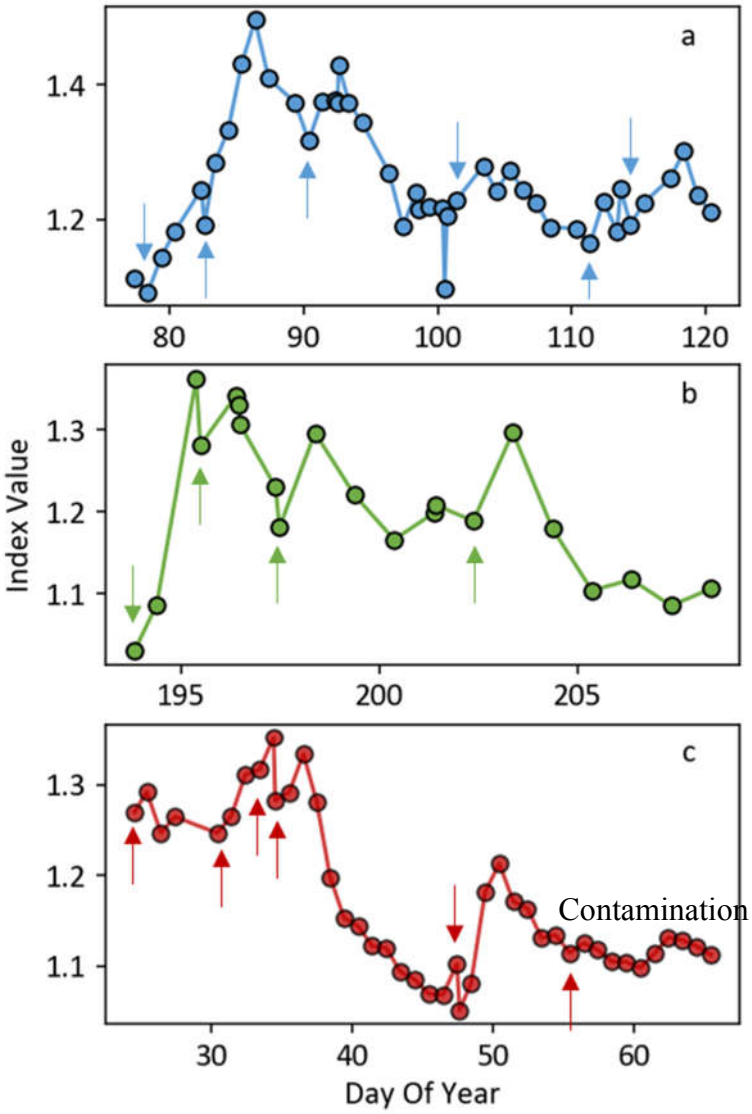

Figure D.9 Examples of nitrogen stress index value response to nutrient addition in outdoor ARID raceway (Waller et al., 2012) experiments in RAFT project. In the three experiments, *Scenedesmus obliquus* (a, RAFT07, 2015), *Chlorella sorokiniana* (b, RAFT21, 2016) and *Monoraphidium minutum* (c, RAFT31, 2017) cultures, nitrogen stress index increased after nitrogen addition (represented by arrows)

4. Conclusions

Under nitrogen-deplete condition, microalgal growth is supported for several days by internal nitrogen storage. The cell quota model provided a reasonable representation of growth rate

reduction caused by nitrogen stress. The intensity of nitrogen stress required for rapid lipid accumulation varied among species, but the degree of lipid unsaturation appeared similarly in the examined microalgae. By taking the advantage of strong correlation between chlorophyll content and cellular nitrogen, as well as light absorbance feature of chlorophyll, the nitrogen stress index can provide a quick and convenient method for evaluating culture nitrogen status.

5. Acknowledgements

This work was supported by the U.S. Department of Energy Bioenergy Technologies Office Regional Algal Feedstock Testbed (RAFT) Project [grant number DE-EE0006269].

6. References

Adams, C., Godfrey, V., Wahlen, B., Seefeldt, L., Bugbee, B., 2013. Understanding precision nitrogen stress to optimize the growth and lipid content tradeoff in oleaginous green microalgae. Bioresour. Technol. 131, 188–194. doi:10.1016/j.biortech.2012.12.143

Adarme-Vega, T.C., Lim, D.K.Y., Timmins, M., Vernen, F., Li, Y., Schenk, P.M., 2012. Microalgal biofactories: a promising approach towards sustainable omega-3 fatty acid production. Microb. Cell Fact. 11, 96. doi:10.1186/1475-2859-11-96

Álvarez-Díaz, P.D., Ruiz, J., Arbib, Z., Barragán, J., Garrido-Pérez, C., Perales, J.A., 2014. Lipid Production of Microalga *Ankistrodesmus falcatus* Increased by Nutrient and Light Starvation in a Two-Stage Cultivation Process. Appl. Biochem. Biotechnol. 174, 1471–1483. doi:10.1007/s12010-014-1126-5

An, M., Wang, Y., Liu, F., Qi, X., Zheng, Z., Ye, N., Sun, C., Miao, J., 2017. Biomass, nutrient uptake and fatty acid composition of *Chlamydomonas* sp. ICE-L in response to different nitrogen sources. Acta Oceanol. Sin. 36, 105–110. doi:10.1007/s13131-017-0984-4

Bligh, E.G., Dyer, W.J., 1959. A rapid method of total lipid extraction and purification. Can. J. Biochem. Physiol. 37, 911–917. doi:dx.doi.org/10,1139/cjm2014-0700

Brennan, L., Owende, P., 2010. Biofuels from microalgae—A review of technologies for production, processing, and extractions of biofuels and co-products. Renew. Sustain. Energy Rev. 14, 557–577. doi:10.1016/j.rser.2009.10.009

Cai, T., Park, S.Y., Li, Y., 2013. Nutrient recovery from wastewater streams by microalgae: Status and prospects. Renew. Sustain. Energy Rev. 19, 360–369. doi:10.1016/j.rser.2012.11.030

Cakmak, T., Angun, P., Demiray, Y.E., Ozkan, A.D., Elibol, Z., Tekinay, T., 2012. Differential effects of nitrogen and sulfur deprivation on growth and biodiesel feedstock production of *Chlamydomonas reinhardtii*. Biotechnol. Bioeng. 109, 1947–1957. doi:10.1002/bit.24474

Chisti, Y., 2007. Biodiesel from microalgae. Biotechnol. Adv. 25, 294–306. doi:10.1016/j.biotechadv.2007.02.001

Converti, A., Casazza, A. a., Ortiz, E.Y., Perego, P., Del Borghi, M., 2009. Effect of temperature and nitrogen concentration on the growth and lipid content of *Nannochloropsis oculata* and *Chlorella vulgaris* for biodiesel production. Chem. Eng. Process. 48, 1146–1151. doi:10.1016/j.cep.2009.03.006

DeManche, J.M., Jr, H.C.C., Lundy, D.W., Donaghay, P.L., 1979. The rapid response of the marine diatom *Skeletonema costatum* to changes in external and internal nutrient concentration. Mar. Biol. 53, 323–333. doi:10.1007/BF00391615

Difusa, A., Talukdar, J., Kalita, M.C., Mohanty, K., Goud, V. V, 2015. Effect of light intensity and pH condition on the growth , biomass and lipid content of microalgae *Scenedesmus*

species. Biofuels 6, 37–44. doi:10.1080/17597269.2015.1045274

Dortch, Q., Clayton, J.R., Thoresen, S.S., Ahmed, S.I., 1984. Species differences in accumulation of nitrogen pools in phytoplankton. Mar. Biol. 81, 237–250. doi:10.1038/470444a

Droop, M.R., 1968. Vitamin B12 and Marine Ecology. IV. The Kinetics of Uptake, Growth and Inhibition in *Monochrysis lutheri*. J. Mar. Biol. Assoc. United Kingdom 48, 689–733.

Geider, R.J., Maclntyre, H.L., Kana, T.M., 1998. A dynamic regulatory model of phytoplanktonic acclimation to light, nutrients, and temperature. Limnol. Oceanogr. 43, 679–694. doi:10.4319/lo.1998.43.4.0679

Griffiths, M.J., Garcin, C., van Hille, R.P., Harrison, S.T.L., 2011. Interference by pigment in the estimation of microalgal biomass concentration by optical density. J. Microbiol. Methods 85, 119–123. doi:10.1016/j.mimet.2011.02.005

Havlik, I., Lindner, P., Scheper, T., Reardon, K.F., 2013. On-line monitoring of large cultivations of microalgae and cyanobacteria. Trends Biotechnol. 31, 406–414.

Hoekman, S.K., Broch, A., Robbins, C., Ceniceros, E., Natarajan, M., 2012. Review of biodiesel composition, properties, and specifications. Renew. Sustain. Energy Rev. 16, 143–169. doi:10.1016/j.rser.2011.07.143

Hu, Q., Sommerfeld, M., Jarvis, E., Ghirardi, M., Posewitz, M., Seibert, M., Darzins, A., 2008. Microalgal triacylglycerols as feedstocks for biofuel production: Perspectives and advances. Plant J. 54, 621–639. doi:10.1111/j.1365-313X.2008.03492.x

Hu, Q., Xiang, W., Dai, S., Li, T., Yang, F., Jia, Q., Wang, G., Wu, H., 2015. The influence of cultivation period on growth and biodiesel properties of microalga *Nannochloropsis*

gaditana 1049. Bioresour. Technol. 192, 157–164. doi:10.1016/j.biortech.2015.04.106

Kaewkannetra, P., Enmak, P., Chiu, T., 2012. The effect of CO2 and salinity on the cultivation of *Scenedesmus obliquus* for biodiesel production. Biotechnol. Bioprocess Eng. 17, 591–597. doi:10.1007/s12257-011-0533-5

Li, Y., Horsman, M., Wang, B., Wu, N., Lan, C.Q., 2008. Effects of nitrogen sources on cell growth and lipid accumulation of green alga *Neochloris oleoabundans*. Appl. Microbiol. Biotechnol. 81, 629–36. doi:10.1007/s00253-008-1681-1

Liu, Z., Wang, G., Zhou, B.-C., 2008. Effect of iron on growth and lipid accumulation in *Chlorella vulgaris*. Bioresour. Technol. 99, 4717–4722. doi:10.1016/j.biortech.2007.09.073

Lourenço, S.O., Barbarino, E., Lavín, P.L., Lanfer Marquez, U.M., Aidar, E., 2004. Distribution of intracellular nitrogen in marine microalgae: Calculation of new nitrogen-to-protein conversion factors. Eur. J. Phycol. 39, 17–32. doi:10.1080/0967026032000157156

Mandal, S., Mallick, N., 2009. Microalga *Scenedesmus obliquus* as a potential source for biodiesel production. Appl. Microbiol. Biotechnol. 84, 281–291. doi:10.1007/s00253-009-1935-6

Mostert, E.S., Grobbelaar, J.U., 1987. The influence of nitrogen and phosphorus on algal growth and quality in outdoor mass algal cultures. Biomass 13, 219–233. doi:10.1016/0144-4565(87)90061-8

Pancha, I., Chokshi, K., George, B., Ghosh, T., Paliwal, C., Maurya, R., Mishra, S., 2014. Nitrogen stress triggered biochemical and morphological changes in the microalgae *Scenedesmus* sp. CCNM 1077. Bioresour. Technol. 156, 146–154. doi:10.1016/j.biortech.2014.01.025

Ramanna, L., Guldhe, A., Rawat, I., Bux, F., 2014. The optimization of biomass and lipid yields of *Chlorella sorokiniana* when using wastewater supplemented with different nitrogen sources. Bioresour. Technol. 168, 127–135. doi:10.1016/j.biortech.2014.03.064

Rashid, N., Ur Rehman, M.S., Sadiq, M., Mahmood, T., Han, J.-I., 2014. Current status, issues and developments in microalgae derived biodiesel production. Renew. Sustain. Energy Rev. 40, 760–778. doi:10.1016/j.rser.2014.07.104

Richardson, B., Orcutt, D.M., Schwertner, H.A., Martinez, C.L., Wickline, H.E., 1969. Effects of nitrogen limitation on the growth and composition of unicellular algae in continuous culture. Appl. Microbiol. 18, 245–50.

Rodolfi, L., Chini Zittelli, G., Bassi, N., Padovani, G., Biondi, N., Bonini, G., Tredici, M.R., 2009. Microalgae for oil: strain selection, induction of lipid synthesis and outdoor mass cultivation in a low-cost photobioreactor. Biotechnol. Bioeng. 102, 100–12. doi:10.1002/bit.22033

Roessler, P.G., 1990. Environmental Control of Glycerolipid Metabolism in Microalgae: Commercial Implications and Future Research Directions. J. Phycol. doi:10.1111/j.0022-3646.1990.00393.x

Rogers, J.N., Rosenberg, J.N., Guzman, B.J., Oh, V.H., Elena, L., Ghassemi, A., Betenbaugh, M.J., Oyler, G.A., Donohue, M.D., 2014. A critical analysis of paddlewheel-driven raceway ponds for algal biofuel production at commercial scales. Algal Res. 4, 76–88. doi:10.1016/j.algal.2013.11.007

Santos-ballardo, D.U., Rossi, S., Hernández, V., Vázquez, R., Rendón-unceta, C., Caro-corrales, J., Valdez-ortiz, A., 2015. A simple spectrophotometric method for biomass measurement

of important microalgae species in aquaculture. Aquaculture 448, 87–92. doi:10.1016/j.aquaculture.2015.05.044

Sharma, K.K., Schuhmann, H., Schenk, P.M., 2012. High lipid induction in microalgae for biodiesel production. Energies 5, 1532–1553. doi:10.3390/en5051532

Thompson, G.A., 1996. Lipids and membrane function in green algae. Biochim. Biophys. Acta 1302, 17–45. doi:10.1016/0005-2760(96)00045-8

Turpin, D.H., 1991. Effects of Inorganic N Availability on Algal Photosynthesis and Carbon Metabolism. J. Phycol. doi:10.1111/j.0022-3646.1991.00014.x

Unkefer, C.J., Sayre, R.T., Magnuson, J.K., Anderson, D.B., Baxter, I., Blaby, I.K., Brown, J.K., Carleton, M., Cattolico, R.A., Dale, T., Devarenne, T.P., Downes, C.M., Dutcher, S.K., Fox, D.T., Goodenough, U., Jaworski, J., Holladay, J.E., Kramer, D.M., Koppisch, A.T., Lipton, M.S., Marrone, B.L., McCormick, M., Molnár, I., Mott, J.B., Ogden, K.L., Panisko, E.A., Pellegrini, M., Polle, J., Richardson, J.W., Sabarsky, M., Starkenburg, S.R., Stormo, G.D., Teshima, M., Twary, S.N., Unkefer, P.J., Yuan, J.S., Olivares, J.A., 2017. Review of the algal biology program within the National Alliance for Advanced Biofuels and Bioproducts. Algal Res. 22, 187–215. doi:10.1016/j.algal.2016.06.002

Vigani, M., Parisi, C., Rodríguez-Cerezo, E., Barbosa, M.J., Sijtsma, L., Ploeg, M., Enzing, C., 2015. Food and feed products from micro-algae: Market opportunities and challenges for the EU. Trends Food Sci. Technol. 42, 81–92. doi:10.1016/j.tifs.2014.12.004

Waller, P., Ryan, R., Kacira, M., Li, P., 2012. The algae raceway integrated design for optimal temperature management. Biomass and Bioenergy 46, 702–709. doi:10.1016/j.biombioe.2012.06.025

Yilancioglu, K., Cokol, M., Pastirmaci, I., Erman, B., Cetiner, S., 2014. Oxidative Stress Is a Mediator for Increased Lipid Accumulation in a Newly Isolated *Dunaliella salina* Strain. PLoS One 9, e91957. doi:10.1371/journal.pone.0091957

Zhang, Q., Hong, Y., 2014. Effects of stationary phase elongation and initial nitrogen and phosphorus concentrations on the growth and lipid-producing potential of *Chlorella* sp. HQ. J. Appl. Phycol. 26, 141–149. doi:10.1007/s10811-013-0091-7

Zhao, Y., Li, D., Ding, K., Che, R., Xu, J.W., Zhao, P., Li, T., Ma, H., Yu, X., 2016. Production of biomass and lipids by the oleaginous microalgae *Monoraphidium* sp. QLY-1 through heterotrophic cultivation and photo-chemical modulator induction. Bioresour. Technol. 211, 669–676. doi:10.1016/j.biortech.2016.03.160